Alma Mater Studiorum – Università di Bologna

DOTTORATO DI RICERCA IN

CHIMICA

Ciclo XIX

Settore Concorsuale di afferenza: 03/C2

Settore Scientifico disciplinare: CHIM/04

From lignocellulosic biomass to rare sugars: hydrolysis and isomerization with heterogeneous catalysts

Presentata da: MATTIA MELLONI

Coordinatore Dottorato — Relatore

Prof. Aldo Roda — Prof. Fabrizio Cavani

Esame finale anno 2017

Abstract

The PhD project presented in this thesis focused on two research topics turned to contribute to the development of a modern model of production, that is able to reduce the environmental impact of the chemical industry. For this purpose, preparation and characterization of heterogeneous catalysts for the transformation of renewable raw materials into valuable chemicals has been studied.

The first part of the work concerned the conversion of lignocellulosic biomass, the most abundant renewable source presents on Earth, into monosaccharides and bio-building blocks, such as HMF, furfural and levulinic acid. Solid acid metal phosphate catalysts were synthetized for lignocellulose transformation; the catalytic behaviors shown by prepared metal phosphates were correlated to their physical-chemical properties: in particular, the role of acid features on the hydrolysis reaction has been studied.

The synthesis of interesting industrial monosaccharides that cannot be obtained in appreciable amount from natural resources, called rare sugars, was the topic of the second part of the work. For this purpose, the rearrangement of glucose by the use of heterogeneous catalysts containing titanium was studied: especially, the influence of the different Ti species on products distribution has been investigated.

TABLE OF CONTENTS

1. Introduction 1
1.1 Biomass & Bio-refinery 1
1.2 Lignocellulose: Nature and Composition 3
1.2.1 Cellulose 4
1.2.2 Hemicellulose 7
1.2.3 Lignin 8
1.3 Lignocellulose: feedstock for a new model of chemical production 9
1.3.1 Mechanism of lignocellulose hydrolysis 11
1.3.2 Bio-building blocks from lignocellulose 17
1.3.3 Lignocellulose hydrolysis in homogeneous acid catalysis 20
1.3.4 Lignocellulose hydrolysis with heterogeneous acid catalysis 23
1.3.5 Lignocellulose pretreatment methods 25
1.3.6 Other lignocellulose transformation processes 27
1.4 Monosaccharides & Rare Sugars 30
1.4.1 Glucose 33
1.4.2 Isomerization of glucose: Fructose & Sorbose 35
1.4.3 Epimerization of glucose: Mannose 40
1.4.4 Heterogeneous catalysis: Titanium-silicalite 43
2. Materials and Methods 47
2.1 Preparation of catalytic systems 47
2.1.1 Catalytic systems for lignocellulose hydrolysis 47
2.1.2 Catalytic systems for rare sugars synthesis 48
2.2 Characterization Techniques 49
2.2.1 Structural properties 49
2.2.2 Composition 50
2.2.3 Surface properties 51
2.3 Catalytic Tests 53

2.3.1 Lignocellulose hydrolysis 53
2.3.2 Rare sugars synthesis 55
2.3.3 HPLC analysis.....57
2.3.4 Expression of results 57
3. Results and Discussion.....59
3.1 Lignocellulose hydrolysis tests 59
3.1.1 Characterization of lignocellulosic substrate 60
3.1.2 Characterization of hydrolysis catalytic systems 63
3.1.3 Catalytic tests of lignocellulose and cellulose hydrolysis.....75
3.1.4 Characterization of spent catalytic systems 90
3.2 Rare sugars synthesis.....93
3.2.1 Characterization of titanium oxide grafted on silica catalysts 94
3.2.2 Characterization of titanium-silicalites 97
3.2.3 Catalytic tests for the synthesis of rare sugars 104
4. Conclusions.....118
5. References.....121

1. Introduction

The large use of petroleum, coal and natural gas in the XX century, allowed our society to achieve a high level of economic wealth and technological development, never reached before.
At the same time, this massive exploitation has led to environmental problems, such as pollution and greenhouse effect, and social-political issues, due to the need of supply of fossil raw materials, that are unevenly distributed on Earth.
In the last years these problems, together with the concern caused by the gradual dwindling of the fossil resources, have stimulated the research and the use of alternative renewable feedstocks for the production of energy, fuel and chemicals. Thanks to the influence of the public opinion on governments, in the last period, this pulse has obtained a renewed force, as demonstrated by the ratification of important agreements signed to stop the climate change[1].

Among the various types of renewable resources, today biomass appears to be highly suitable as alternative raw material for the chemical industry: it represents the main resource of renewable organic carbon on Earth, and for this reason, it is the principal candidate to replace fossil feedstocks in the production of fuels and chemicals, based on the model of bio-refinery[2, 3, 4, 5, 6].

1.1 Biomass & Bio-refinery

The term biomass indicates any organic and bio-organic material derived from a photosynthesis process, except fossil fuels; in other words, biomass represents all that is part of the life cycle in biosphere.
At present, the world production of biomass is about 180000 million of tons per annum[2, 4], that are classified in function of their production: biomass of first generation derived by dedicated culture, which, however, presents ethical issues

caused by the competition in the utilization of resources used to satisfy food demand; biomass of second generation, that are collected by agricultural, forestry, industrial and urban waste and by non-food crops grown on unusable soil for human supply.

The use of biomass as raw material is closely related to the bio-refinery concept, the aim of which is to develop a new production chain based on the direct transformation of renewable materials into fuels and chemicals, that are able to replace the classical production model based on fossil resources in the traditional refinery (Figure 1.1)[7].

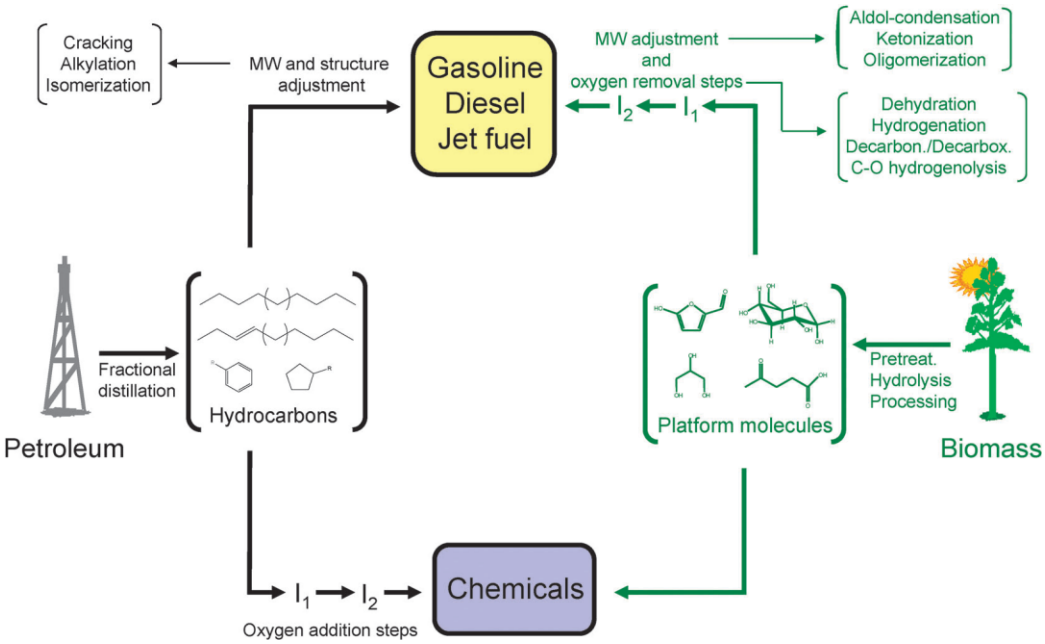

Figure 1.1 Comparison between traditional and bio refinery[7].

As represented in Figure 1.1, in the bio-refinery the theoretical production pathway is comparable to the traditional one: from raw materials to platform molecules, and subsequent transformation into fuels and chemicals.

Actually, depending on the complex chemical structure and on the variable composition of biomass, often due to the seasonal nature of the material, the

approach to the transformation into the desired product must be necessarily different compared to the traditional refinery. Therefore the bio-refinery model is based on an alternative concept of production: the plants have to use different technologies, and especially have to be more flexible in production, in order to be suitable for the transformation of the different types of biomass[3, 4, 8, 9].
Therefore, the development of an industrial chemistry based on biomass requires a more important phase of study and improvement of the technologies, which includes engineering and chemical aspects, such as operative conditions and catalysts design: hence the need of important financial investments for the realization of new plants or the adjustment (revamping) of the old technologies to the alternative ones.

The economic aspect is probably the most important factor that has limited the development of the bio-refinery model, especially if we make a comparison with the investments which are still made in traditional refinery.
The possible solution to overcome this economic gap is the model of bio-refinery that is being developed in recent time, which is further differentiated from the traditional one by the amount of compounds annually produced. The realization of plants that are operative in a relatively smaller scale has allowed the bio-refinery model to improve and become competitive. This model includes the transformation of a particular type of biomass, which today represents one of the most promising resource for this alternative chemistry, which is lignocellulose.

1.2 Lignocellulose: Nature and Composition

Lignocellulose is a particular type of biomass and currently represents the most abundant, various and widely distributed natural raw material produced every year in the world: it is estimated that the production of lignocellulose is roughly 820 million of tons per annum[10].

This particular type of biomass presents a complex composition; it consists mainly of three natural polymers: cellulose, hemicellulose and lignin. There are also other minor components such as oils, waxes, proteins and minerals[2,7].

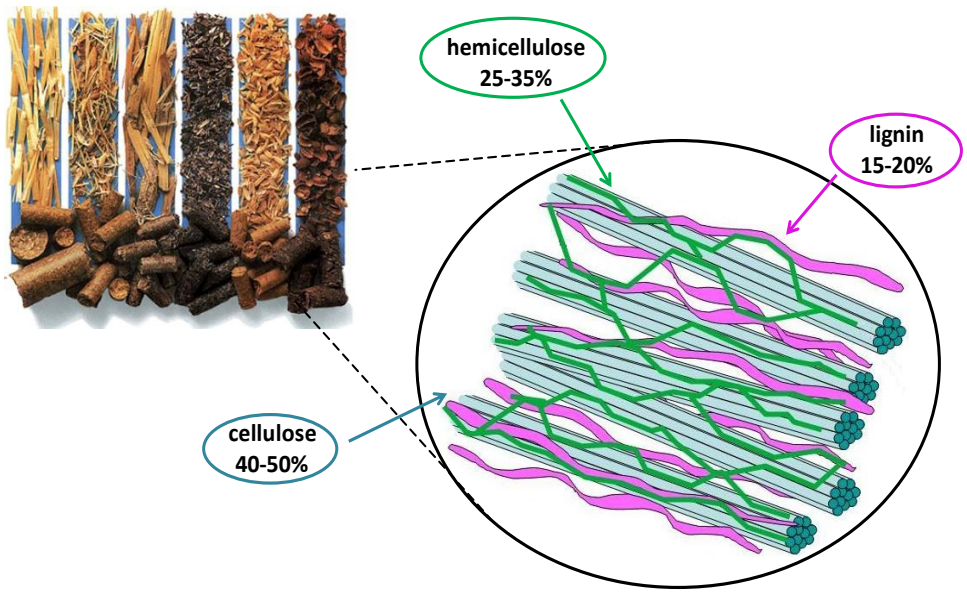

Figure 1.2 Lignocellulose structure and composition.

As represented in Figure 1.2, lignocellulose presents a structure made by two polymers of carbohydrates (cellulose and hemicellulose), that are tightly covered and tied by a phenolic polymer (lignin).

The amount of these three main components is variable in function of the type of lignocellulose, and of other factors such as seasonality and place of collection; usually, cellulose represent the main fraction (40-50%), whereas hemicellulose and lignin are present in comparable amount (15-35%).

1.2.1 Cellulose

Cellulose is the most abundant bio-polymer present on Earth and one of the main polysaccharides. It is made by units of D-glucose linked together with 1,4-

β-glycosidic bond; in cellulose, the degree of polymerization ranges between 300 and up to 10000 units of glucose[3, 11].

The D-glucose is present in cellulose with its β-anomeric form, that is a six member cycle, derived from the cyclization of linear glucose, which involves the hydroxyl group on C5 and the reducing-end (-CHO), with the –OH group on C6 in equatorial position (Figure 1.3).

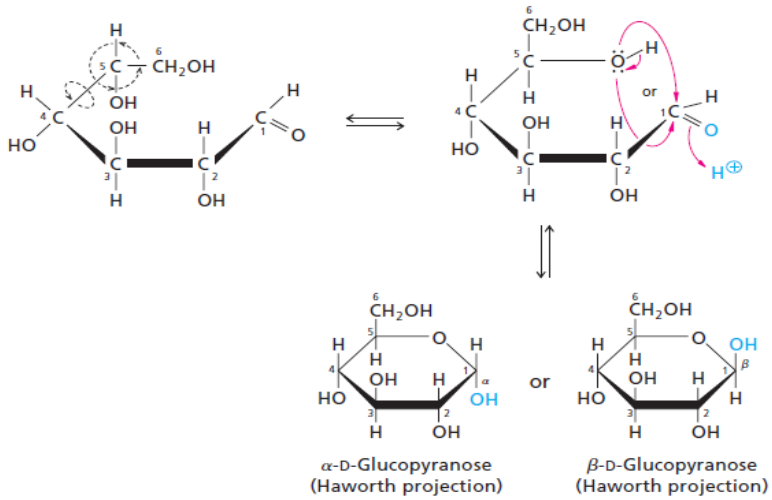

Figure 1.3 Cyclization of linear glucose to give α- and β-D-glucose.

This distinguishes cellulose form the other important natural polysaccharide, i.e. starch, that is made of units of D-glucose bound together via 1,4-glycosidic linkage, but in their α-anomeric form (with the –OH group on C6 in axial position)[12].

This means that cellulose and starch, that is composed by several bio-polymers such as amylase and amylopectin, present very different structure and properties (Figure 1.4).

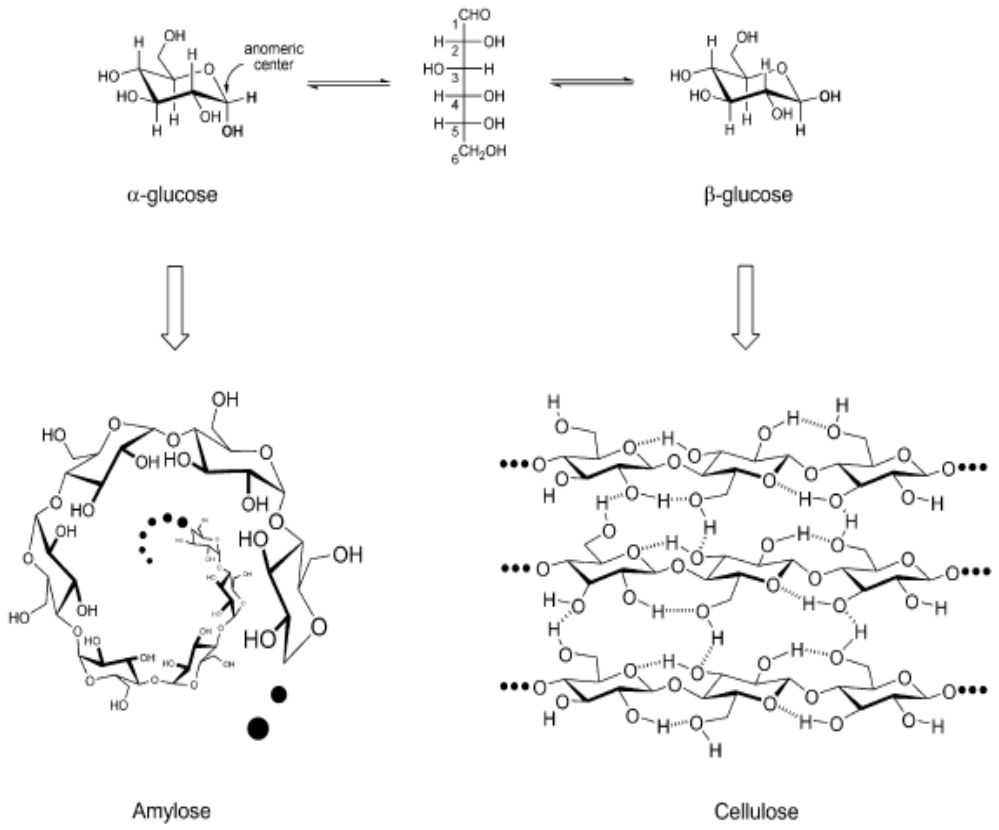

Figure 1.4 Comparison between natural polymers of different anomeric form of D-glucose[12].

As visible in Figure 1.4, amylase presents an helicoidal structure due to the arrangement of the pyranose rings one beneath each other of the pyranose rings, that is characteristic of the 1,4-α-glycosidic bond of the α-anomeric form; this results in a structure that is very accessible to enzymes and chemicals.

On the other hand, cellulose presents a side-by-side disposition of the pyranose rings, that results in a linear chain structure, with an intense intramolecular hydrogen bonding interaction between the close groups to the glycosidic bond[13]. In this way, the polymer chains of cellulose can be packed very tightly through intermolecular interaction, thus making most of the functions of cellulose not accessible to enzymes and chemicals.

1.2.2 Hemicellulose

Hemicellulose is the second and less abundant polysaccharide present in lignocellulose. In contrast with cellulose, this polymer is made of different types of sugar: both C6 terms like glucose, mannose and galactose, and C5 terms such as xylose (usually the main component) and arabinose; moreover, it is possible to observe the presence of sugar in their oxidized form, such as glucuronic and galacturonic acid. Furthermore, hemicellulose presents a lower degree of polymerization, with a chain from 500 to 3000 monomer units, and a characteristic branched structure (Figure 1.5)[12].

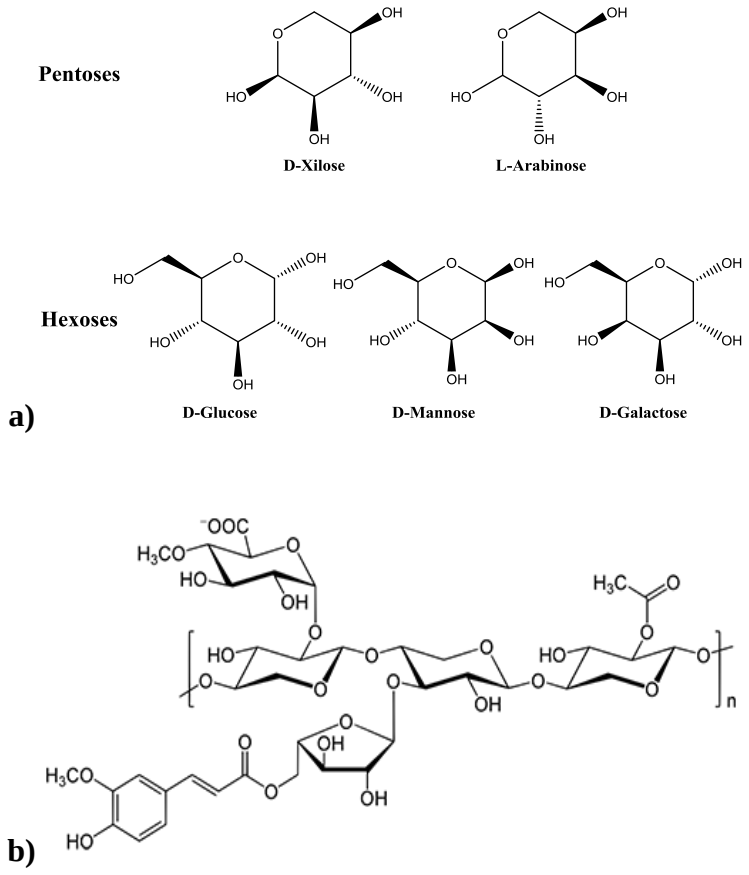

Figure 1.5 a) Monomer units of hemicellulose **b)** Structure of hemicellulose.

Depending on the way by which the different monomers can be linked together, hemicellulose is divided into: xylan (mainly xylose units), glucoroxylan (glucoronic acid and xylose units), arabinoxylan (arabinose and xylose units), glucomannan (mannose, glucose and galactose units), and xyloglucan (xylose, glucose and galactose units).

1.2.3 Lignin

Lignin is a natural complex polymer that presents itself mainly in the external cellular side of the plant, with the role to confer thermal, mechanical and chemical resistance to the inner part made by microfibrils of cellulose and hemicellulose.

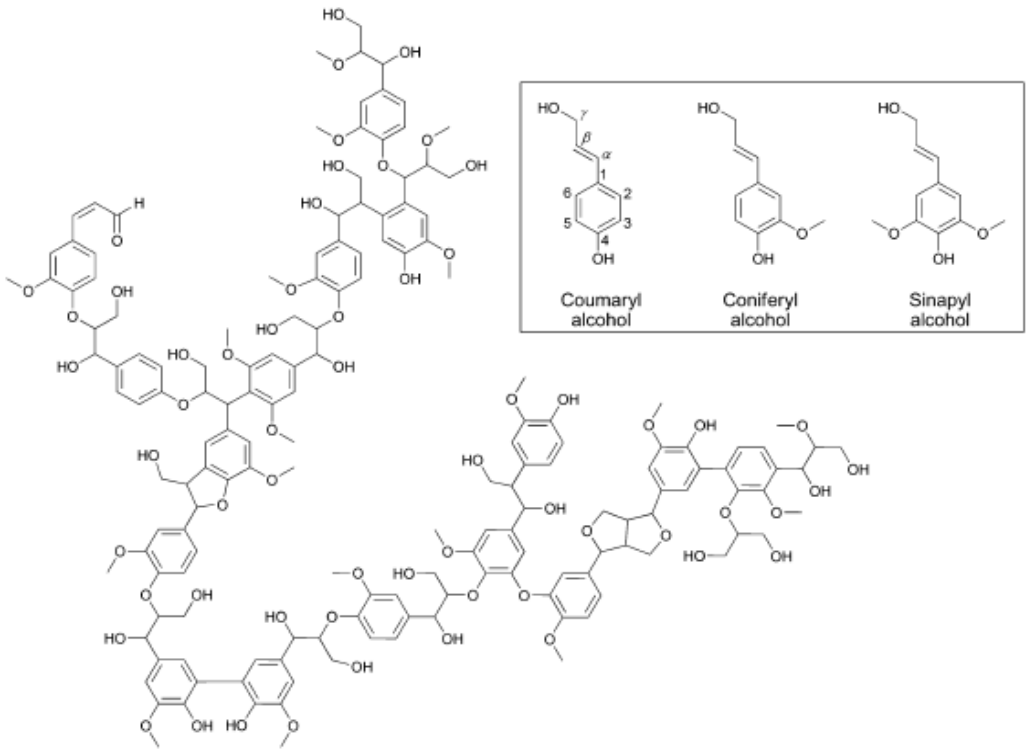

Figure 1.6 Monomer units and example of structure of lignin[12].

The structure and the composition of lignin are closely linked to the type of wood and the part of the plant taken into account. It is a copolymer of phenolic units, that are mainly *p*-coumaryl, synapyl and coniferyl alcohols; these units polymerize randomly by coupling reactions, which results in a very complex three dimensional structure (Figure 1.6)[12, 14].

1.3 Lignocellulose: feedstock for a new model of chemical production

Lignocellulosic biomass has been used by humankind for millennia as a raw material: it represents probably the oldest resource used to produce energy, by its burning or heating.

Starting from the end of the XIX century, the development of the knowledge in the chemical sector allowed to develop a better understanding of the nature of lignocellulose and of its potential as feedstock for the production of fuels and chemicals.

During the first half of the XX century, a high number of reactions and processes were proposed for the conversion of lignocellulose into products of industrial interest. These processes, however, were not sufficiently cost-efficient, especially compared to the high profitable petrochemical production, and this limited their development.

During latest years the use of lignocellulose as a raw material has been representing the base of the bio-refinery model, whose production chain can be summarized in Figure 1.7: it is possible to observe that from a natural and renewable material, a wide range of products such as fuels, polymers, resins, lubrificants, chemicals, solvents, and adhesives can be obtained[5, 10, 15, 16].

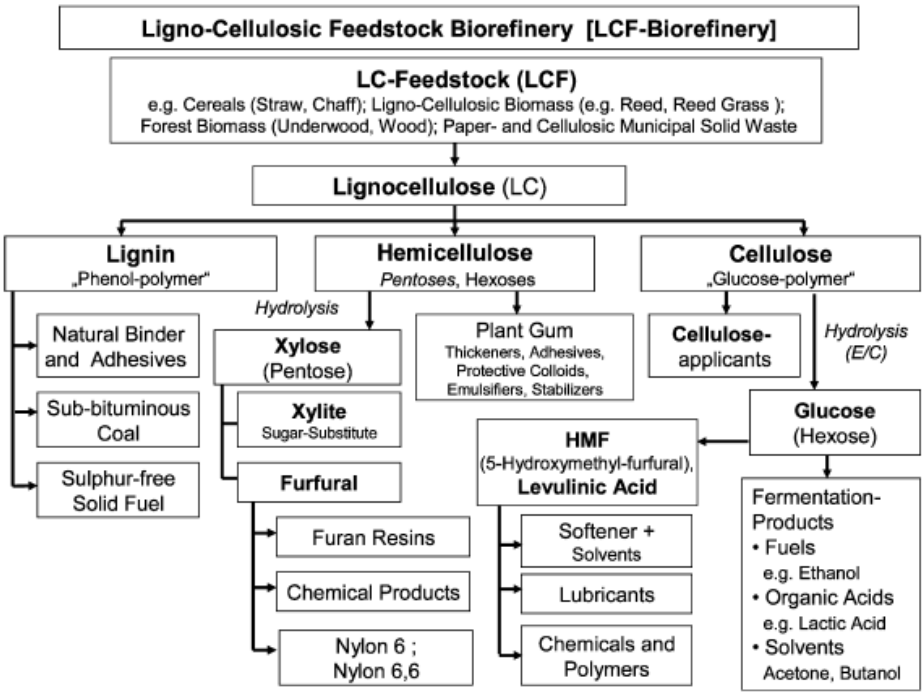

Figure 1.7 The bio-refinery model from lignocellulose feedstock[16].

At present, the transformation of lignocellulose is based on hydrolysis process, that is divided in two fundamental steps. The first step consists in the degradation of the biomass with the deconstruction of lignocellulose into its three main components. In the second step, cellulose and hemicellulose are depolymerized under controlled conditions, in order to prevent the degradation of the obtained monosaccharides, that can be used directly, or even further transformed into bio-building blocks such as 5-hydroxymethylfurfural (HMF), furfural (F) and levulinic acid (LA). For this type of process, the use of catalytic systems with acid peculiarities results to be fundamental, able to promote the two reaction steps for the transformation of lignocellulose.

As regards the lignin fraction, its transformation is more difficult, due to the complexity of its composition. Breaking the polymer structure of lignin in order to obtain monomers requires stronger conditions[17, 18, 19]. In general, this is made

by pyrolysis treatment at very high temperature (above 400°C), or by deoxy and hydro treating, such as hydrogenolysis and deoxygenation, at high pressure and temperature, or even with the use of a strong base such as concentrated sodium hydroxide.

Besides the presence of lignin, that reduces the processability of cellulose and hemicellulose because of its natural protective prerogative, the process is also limited by another issue: the high crystallinity of cellulose. As described above, the particular linear structure of cellulose microfibrils results in a tight packing, thanks to the intense intermolecular interaction, that protects the 1,4-β-glycosidic bond from the hydrolysis.

1.3.1 Mechanism of lignocellulose hydrolysis

The hydrolysis of lignocellulose is a very complex process, that is hard to summarize in a general reaction mechanism, due to the variable nature and composition of the substrate.
While most of the conducted studies on this transformation are basically in agreement on the way the lignocellulose is cleaved into its three main components, it is more difficult to find in literature a shared explanation for the conversion of cellulose and hemicellulose fractions. Especially the mechanism of cellulose depolymerization in acid solution is a very debated matter[12, 20, 21, 22].
In the cleavage of 1,4-β-glycosidic bond, the crucial step appears to be the initial formation of a carbocation, by means of addition of a proton to the substrate, due to acid conditions. As summarized in Figure 1.8, the protonation can take place either on the bridging oxygen atom of the bond (glycosidic oxygen), with the consequent formation of a cyclic carbocation, or on the pyranic oxygen, that results in an acyclic carbocation formation.

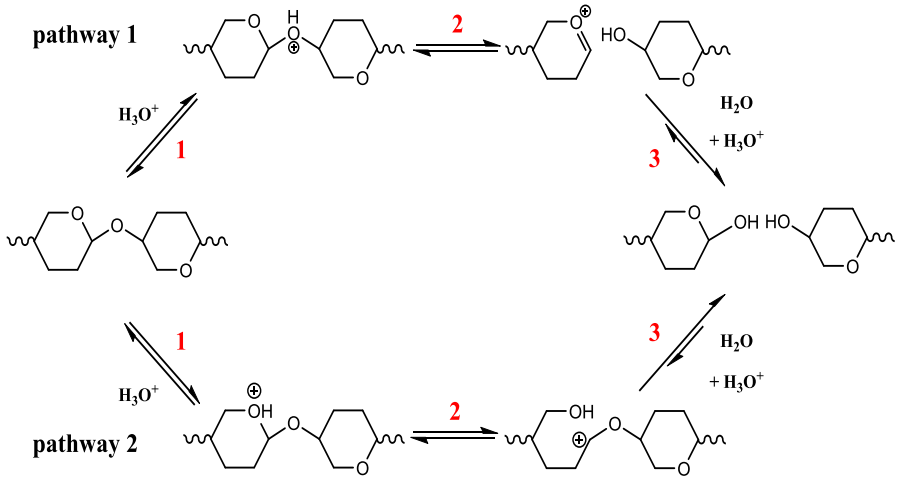

Figure 1.8 Proposed catalytic cycle for the hydrolysis of cellulose.

The synthetic route via cyclic carbocation (pathway 1) is considered the most probable by several authors[20, 23, 24, 25].The formation of this cyclic ion involves conformational changes in pyranose ring that undergoes a tipping of the structure to obtain a half-chair configuration; the high hindrance caused by intra and intermolecular interactions, characteristic of cellulose structure, makes this step the most energetically relevant. In the last step of the hydrolysis mechanism, water reacts with the formed carbocation, to regenerate the anomeric center and the catalytic proton.

The kinetic model of this reaction can be summarized as reported in Equation 1.1[23]:

$$R + H_3O^+ \underset{k_{-1}}{\overset{k_1}{\rightleftharpoons}} RH^+ + H_2O \underset{k_{-2}}{\overset{k_2}{\rightleftharpoons}} P$$

Equation 1.1 Kinetic model for cellulose hydrolysis, where: R stands for substrate, RH^+ for protonated substrate, P for product.

This model shows that the rate of cellulose hydrolysis is a first order reaction with respect to the concentration of the acid H_3O^+ species. The studies conducted on the hydrolysis have also demonstrated that the kinetic of the process is affected by the presence of crystalline and amorphous domains in the substrate that influences the rate and the apparent activation energy[20, 26, 27, 28].
Amorphous domains are more accessible and easier to hydrolyze compared to crystalline ones, with a consequent higher cellulose deconstruction rate at the beginning of the process. As the reaction proceeds, the residual crystalline domains are depolymerized at a lower reaction rate, resulting in the leveling-off degree of polymerization (LOPD)[20, 29]. Moreover, in literature[30] it has also been proposed the presence of weak points in the cellulose structure, which can be formed by the insertion of other monosaccharides in cellulose chains during its formation, a point that is possible but difficult to prove, or as result of partial oxidation of glucose units during degradation of lignocellulose. These weak sites are supposed to contribute to both the decrease of the activation energy and the higher hydrolysis rate.

The monosaccharides obtained by hydrolysis of lignocellulose (glucose from cellulose and a mix of hexoses and pentoses from hemicellulose) can be further transformed by degradation reactions, thanks to the presence of water and acid conditions.
The transformation of hexoses, mainly glucose, involves an initial dehydration to form the intermediate product 5-hydroxymethylfurfural (HMF) that subsequently is hydrated to levulinic acid (LA) and the by-product formic acid (FA)[31, 32].

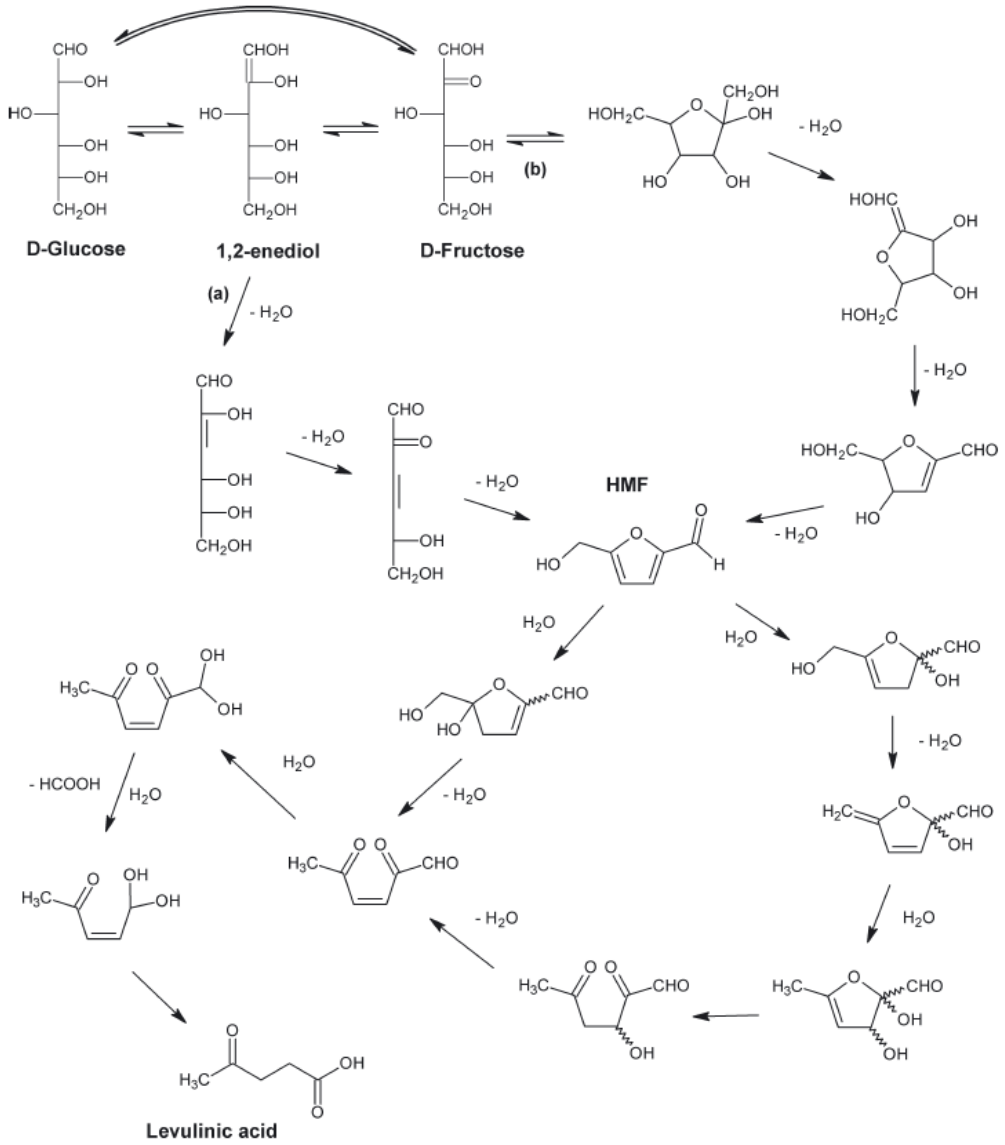

Figure 1.9 Reaction mechanism for the conversion of hexoses to LA[32].

As reported in Figure 1.9, the dehydration mechanism of hexoses includes isomerization equilibria between glucose and fructose via keto-enol tautomerization. Two possible routes are proposed for this reaction: acyclic dehydration route from 1,2-enediol intermediate and cyclic dehydration route from fructose. The acyclic route is generally accepted as the prevalent

mechanism from glucose substrates while cyclic route preferentially prevails for fructose substrates.

The subsequent hydration of HMF results from water addition to the C2-C3 bond of the HMF furanic ring, that gives LA and FA (the formation of the by-product FA results to be inevitable).

From the thermodynamic point of view[33], the first dehydration step is highly endothermic, while, the subsequent hydration step is exothermic, even if the dehydration of fructose to HMF is easier and faster than that of glucose. This indicates that the first step presents a higher activation energy and, therefore, it controls the overall progress of the reaction; in fact, the conversion of HMF to LA is much faster than the conversion of hexoses to HMF.

From the kinetic point of view[34], the model proposed by several authors predicts a pseudo-homogeneous and partly irreversible consecutive first-order reaction sequence. The reaction rate depends on substrate concentration (R_i), temperature (T) and acid hydrogen ion concentration (A_{H+}) by means of kinetic constants for the two steps (k_{iH} and k_{iP} defined by Arrhenius equation), as shown in the Equation 1.2:

$$\frac{dR_i}{dt} = -x(R_i)^{\sigma}(A_{H+})^{\varphi}\left(k_{ip}\exp\left[\frac{E_{ip}}{Rf(T)}\right]+k_{iH}\exp\left[\frac{E_{iH}}{Rf(T)}\right]\right)$$

Equation 1.2 Simplified kinetic model for hexoses degradation to LA; where σ is order of the reactant, φ acid hydrogen ion concentrations, E_{iP} is activation energy of the decomposition products, E_{iH} is activation energy of humins, R is the universal gas constant[32].

For pentose monosaccharides derived from the hydrolysis of hemicellulose, the transformation via degradation is similar to that observed for hexoses: C5-sugars are dehydrated to furfural (F), with a reaction mechanism that is similar to that one shown by hexoses, as shown in Figure 1.10[32, 35].

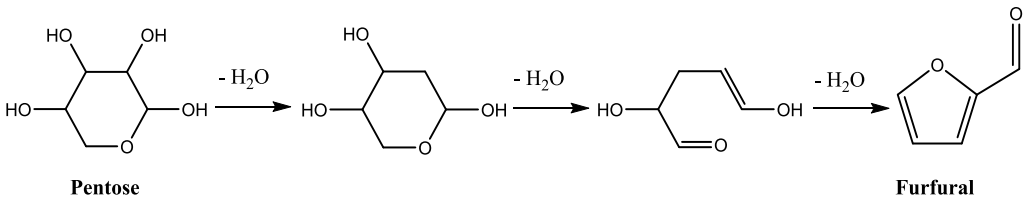

Figure 1.10 Reaction mechanism for the conversion of pentose to furfural.

In acid conditions, besides the degradation reaction described above, which results in the formation of high value products, condensation reaction involving glucose and HMF many also occur[36, 37, 38].

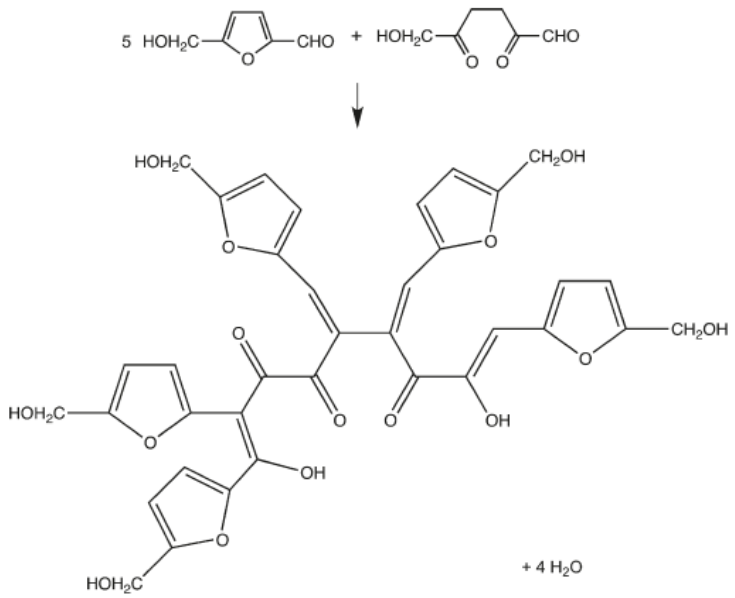

Figure 1.11 Example of humins formation from HMF[38].

As reported in Figure 1.11, this polymerization leads to the formation of undesired black insoluble materials, called humins. The activation energy and the reaction order for humins formation from glucose and HMF, are significantly higher than those for the other reactions. This means that the

kinetic of humins formation is the most sensitive to temperature and substrate concentration: a higher temperature or substrate concentration results in a higher production of humins.

1.3.2 Bio-building blocks from lignocellulose

5-Hydroxymethylfurfural (HMF), furfural (F) and levulinic acid (LA), as explained in the previous paragraph, are the products of the acid transformation of monosaccharides obtained by hydrolysis of lignocellulose; these molecules represent three of the most promising bio-building blocks on which the bio-refinery model for the production of chemicals and fuels is based[2,3,8].

5-Hydroxymethylfurfural, that is obtained from the direct dehydration of glucose, is a furanic compound containing two different functional groups: aldehyde and alcohol. It represents an important intermediate for the production of polymers and fuels through various reactions, as shown in Figure 1.12[39, 40, 41].

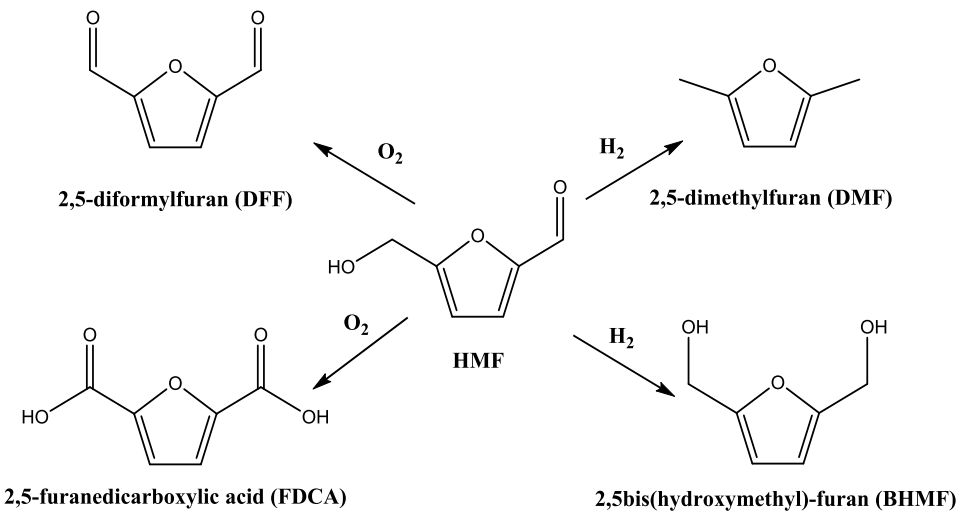

Figure 1.12 Derivatives of HMF.

By oxidative treatment, HMF can be converted into 2,5-diformylfuran (DFF) and 2,5-furanedicarboxylic acid (FDCA), that present a high potential in polymer production as a replacement for terephthalic acid and the widely used polymers such as polyethylene terephthalate (PET) and polybutylene terephthalate (PBT).

On the other hand, reductive reaction of HMF leads to the formation of 2,5bis(hydroxymethyl)-furan (BHMF), a diol which can be used in the production of bio-polymers as polyurethane and polyesters, and 2,5-dimethylfuran (DMF), that is a promising component of bio-fuel with an energy density comparable to that of gasoline.

As seen from the mechanism of lignocellulose hydrolysis, in acid condition HMF is converted into LA, whose properties are summarized below.

Furfural is also a furan ring, obtained from the dehydration of a C5 sugar, such as xylose, with only the aldehyde function, that reduces its possible uses compared to HMF, as shown in Figure 1.13[6, 15, 42].

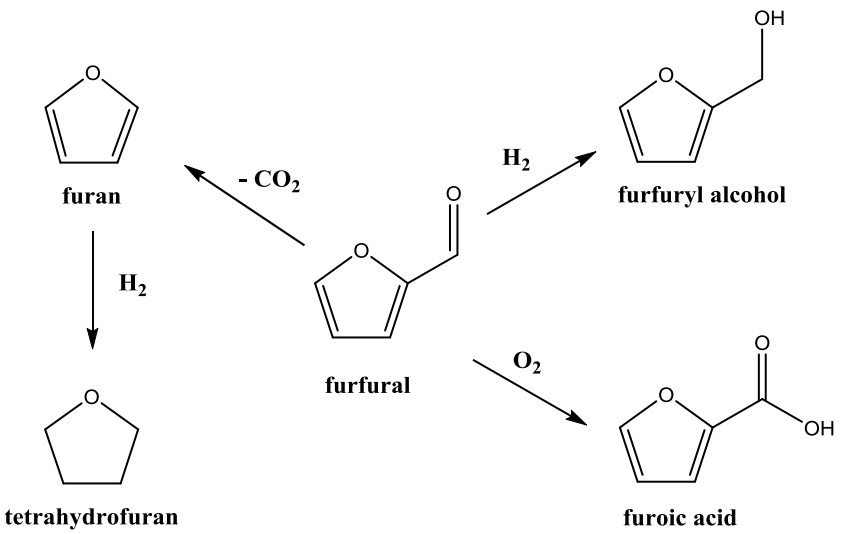

Figure 1.13 Derivatives of Furfural.

Furfural finds important industrial use when treated in reductive conditions to obtain furfurylic alcohol, which is employed for the production of monomers, solvents, adhesives, wetting agents and fuels.

LA, as explained above, is obtained by hydration of HMF. In 2004, it was included in the top-twelve promising building blocks list compiled by NREL[43].

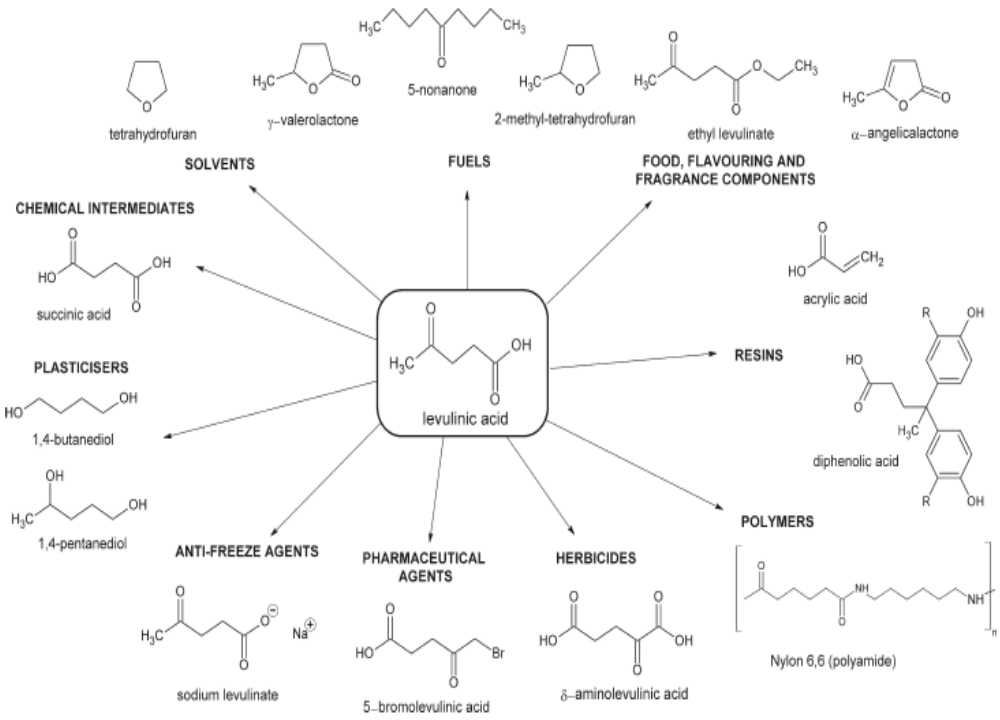

Figure 1.14 LA as a platform chemical for products and fuels[32].

LA presents a wide range of applications[32, 41, 44], as shown in Figure 1.14, thanks to the different possible transformations involving its functional groups:

- carboxylic group: esterification reactions with alcohol in presence of an acid catalyst; esters of LA, like ethyl levulinate, which can be used as additives in diesel, as flavoring and fragrance agents and as plasticizer.

- carbonyl group: addition of nucleophiles, like nitrogen, ammonium or heterocyclic nucleophiles, leads to value-added products, such as diphenolic acid, used as a pharmaceutical intermediate and in the production of polymers, lubricants, fire-retardant materials and paints.
- methyl group: halogenation with bromide or chloride forms organic halides, like bromolevulinic acid, employed as intermediates in the production of drugs and herbicides.
- oxidation reactions: high-temperature catalytic oxidation with heterogeneous catalysts such as vanadium oxide, leads to oxidation products such as succinic acid or acrylic acid, that can be used as pharmaceutical and agrochemical intermediates and in the production of polymers and solvents.
- reduction reactions: catalytic hydrogenation with heterogeneous catalysts such as platinum oxide, nickel-Raney, copper-chromite, rhodium and ruthenium complex, produces compounds like γ-valerolactone, which find important use as solvents, lacquers, insecticides, adhesives and as additives in gasoline.

1.3.3 Lignocellulose hydrolysis in homogeneous acid catalysis

As described above the acid-catalyzed hydrolysis represents the starting point of the bio-refinery model. The most common processes for the conversion of lignocellulosic biomass make use of homogeneous mineral acid systems, typically with the use of diluted or concentrated solution of H_2SO_4 and HCl (even if other Brønsted acid as HNO_3, HBr and HF have been used with interesting results)[34, 45].

The study and the development of processes based on this type of technology started at beginning of the XX century.

The Scholler process[46], improved during the 1920s, was the first technology for the acid degradation of lignocellulose: at 170°C and 20 bar, a 0,5%wt H_2SO_4 solution is forced to pass in a brick-lined percolator that contain compressed sawdust, with a residence time of 45 minutes; the yields in monosaccharides is about 50%, and the remaining 50% is represented by a mixture of partial hydrolyzed oligomers and furanic derivatives. In 1946, Madison[47] proposed an improvement to the Scholler process: the biomass is treated at a temperature between 150 and 180°C with a continuous flow of a 0,5 wt% solution of H_2SO_4, thus allowing a short reaction time, resulting in a lower production of degradation products and a higher selectivity to monosaccharides.

As an alternative to the use of sulfuric acid, during the 1930s Bergius[48] studied a process for the conversion of lignocellulose with concentrated HCl solution in two steps. At first, the substrate is treated with acid at room temperature for several hours, this allows solubilization of cellulose and hemicellulose fraction, and successive production of monosaccharides without any formation of degradation products. Then, the remaining hydrolyzate, containing 1-2%wt of HCl, is heated at 120°C to complete the transformation. This process was resumed in 1987 by Ragg et al.[49], that proposed the use of salt, like $CaCl_2$ or LiCl, to promote the transformation of lignocellulose, with a consequent increase in monosaccharides production. This study exploited the positive effect of the dissolution of ions in the solution on the reaction rate, that had been demonstrated a few years before.

In 1985, Noguchi[50] presented an alternative approach in the hydrolysis of lignocellulose with the use of gaseous HCl: at first, the substrate is treated in a flow of acid steam at 120°C, with the extraction of the monosaccharides produced in a counter-current water flow; then, the hydrolysis of the residues, that contain a higher concentration of acid, is finished at higher temperature.

More recently, processes based on innovative reactor technology have been developed to improve the performances and the economic return: in 1979, Thompson et al.[51] proposed the use of a plug-flow-reactor (PFR) for the

conversion of a slurry made of lignocellulose and a 1%wt H_2SO_4 solution at 240°C with a very short reaction time (0,22 minutes). Then, this process was improved by Harris et al.[52], by splitting the hydrolysis in two steps (the second step needed for the transformation of the most recalcitrant part), that allows to work with lower temperature and acid concentration.

In 1999 Ghorpade and Hanna[53] developed a process for the conversion of biomass based on the concept of a reactive extrusion: a slurry of lignocellulose and a 5%wt H_2SO_4 solution is fed continuously to a twin-screw extruder with a variable temperature profile (80-100°C, 120-150°C, 150°C), this allows a reduction of side reactions.

Despite years of development, these processes for the transformation of lignocellulose with homogeneous acid catalysis were abandoned, or, in some cases, they have never gone beyond the theoretical level. In fact, they presented several operative drawbacks: the use of mineral acids requires special materials for reactor and other process units, due to the highly corrosive conditions; the recovery of the mineral acid for the following processes is difficult, with at least one neutralization step, that increases the amount of waste. That caused an increase of the operative costs, which made these processes not effective[2, 4, 34].

Although some examples of industrial plants that still operate in homogeneous catalysis for the production of chemicals by hydrolysis of lignocellulose, such as the process based on the Biofine technology, that has been proposed in 1995 by Fitzpatrick[54], and also used in Italy by Le Calorie in Caserta, for the reasons described above, the research is nowadays addressed to the development of alternative catalytic systems that can replace mineral acids.

In this sense, the results obtained with the use of organic acid, such as trifluoroacetic acid (TFA) or paratoluensulfonic acid (PTFA), appears to be interesting, thanks to the easier recovery of the catalyst and the lower amount of waste produced, although this technology is still at the laboratory scale[55, 56].

However, the use of solid acid systems in heterogeneous catalysis represents the most promising route for the hydrolysis of cellulose.

1.3.4 Lignocellulose hydrolysis with heterogeneous acid catalysis

The use of solid catalytic systems usually represents the preferred choice for most industrial processes, in fact now heterogeneous catalysis is used in about the 85% of chemical processes[57]. The main reason for this is the easy catalyst recovery after reaction; at present, the costs associated to separation, purification and recovery represent a considerable fraction of the total cost for a chemical process. Therefore, together with the selectivity to the desired products, the separation costs are a fundamental factor in the successful development of novel processes[28, 57]. Homogeneous catalysts and enzymes are generally more selective compared to heterogeneous systems, but the higher problems in recovery, and the poor versatility of enzymes, make the use of solid catalytic systems preferred.

As described in the previous paragraph, the hydrolysis of lignocellulose is no exception to this analysis; moreover, the use of solid acid systems in place of mineral acids reduces the risks and the environmental costs of the process.
Biomass hydrolysis in heterogeneous acid catalysis results to be limited by other factors, mainly caused by the biomass nature and the way it can interact with the solid catalysts[58, 59, 60].
Lignocellulose is a natural polymer, with a particular composition that protects its internal functional groups from the penetration of chemical agents; this means that in its natural form, it is not soluble in the common polar solvents, including water. For this reason, the effective interactions between the substrate and the active surface of the solid catalysts are very limited.
Another fundamental role in heterogeneous catalysis is represented by catalyst porosity, that influences catalytic activity and selectivity. Based on the size of the pores, materials are classified in: microporous (pore size < 2nm), mesoporous (pore size between 2 and 50 nm), macroporous (pore size > 50nm).

Therefore, the activity of a solid catalyst in lignocellulose conversion is also limited by its high molecular dimension, which hinders the diffusion inside catalyst pores.

Consequently, the use of heterogeneous catalysts for lignocellulose hydrolysis requires pretreatment steps, in order to make the substrate more suitable for the hydrolysis, and also the use of a high catalyst/substrate weight ratio, with an amount of catalyst which is comparable to that one of the reagent. Also high temperature and long reaction time are necessary in order to obtain the highest substrate conversion, though often this leads to a decrease of selectivity to the desired products with a higher formation of by-products.

At present, another issue that limited the implementation to industrial plants of heterogeneous technology is the real ability to recover the solid catalyst from the reaction mixture: the direct separation is generally prevented by the formation of solid residues, as unconverted lignin and insoluble humins.

Many solid catalysts have been studied and proposed at the laboratory scale[32, 41, 61, 62, 63] from the most common systems widely used in petrochemistry like zeolites and doped zeolites, metal and sulfated-metal oxides, metal supported materials, heteropolyacids, to more exotic ones with a hard applicability, such as metal halides and sulfated graphene oxide.

Currently, the systems that have presented the most interesting and promising performances in hydrolysis of lignocellulose are those which reproduce the peculiarity of mineral acids in solid systems:

- acid functionalized resins showed activity comparable to that one obtained with the best mineral acids. Amberlyst, that is a co-polymer of styrene-divinylbenzene with sulfonic groups ($-SO_3H$), was proposed for the first time as a catalyst for biomass hydrolysis by Schuth et al.[64], and Nafion, a sulfonated tetrafluoroethylene co-polymer, used by Lucht et al.[65] supported on amorphous silica, provided good performances in terms of biomass conversion, very close to 100%, and yields to desired

products, up to 15% for glucose. The issues related to catalyst recovery, caused by the organo-polymeric nature comparable to that of humins, have not yet been solved.

- sulfonated carbon-based materials, prepared by sulfonation of incompletely carbonized natural polymers such as cellulose and starch, have demonstrated a superior catalytic activity, with a conversion of 68% and yields in glucose of 4% in only three hours of reaction, as reported in the study of Hara et al[66]. This material, which consists of uniform graphene sheet functionalized with sulfonic, phenolic and carboxylic groups, manifests a high capability of incorporation of hydrophilic molecules, that makes an easier interaction of lignocellulose with $-SO_3H$ groups. This results in an increased catalytic performance; moreover, tests showed a good recovery and reuse.

1.3.5 Lignocellulose pretreatment methods

To reduce the difficulty in the hydrolysis of lignocellulose due to the strength of lignin and crystallinity of cellulose (as described in paragraph 1.3), a pretreatment of the substrate can be an efficient option. The role of the pretreatment is to separate the lignin from the inner part of lignocellulose, to reduce the crystallinity of cellulose and also to increase the porosity of the material, as represented in Figure 1.15[67].

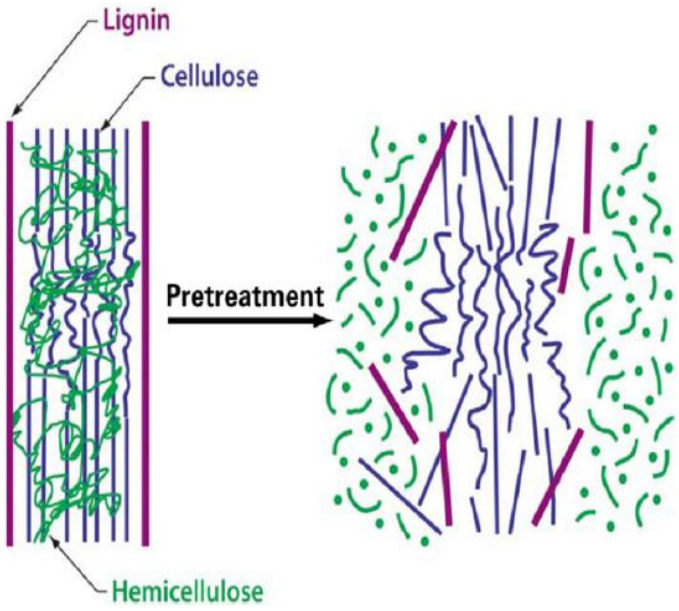

Figure 1.15 Schematic representation of pretreatment on lignocellulose material[67].

This permits to operate in milder condition during the subsequent hydrolysis, and hence to reduce the degradation of the desired products, that means an improved economic return.

The pretreatment of lignocellulose can be mainly classified into three different categories: physical, chemical and physical-chemical[67, 68, 69].

Physical Pretreatment:

- mechanical crushing, that consists in the pulverization of lignocellulose in a ball-mill with a reduction of the average size from 10-30 mm to 0,2-2 mm; it is one of the most common pretreatment for lignocellulose, thanks to its relative simplicity and economy;

Chemical Pretreatment:

- the use of diluted base or acid solution, such as NaOH and H_2SO_4, at room temperature and pressure, permits to increase the rate of the

following hydrolysis process and the yield in monosaccharides; for the diluted base solution, the treatment can last several hours or even days, and the efficacy depends on the amount of lignin present;

- ozonolysis is a treatment especially used for the degradation of lignin, but due to the high energy cost and ozone consumption, it is not much used.

Physical-chemical Pretreatment:

- steam explosion in which lignocellulose is treated with saturate vapour (160-260°C) at high pressure (10-50 bar) for several minutes; then, a very fast reduction of the pressure is applied in order to expose the material to an explosive decompression. This results in a substrate more easily hydrolysed, with a low operative cost and environmental impact; it is also possible to add ammonia to the saturate vapour (Ammonia Fiber Explosion AFEX), or use carbon dioxide instead of vapour (Carbon Dioxide Explosion) to reduce the temperature of the treatment and prevent the degradation of monosaccharides.

There are also types of pretreatment[68] that are used in laboratory or on a very small scale, like the biological pretreatment, that uses microorganisms such as fungi, or the pulsed electric field pretreatment (PEF), in which a short burst of high voltage is applied on the substrate.

1.3.6 Other lignocellulose transformation processes

Besides the processes of acid hydrolysis described above, lignocellulose can be used as feedstock in other production processes, which are based on different types of technology and concepts.

Enzymatic hydrolysis:

The enzymatic hydrolysis is an alternative to the classical hydrolysis with traditional catalytic systems; this approach involves the use of microorganisms, like bacteria and fungi, that are able to produce enzymes which can degrade lignocellulose.

The principal enzymes for the degradation of lignocellulose belongs to the family of cellulase, and is a tri-component system composed by β-glucosidase, endo-β-glucanase and eso-β-glucanase; in general, this type of enzyme is synthetized by microorganism such as *Trichoderma Reesei* e *Aspergillus Niger*[70, 71, 72].

From an operative point of view, this system is active in the hydrolysis of cellulose, as it is able to cleave the 1,4-β-glycosidic bond, in milder conditions compared to traditional processes mediated by catalysts. The ability to operate hydrolysis at lower temperature, allows enzyme to obtain glucose with higher selectivity, thanks to the limitation of degradative reactions, and to reduce the energy cost of the process.

However, the use of enzymes presents several issues[73]: enzymes are extremely sensible to the variation of the reaction conditions, in particular temperature and pH, and are active in a very narrow operative range. In addition, the lack of flexibility towards the type of substrate, the low productivity due to the need of long reaction time, the difficult recovery at the end of the reaction and the high cost, have limited the development of this process on an industrial scale.

Thermochemical transformation:

Thermochemical processes for the conversion of lignocellulose operate generally at high temperature, above 700°C. It is possible to distinguish two types of processes, in function of the presence or absence of oxygen.

Gasification is a high-temperature treatment of lignocellulose in the presence of a small amount of oxygen, in which the result is the production of syngas (CO + H_2), that can be fed to a Fischer-Tropsch unit for the synthesis of a diesel-like fuel mixture of hydrocarbons (Biomass to Liquid Process)[11].

Conversely, pyrolysis is the thermal process conducted in absence of oxygen, with the production of a mixture of gas, oil and tar[74].

These processes have been known since many years, but they are not commonly used in commercial scale, due to their many drawbacks, such as the low selectivity to the desired products, the formation of heavy products with no value and the high cost due to energy consumption.

Hot Compressed Water:

Lignocellulose can be hydrolyzed with hot and compressed water (in sub- or super-critical condition), in the absence of a catalytic system; the substrate is treated at a temperature between 200-400°C and a pressure above 200 bar, for a short residence time[11].

Several issues, such as the low selectivity to the desired products, due to the high contribution of degradation reactions, corrosion phenomena caused by super-acid character of super-critical water and high energy costs have limited the development of this technology.

One-pot transformation of lignocellulose:

The catalytic conversion of lignocellulose is not limited to the acid hydrolysis: during latest years, bi-functional catalytic systems for the one-pot synthesis of chemicals directly from the biomass have been developed[13].

In general, this strategy consists in coupling an acidic property, that is necessary for the first hydrolysis step, with a redox functionality, for the further transformation into the desired products.

Under reducing conditions, the direct synthesis of sugar alcohols, sorbitol and mannitol is an example of this approach. These compound are used in pharmaceutical and food industry; they are obtained at high temperature (200°C) and high pressure of H_2, by means of a catalyst made by deposition of a transition metal, such as platinum or ruthenium, on a solid acid support, like a zeolite.
The direct production of ethylene glycol from lignocellulose, with a catalytic system made of tungsten carbide on activated carbon, and with nickel as a promoter, is another example of bi-functional reaction.

In oxidative conditions, it is possible to mention the direct synthesis of gluconic acid in the presence of oxygen, that is an intermediate for the food and pharmaceutical industry; in this process, catalysts based on nano-gold or platinum-bismuth supported on carbon are used[75].

1.4 Monosaccharides & Rare Sugars

Monosaccharides or sugars, as described in previous paragraphs, represent the base units of the most abundant bio-polymers on Earth: carbohydrates. The term carbohydrate derives from the initial studies that were conducted on these molecules, which wrongly attributed the same number of carbon atoms and water molecules, with general formula $(C_n(H_2O)_n)$. Recent studies have demonstrated the absence of water molecules in carbohydrates structure, thus defining more correctly these molecules as polyhydroxyaldehydes and polyhydroxyketones[76, 77].
Carbohydrates represent important constituents for organisms and play fundamental biological functions: metabolic energy sources, elements of cell structures, regulators of the gene expression and recognition sites on the cell surface.

Monosaccharides are distinguished in aldoses and ketoses according to the nature of the carbonyl group; moreover, they are also classified in function of the number of carbon atoms, that can be between 3 and 9.

From a configurational point of view, sugars are divided into D series and L series, depending on the conformation of the farther asymmetric carbon from the carbonyl group (Fischer projection)[77]. To indicate the rotation of polarized light, it is used the symbology + or -, that stands for rotation of the light to the right and rotation of the light to the left respectively, as shown in Figure 1.16.

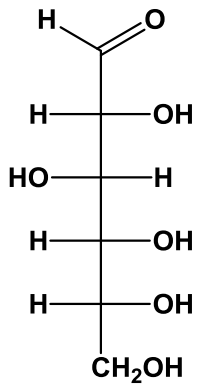

Figure 1.16 Fischer projection for D-(+)-Glucose.

Besides the essential biological functions mentioned above, monosaccharides also represent an important industrial resources. In fact, besides classical uses in food and cosmetic fields, sugars raised a great interest in the pharmaceutical field and especially as intermediates for the production of bio-building blocks and bio-fuels, as described in paragraph 1.1[2, 4, 78, 79, 80].

For these reasons, the supply of monosaccharides for the development of industrial processes is becoming an increasingly important aspect.

The only source of these molecules is represented by carbohydrates synthesized in nature, that are mainly found in plants and vegetal organisms; from these raw

materials it is possible to isolate the desired sugars by means of separation and extraction processes, like the hydrolysis of lignocellulose, widely discussed in paragraph 1.3.

The amount of monosaccharides obtainable from natural resources is closely dependent on the composition of the feedstock: in fact, in addition to the most common sugars like glucose and xylose (which can be obtained in large amounts) there is a group of monosaccharides, called rare sugars, such as mannose, galactose, ribose, whose achievable quantity is very low[78].

Rare sugars show very interesting properties and possible uses: as sweeteners in place of common sugars (glucose and sucrose) thanks to their low calories, marginal alteration of sugar level in blood and anticaries effects; but also for the production of new type of drugs, like antitumorals; as chemical intermediates and monomers for the synthesis of bio-polymers and bio-fuels, after hydrogenation to sugar alcohols. However, their amounts are generally too small to make their separation or extraction from natural source economically sustainable.

Therefore, the only possible alternative to obtain these monosaccharides is to synthesize them from more abundant sugars, like glucose, by structural rearrangement reactions, such as isomerization and epimerization[81].

At present, the employment of bio-catalysts and enzymes represents the most used option for the production of rare sugars: bio-systems reproduce the transformation of sugars that occur in organisms, but these processes show several issues, that are already discussed in paragraph 1.3.6 for the enzymatic hydrolysis of lignocellulose.

For this reason, the development of catalytic systems that are less expensive and more functional in the production of rare sugars, represents nowadays one of the most challenging discussed research topics.

1.4.1 Glucose

Glucose is the most abundant monosaccharide in nature, it is soluble in water but slightly soluble in common organic solvents. It is possible to find it in its single form in a variety of fruits and organic liquids or, in its combined form, in natural oligomers and polymers as energy reserve, in animals as glycogen, and in vegetal as cellulose and starch.

From a chemical point of view, glucose is an aldose monosaccharide with six atoms of carbon and it exists in both enantiomeric configurations, even if D-glucose is the more common conformation, as reported in Figure 1.17[76].

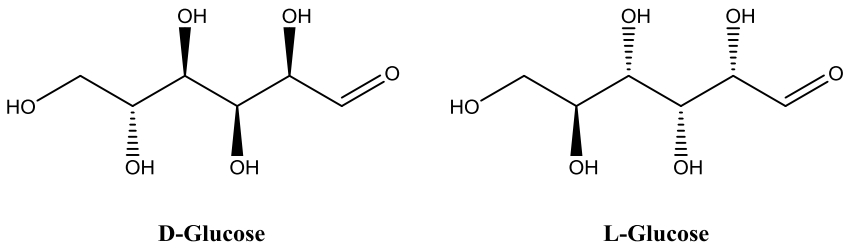

Figure 1.17 D-Glucose and L-Glucose structure.

In water, glucose undergoes cyclization reaction via condensation between the carbonyl group and a hydroxyl group, that results in a pyranose cycle with a new stereogenic center, that is defined anomeric carbon.

In aqueous solution glucose is in equilibrium between its linear form and the two cyclic forms, that differ each other for the configuration of the anomeric carbon: α conformation with hydroxyl group in axial position, and β conformation with hydroxyl group in equatorial position, as shown in Figure 1.18[82].

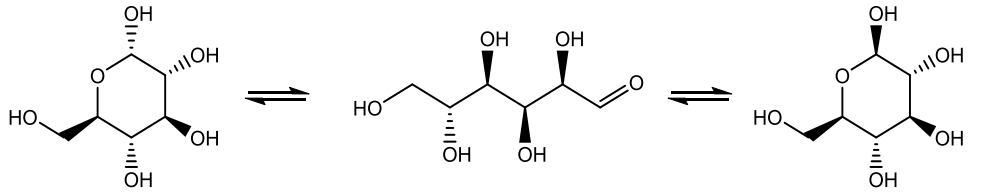

Figure 1.18 Equilibrium forms of D-glucose in water and relative percentages at pH = 7.

Glucose, as previously mentioned, presents several industrial uses in confectionary, pharmaceutical and textile fields; moreover, it is also employed as a substrate in fermentative processes for the production of alcohols or for the synthesis of enzymes, and as intermediate for the production of bio-polymers, bio-fuels and bio-building blocks.

Glucose is a polyfunctional molecule, with both hydroxyl and carbonyl functions in its structure; thanks to these different functionalities, glucose is a highly reactive molecule in reduction, oxidation and esterification reactions, that lead to important products with high added value.

Simultaneously to these reactions, glucose, in particular conditions, can also be subjected to structural rearrangement that are fundamental for the synthesis of rare sugars[78]. These reactions, conducted with enzymes, allow to obtain high yields and selectivity in rearrangement products: the process proposed by Muntz et al.[83], through the use of reducing agents and sorbitol dehydrogenase, permits to obtain a yield of 90% in fructose starting from glucose. However, the industrial scale up of processes based on this type of catalysis is made very difficult by the high cost and the low strength and flexibility of enzymes.

Structural rearrangement of glucose conducted via chemical processes, both in acid and basic conditions, present comparable issues, caused by the high reactivity of glucose: in the presence of mineral acids or bases, at the temperature needed for the transformation, glucose may undergo irreversible degradation reactions. Therefore, in the last years the research has been focused

on the development of acid solid systems, which combine mild acidic peculiarities necessary to promote the rearrangement reactions and prevent the degradation, with the typical advantages of heterogeneous catalysis.

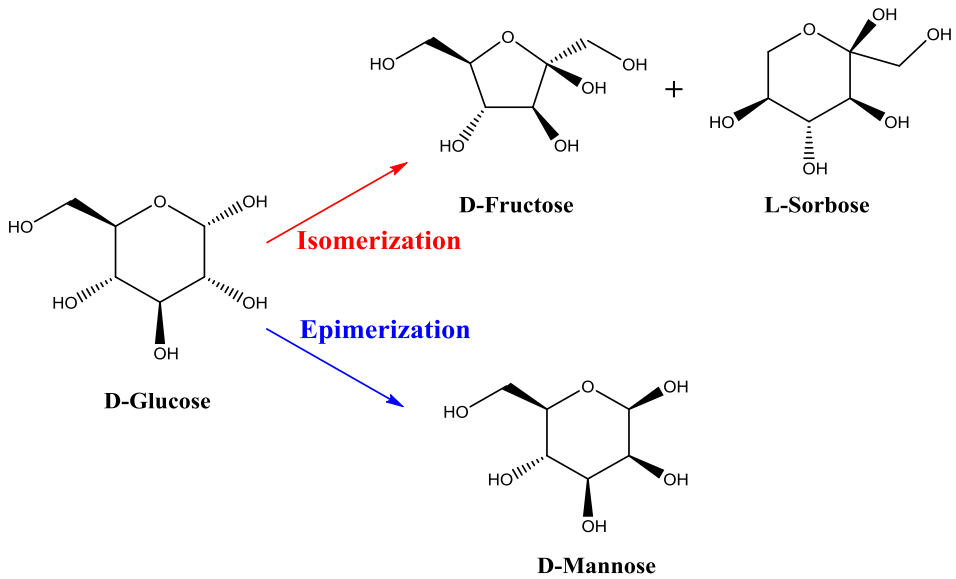

Figure 1.19 Schematic representation of D-glucose structural rearrangement in acid conditions.

The use of these acid solid catalysts allows to obtain the products of structural rearrangement; in particular, as summarized in Figure 1.19, D-fructose and L-sorbose via isomerization, and D-mannose via epimerization[78, 81, 84, 85].

1.4.2 Isomerization of glucose: Fructose & Sorbose

Fructose and sorbose are two structural isomers of glucose, in other words these two monosaccharides have the same chemical formula of glucose but a different molecular structure[77].

Fructose is a monosaccharide with six carbon atoms, but unlike glucose which is its constitutional isomer, it presents a ketone carbonyl group and a furanose

cycle made by 5 terms. This is the result of a different cyclization reaction, that involves the hydroxyl group and the ketone function, as represented in Figure 1.20. Moreover fructose is a levorotatory sugar[76].

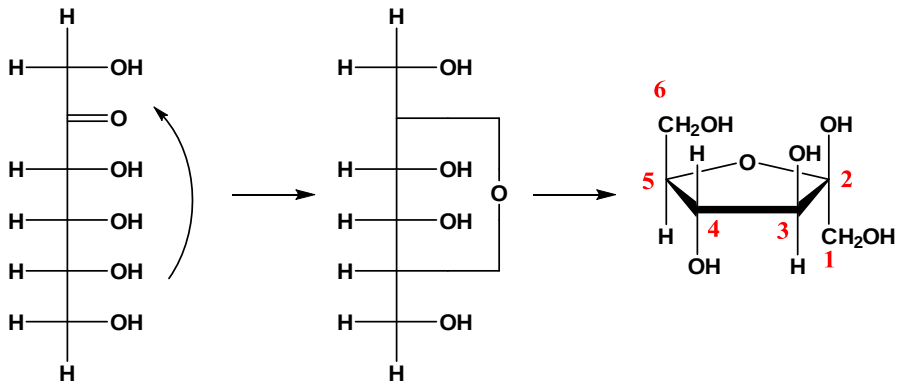

Figure 1.20 Cyclization reaction of fructose.

Also for fructose the D conformation is the most common, and the cyclization leads to the formation of an anomeric center on the C2 that results in two possible anomers, α and β, in function of the position of the hydroxyl group: β-D-fructose is the most common form in nature, thanks to its higher stability.

D-(-)-fructose is present in its single form in many fruits, and in its combined form in oligomers, such as sucrose, a dimer formed by condensation with glucose. Therefore, it is possible to obtain it in large amounts by direct extraction or by enzymatic hydrolysis of starch, with consequent isomerization of the formed glucose with xylose ketoisomerase[78, 81].

Industrially fructose is widely used in food field, like in Maillard reaction for the production of particular flavor by reaction with molecules having the amino moiety at 140°C[86]. Moreover, fructose can undergo fermentative processes for the production of ethanol, or, as described in 1.3.1 paragraph, dehydrated for the synthesis of bio-building blocks.

Sorbose is a monosaccharide with six carbon atoms and, like fructose, which is epimer at C5, is a ketose sugar. The prevalent conformation in nature is L-sorbose and, from its cyclization, a six terms cycle is obtained[76].

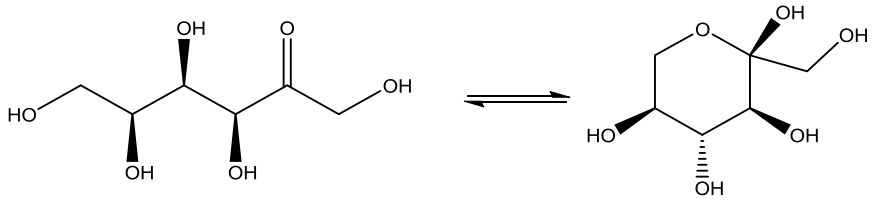

Figure 1.21 Linear and cyclic structure for L-sorbose.

The name sorbose derives from sorb fruit, from which it is obtained through fermentation. At present, sorbose is produced industrially by enzymatic process from glucose, and it represents an important intermediate for the synthesis of ascorbic acid (vitamin C)[85].

The first studies on the isomerization reaction of glucose have been conducted in 1885 by Lobry de Bruyn, Alberda and Van Ekenstein. These studies demonstrated the ability of glucose to do structural rearrangement reaction without the breaking of C-C bonds in the main chain, in the presence of a strong base, as sodium or calcium hydroxide, at room temperature[81].
The mechanism for this transformation, that has been proposed recently by Carraher et al.[87], is based on four steps, as summarized in Figure 1.22: ionization of the cyclic glucose, to give an equilibrium between linear and cyclic anionic form of glucose; loss of an hydrogen atom from C2, with the formation of 1,2-ene-diol intermediate; rearrangement to the anionic acyclic form of fructose; protonation by water, with the formation of fructose.

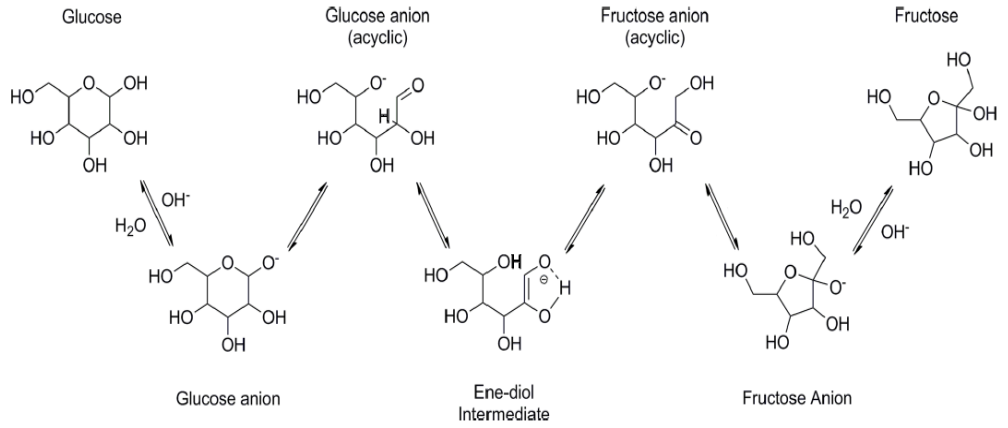

Figure 1.22 Proposed mechanism for glucose-fructose isomerization in basic conditions.

In alkaline conditions, fructose is the main product of this reaction, even if its selectivity decreases with the conversion of glucose, because of the presence of side reactions, such as retro-aldol fragmentation and 1,2-ene-diol isomerization. To increase fructose selectivity in alkaline conditions, the addition of borates and aluminates, or the use of organic base, such as triethylamine, have shown important improvements.

Acid systems with Lewis-type peculiarities, proved to be an attractive alternative to the bases. In fact, the use of solid Lewis acids permits to catalyze isomerization of glucose, with a good selectivity to desired products. These systems, such as supported metal catalysts, allowed the typical advantages of heterogeneous catalysis, which have been discussed in paragraph 1.3.4[85, 88, 89].
As reported by Moliner et al.[90], with a Sn-β zeolite, the reaction mechanism is quite different from that one described in the presence of bases.

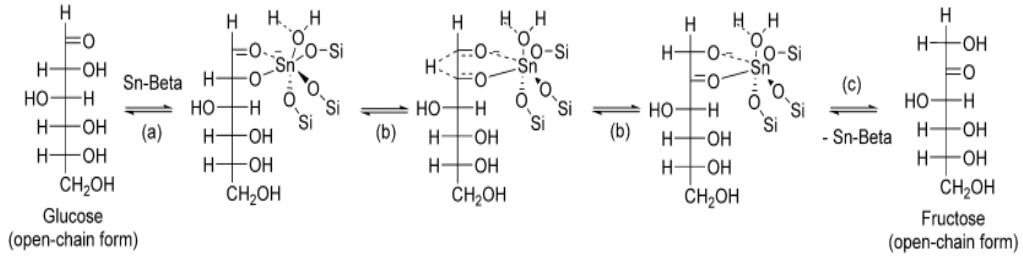

Figure 1.23 Proposed mechanism for glucose-fructose isomerization with Lewis acid systems[90].

Lewis acids coordinate glucose in a bidentate mode, as represented in Figure 1.23: the bond with glucose occurs on the oxygen atom of the aldehydic function (C1) and on another oxygen of glucose hydroxyl groups, in general on C2; the subsequent intramolecular C2-C1 shift of the thus formed hydride, leads to the formation and desorption of fructose.

The use of Lewis acid systems in glucose isomerization, also allowed to obtain synthetic sorbose; in fact, when the bidentate coordination of glucose occurs on the aldehydic C1 oxygen and the hydroxyl group on C5, intramolecular C5-C1 shift of the formed hydride takes place, followed by a rotation of 180° for the desorption of sorbose, as summarized in Figure 1.24[81, 91].

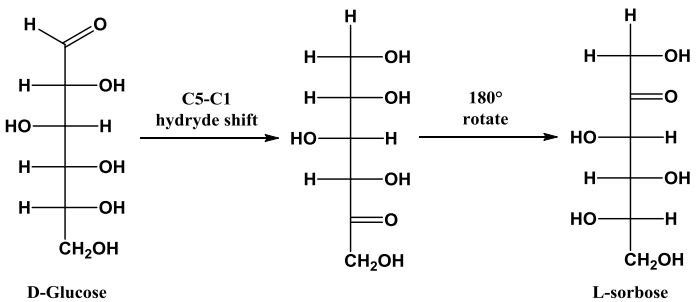

Figure 1.24 Simplified mechanism for glucose-sorbose isomerization with Lewis acid systems.

1.4.3 Epimerization of glucose: Mannose

Mannose is an epimer of glucose, which presents the same chemical formula of glucose, but differs from it for the configuration of only one stereocenter, that is the C2: on this carbon atom, the hydroxyl group is in axial position, compared to equatorial position in glucose, as represented in Figure 1.25[77].

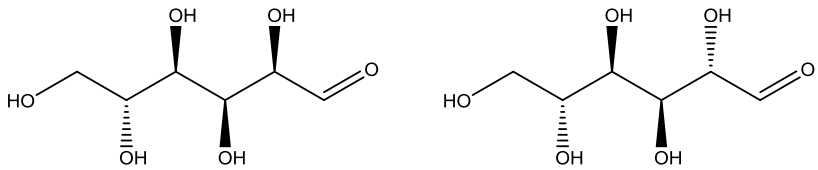

Figure 1.25 Comparison between D-glucose and D-mannose.

Mannose is a monosaccharide with six carbon atoms and it is an aldose: the most abundant configuration is D-mannose.

It is found in its single form in few quantities, in some fruits. For this reason it is considered a rare sugar; while, in its combined form, it is present in many polysaccharides: it is one of the component of hemicellulose in lignocellulose, and also it can be combined with galactose to form galactomannans, natural polymers industrially used as thickeners[76, 78].

Mannose is present in glycoproteins, and represents one of the key messengers of the cell membrane in the glycosylation process; thanks to these molecules, the cell is able to exchange vital information with the surrounding extra-cellular environment. Mannose is used in food industry, pharmaceuticals, for production of antiviral and anti-inflammatory drugs, and for the synthesis of bio-building blocks.

At present, mannose is obtained in commercial amounts through enzymatic synthesis: the Takasaki and Ohya process[92] uses mannose-isomerase from D-

fructose. Otherwise, it is also possible to extract it from its natural sources: Zhang at al.[93] proposed the use of sulfuric acid to degrade mannans. These processes, as widely described in previous paragraphs, present several issues, due to costs, operating conditions and environmental aspects.

Therefore, synthesis of mannose by glucose epimerization appears to be an attractive alternative to obtain this important rare sugar in appreciable amounts.
The studies conducted on this type of reaction, have demonstrated that epimerization can be catalyzed both with bases and with Lewis acid systems.

The mechanism of epimerization was exhaustively described in 1972 by Bilik[94], and subsequently confirmed by experimental tests. He studied the epimerization of glucose in homogeneous catalysis with molybdic acid: a mixture of the two epimers in thermodynamic equilibrium is obtained, with a molar ratio between mannose and glucose equal to 28:72.
According to the Bilik mechanism, epimerization occurs through three steps, as summarized in Figure 1.26. Initially glucose forms a bidentate coordination complex with catalytic center, in this case MoO_4^{2-} ion, on C2 and C3 of glucose; that results in a rigid structure, which maintains atoms in the final conformation, while a stereospecific 1,2-shift occurs through the breaking of the C3-C2 bond and the formation of new C3-C1 linkage that results in a position change between C1 and C2 and the formation of a new C2 with a reversed configuration. Finally, mannose desorbs from the catalyst.

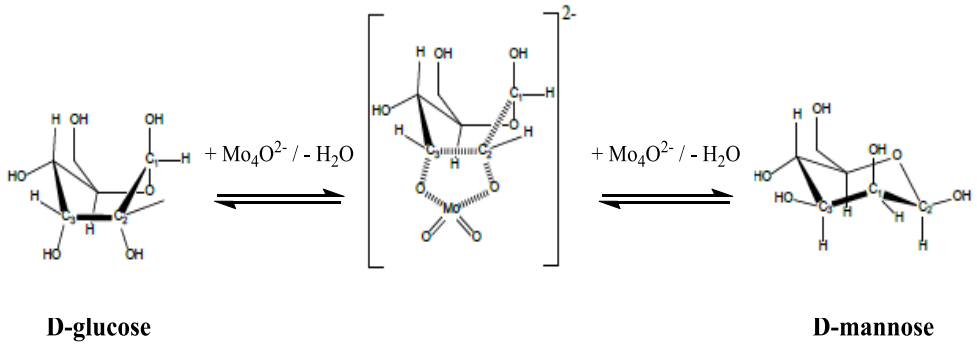

Figure 1.26 Simplified Bilik mechanism for glucose-mannose epimerization with molybdic acid[94].

Using a base catalyst, such as calcium hydroxide proposed by Kusin[95], or nickel complexes formed with ammines described by Yoshikawa[96], the epimerization of glucose takes place in the same way as that one described by Bilik; but, in these cases, formation of fructose as a by-product is also reported.

In 2012, the studies conducted by Gunther et al.[89], introduced heterogeneous catalysis as an option for the epimerization of glucose. He demonstrated that Sn-β zeolite systems, in the presence of borates, are able to synthesize mannose with high selectivity: borates form complexes with glucose that prevent the isomerization, and the consequent formation of fructose; then, epimerization proceeds via a rearrangement of the carbon skeleton similar to that one described by Bilik.

Therefore, the opportunity for the use of heterogeneous catalysis in epimerization reaction, with its advantages compared to homogeneous catalysis, represents nowadays a very important research topic, with an increasingly higher number of conducted studies.

1.4.4 Heterogeneous catalysis: Titanium-silicalite

As mentioned above, the applications of rare sugars, combined with their little amount available in nature, has led to the need of synthesizing these important monosaccharides. Extractive processes and enzymatic synthesis are not competitive due to the several issues that have been described in previous paragraphs.

For this reason, heterogeneous catalysis appears to be the most suitable route for the production of rare sugars by isomerization and epimerization of glucose. In the last years, in fact, research and development of Lewis acid solid systems for these reactions have grown, focusing on different materials and solutions.

Titanium, as known, is an interesting element for the promotion of the structural rearrangement of glucose, thanks to its Lewis acid peculiarities[78, 81]; in fact, in literature, titanium supported on acid systems, such as zeolite, are proposed as catalysts for this reaction[91, 97].

A particular class of solid materials containing titanium, whose catalytic properties are well known for other processes, can be also used for promoting isomerization and epimerization of glucose.

Titanium-silicalite, referred to as TS-1[98, 99, 100], is a synthetic zeolite obtained by incorporation of Ti in the silicalite, that is a polymorph of silica: more precisely, this material is achieved by substitution of Si atoms with Ti atoms in the structure of a dealuminated zeolite In this way, the material presents the resistance and hydrophobicity typical of zeolites, but the absence of H^+ protons, necessary to compensate electronics vacancies generated by the Al atoms in classical zeolites, prevents the formation of a Brønsted acidity, that is detrimental for selectivity in the structural rearrangement of glucose, because it favors degradation of monosaccharides.

TS-1 presents a zeolitic structure with MFI type morphology: atoms of the crystal form a 3-D structure where the elementary units are represented by tetrahedral SiO_4 arranged in pentasilic chains; each term in the pentasil is made in turn by 5 ring terms. The adjacent pentasilic units interconnected with oxygen bridges, to form a lamellar structure corrugated to 10 channels, with dimensions 5,1-5,6 Å, as represented in Figure 1.27[101], [102].

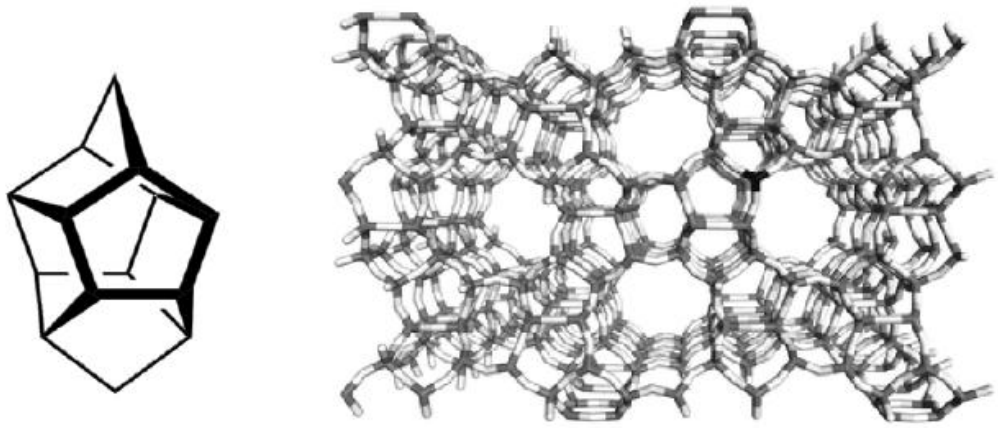

Figure 1.27 Pentasilic units and 3-D modelling structure of TS-1.

Fundamental for the chemical properties of TS-1, is the distribution of Ti species in the crystalline structure. In TS-1, Ti(IV) species are typically distributed in anisotropic mode inside tetrahedral cavities of the crystal, thus replacing SiO_4 units; this incorporation results in an increase of the tetrahedral units volume, due to the higher length of Ti-O-Ti bond respect to Si-O-Si.

Titanium distributed in this way and with this coordination is defined as "framework Ti"; it is also possible to note that the amount of Ti incorporated in TS-1 is proportional to the increase of the tetrahedral units volume. This effect is maintained up to the 3% wt of incorporated Ti, expressed as TiO_2[99, 100].

Further additions of Ti in TS-1 results in the formation of distributed species with a different nature compared to framework tetrahedral Ti: in particular, the

excess of Ti arranges mainly on the surface and in the pore system of TS-1, rather than in the tetrahedral positions of the crystal. This type of Ti is called "bulk Ti", and is made of colloidal aggregates of TiO_2 nanoparticles, with the anatase structure, having the symmetry of the orthorhombic cell.
In TS-1, it is also possible to find a third species of Ti, called "amorphous Ti"; this species is distributed in the crystalline structure of TS-1, but its chemical nature is a very debated issue in literature: in some cases it is supposed to form species that present a octahedral coordination; instead, in other cases, it forms of polymers aggregates $[TiO_x]_n$ with a higher coordination than tetrahedral[103].

The different Ti species that can be present in TS-1 influence the catalytic performance of these materials.
Their nature and relative amount, are closely related to the synthesis method used; therefore, the control of the various synthetic steps is fundamental in order to achieve a material with the proper catalytic activity.
The first recipe for the synthesis of TS-1 was proposed by Taramasso et al.[98] in 1983; in this method, the fundamental components for the production of TS-1 are: tetraethylorthotitanate (TEOT) or tetrabutylorthotitanate (TBOT) as the source for titanium, tetraethyl silicate as the source of SiO_2, and tetrapropylammonium hydroxide (TPAOH) as templating agent for the development of the MFI type structure. This synthesis is carried out under hydrothermal conditions at 130°C, and requires very long reaction time: up to 30 days to obtain a crystalline precursor that, after calcination at 550°C, results in the desired TS-1 material.
An alternative method has been proposed by Vasile and Tomoiaga in 2012[104]; this permits to obtain a TS-1 material with a crystalline structure and a distribution of Ti species comparable to those of the TS-1 synthesized by Taramasso, but using cheaper and easily available reactants. These are: tetrapropylammonium bromide (TPABr) as templating agent that, besides being less expensive, does not present alkali metals, which can compromise the

success of TS-1 synthesis, an aqueous solution of tetrabutylorthotitanate (TBOT) as titanium source, and fumed silica as SiO_2 source. As described for the previous method, the synthesis is realized in hydrothermal conditions at 170°C for 24 days; the material thus obtained is then calcined at 550°C, to develop the desired TS-1 catalyst.

Thanks to its peculiar structure and composition, TS-1 has been employed as catalyst in selective oxidation processes[105, 106]: hydroxylation of alkanes or aromatics and epoxidation of olefins are successful examples. In fact, TS-1 is able to activate H_2O_2, allowing to operate at lower temperature and to obtain the desired products with higher selectivity compared to classic catalysts. However, until now, its use as catalyst in the aqueous phase glucose isomerization and epimerization yet has not been studied. Indeed, it is known that Ti^{4+} ions can show Lewis acid properties.

2. Materials and Methods

In this Chapter, the preparation methods and the techniques used to characterize the catalytic systems are described. Moreover, the operating conditions used for reactivity experiments, and the methods used to analyze the reaction mixtures are outlined.

2.1 Preparation of catalytic systems

The description of the synthesis procedure adopted for catalysts preparation (or in some cases of the supplier, when commercially available samples were used) has been divided according to the type of reaction performed.

2.1.1 Catalytic systems for lignocellulose hydrolysis

Zirconium phosphate (Zr/P/Osynt)

Zr/P/Osynt has been synthesized by precipitation, according to the method reported by Kamiya et al[107]. In a typical preparation, 64 ml of 1M solution of $NH_4H_2PO_4$ are added slowly to 32 ml of 1M solution of $ZrOCl_2 \cdot 8H_2O$, under continuous stirring: a white precipitate, with P/Zr molar ratio = 2 is obtained. Then, the precipitate is filtered, washed with water and dried at 120°C; finally, it is calcined at 400°C for 3 hours, with 10°C/min heating rate.

Commercial Niobium phosphate (Nb/P/Ocomm)

Nb/P/Ocomm system has been provided by the Brazilian company CBMM. Before use, the catalyst has been calcined at 400°C for 3 hours, with 10°C/min heating rate.

Synthesized Niobium phosphate (Nb/P/Osynt)

Nb/P/Osynt has been prepared by precipitation, according to the method reported by Mal and Fujiwara[108]. In a typical synthesis, 50 ml of 0.4M solution of H_3PO_4 are added slowly to 50 ml of 0.2M solution of $NbCl_5$, and the mixture is continuously stirred for 30 minutes; then, 25% aqueous ammonia solution is added until pH 2.6, and a white precipitate is obtained. The resulting precipitate is filtered, washed several times with water and combined with 10 ml of a 0.6M solution of hexadecylamine, in a Teflon beaker; the mixture is continuously stirred for 30 minutes; then, a H_3PO_4 solution is added until pH 3.9. The resulting gel is heated in a Teflon autoclave at 65°C for 2 days in autogenous pressure; finally, the product is filtered, washed with water, dried at 120°C, and calcined at 400°C for 3 hours, with 10°C/min speed.

2.1.2 Catalytic systems for rare sugars synthesis

Titanium oxide grafted on silica (TOS)

Five catalysts, which differ in the nominal titanium loading (0.5%, 1%, 2%, 4% and 8%), based on titanium oxide (TiO_2) grafted on silica, have been prepared according to the method described by Hamilton et al.[109]: as titanium precursor, Ti(IV) tetrabutoxide was used, instead of the prescribed Ti(IV) isopropoxide.
In a typical synthesis, commercial silica support (Grace DAVICAT SI-1301) is dried at 130°C for 16 hours; 5 g of dried silica is dispersed in 150 ml of isopropanol, then a 1:4 weight mixture of Ti(IV) tetrabutoxide:isopropanol is added under continuously stirring for 2 hours. The amount of Ti(IV) tetrabutoxide, used is a function of the desired final titanium loading. The resulting system is filtered, washed several times with isopropanol and dried at

80°C for 2 hours; finally, it is calcined at 200°C for 2 hours, with 0.5°C/min heating rate, and then at 550°C for 2 hours, with 1.5°C/min heating rate.

Titanium silicalite (TS-1)

The three TS-1 catalysts studied were provided by an external company; therefore, the method of synthesis for these systems is not known. It can be assumed that they were synthesized following the classical method described in paragraph 1.4.4, but varying some parameters during the synthesis, finally resulting in materials with different properties.

2.2 Characterization Techniques

The description of the techniques used to characterize catalysts is divided in function of the physical-chemical property investigated.

2.2.1 Structural properties

Specific surface area (BET)

The specific surface area of catalysts was determined using the Brunauer-Emmet-Teller model of multi-layer physical adsorption in single point (simplified as BET model).

This model is applied by means of the instrument *Carlo Erba Sorpty 1700*. In a typical analysis, 0.5 g of catalyst are loaded in the sample holder, and heated up to 150°C under vacuum, in order to desorb water molecules and impurities adsorbed on catalyst surface; after this pretreatment, the catalyst is thermostated in a bath of liquid nitrogen, at -196°C, and a flow of gaseous nitrogen is adsorbed on the surface and in the pores of the solid sample. The instrument measures the volume of adsorbed nitrogen and, using the equation of BET model, provides the value of specific surface area.

X-ray diffraction(XRD)

X-ray diffraction allows to obtain information about crystalline properties of the catalysts, such as nature of the crystalline phase, crystal size and possible distortions of the lattice. The instrument used for XRD analysis is a vertical goniometric diffractometer *Philips PW 1050/81* with a *PW 1710* chain counting, and the powder method has been chosen to collect diffraction patterns. The CuKα radiation, made monochromatic thanks to the use of a nickel filter with λ of 0.15418 nm, is used for analysis; the acquisition band is $5° < 2\theta < 80°$, with steps of 0.1° and count of intensity every 2 seconds.

Attenuated total reflectance IR-spectroscopy (ATR-IR)

ATR spectroscopy is a IR technique used to collect information about binding force and molecular geometry of the catalyst; this method is based on attenuated total internal reflectance phenomena of IR radiation, which is transmitted through a high refractive index material placed closely to the sample. *Brucker Alpha Platinum* IR spectrometer is used for these analysis, and no pretreatment of the sample is necessary.

2.2.2 Composition

X-ray fluorescence (XRF)

X-ray fluorescence permits to obtain information about the amount of each element in catalysts. *PANalytical Axios Andvanced* dispersive wavelength spectrometer is used for analysis; this instrument is equipped with rhodium tube of 4 kW power, and usually uses radiation in the KeV order, that involves exclusively the core electrons.

Diffusive reflectance UV-spectroscopy (DR-UV)

DR-UV spectroscopy measures the reflected fraction of the analytical radiation, which just results attenuated after the interaction with the sample; this technique, which is complementary to molecular adsorption spectroscopy, allows to determinate the different chemical species of an element (oxidation state, coordination). *Perkin Elmer Lambda 19* spectrometer, equipped with a calcium sulfate integrating sphere, is used for analysis; the band of analysis is 190 nm < λ < 450 nm, and no pretreatment of the sample is necessary.

Thermogravimetry (TGA)

TG analysis permits to quantify the weight loss of the spent catalysts (systems recovered at the end of the reaction), as a function of the temperature. *Perkin Elmer TGA7* instrument is used for the tests; in a typical analysis 0.01 g of sample are loaded and 100 ml/min of air continuously fed; then, the sample is heated up to 400°C with a ramp of 5°C/min and maintained at this temperature for 20 minutes.

2.2.3 Surface properties

Temperature programmed desorption (TPD)

By means of ammonia as the probe molecule, temperature programmed desorption permits to determine the total acid sites concentration of catalysts, and, in function of the desorption temperature, also the strength of these sites. The instrument used for these analysis is a *Micromeritics Autochem 2*. In a typical analysis, 0.1 g of sample are pretreated at 400°C in a flow of helium, in order to desorb water molecules and impurities; then, at 100°C in a flow of 10% NH_3 in helium, ammonia is adsorbed on the sample until saturation. Finally,

sample is heated up to 650°C for 30 minutes, with a ramp of 10°C/min, and the desorbed ammonia is measured by TCD detector and quadrupole MS.

Fourier transform IR-spectroscopy analysis (FT-IR)

From FT-IR analysis, by means of adsorption and desorption of pyridine as probe molecule, it is possible to discriminate the different acid character of the catalytic acid sites: especially, this technique allows to quantify Lewis and Brønsted acid sites. *Perkin Elmer Spectrum One* spectrometer, equipped with silicon carbide (SIC) cylinder as source of analytical radiation, a KBr beam splitter and a detector of doped triglycine sulfate (DTGS), is employed for the measurements. In a typical analysis, a thin film-shaped catalyst, obtained by pressing the powder at 10 ton/cm^2, is positioned inside a cell equipped with KBr windows; then, it is pretreated under vacuum (10^{-6} mbar) up to 500°C, with steps of 100°C for 30 minutes. Thereafter, at room temperature and under vacuum, pyridine is adsorbed on the sample, until saturation. Finally, the sample is heated, still under vacuum, up to 400°C, and at the same time IR spectra are recorded, in steps of 100°C.
In order to reproduce the aqueous reaction medium, the FT-IR analysis of the catalysts were also conducted with the co-adsorption of water and pyridine; the procedure is the same described above: in particular, after the pretreatment step, water and pyridine are adsorbed on the sample.

Gas-phase dehydration of ethanol

The dehydration of ethanol in the gas-phase, used as a model reaction, permits to investigate the acid properties of the catalytic systems.
The reaction is carried out in a fixed bed reactor (30 cm diameter), loaded with 0.4 g of pellet-shaped catalyst (0.3-0.6 mm size range), and fed with a continuous flow of 15.6% V/V gaseous ethanol in nitrogen, in order to maintain

a contact time of 0.4 second; in these conditions, the reaction is conducted at 250°C for 110 minutes.

Agilent 3000A micro-GC, equipped with an Agilent Plot Q column (stationary phase polystyrene-divinylbenzene) and an AgilentOV1 column (stationary phase 100% dimethylpolysiloxane), is used for the analysis of the outlet gaseous flow from the reactor.

2.3 Catalytic Tests

The description of the operating procedures and apparatus used to carry out catalytic tests, and the analytical techniques for the determination of products, have been divided according to the type of reaction performed.

2.3.1 Lignocellulose hydrolysis

Hydrolysis of lignocellulose and cellulose substrates have been conducted in a stainless steel autoclave in water, heated at 150°C and stirred at 300 rpm; in these conditions, an autogenous pressure of 4.76 bar develops. A scheme of the apparatus used for reactivity experiments is represented in Figure 2.1.

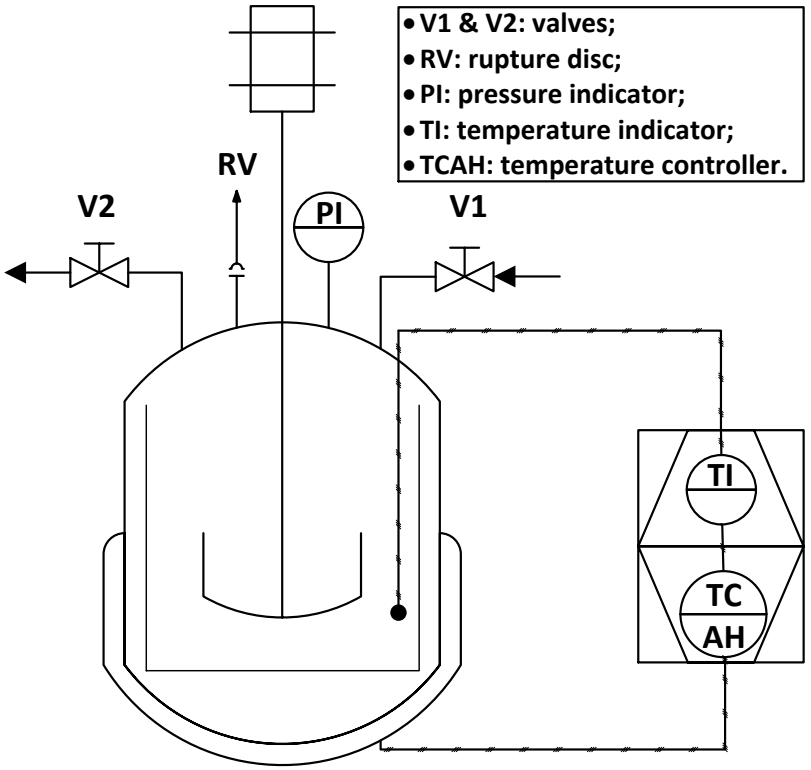

Figure 2.1 Simplified scheme of stainless steel autoclave used for lignocellulose and cellulose hydrolysis.

In a typical test, the biomass and the catalyst are loaded in a glass volume reducer, with a substrate/catalyst weight ratio of 1; then, 50 ml of distilled water are added. The reducer is loaded in the 300 ml stainless autoclave system, which is then sealed, stirred and heated; reaction time is started when the autoclave reaches the desired temperature of 150°C. At the end of reaction time, the heating and the agitation are stopped, and the autoclave is immediately quenched in ice.

After cooling, the autoclave is opened and the glass volume reducer is recovered. The reaction mixture is separated by filtration in a Buchner filter: the volume of the obtained liquid phase is measured, and a fraction is further filtered with a 0.45 µL syringe filter, for HPLC analysis; the solid residue is

recovered, dried overnight at 80°C in oven, and then weighed to determine the conversion of the biomass substrate.

In order to quantify the amount of oligomers produced by hydrolysis of lignocellulose and cellulose, which is not possible to determine directly by HPLC analysis, the procedure described by Sluiter et al.[110] was followed.
The pH and volume of the recovered liquid hydrolysate is measured: according to the recipe reported, the prescribed amount of 96%wt H_2SO_4 is added to the hydrolysate in a glass volume reducer; the reducer is loaded in the 300 ml stainless autoclave system, which is then sealed, stirred and heated at 121°C for 1 hour. At the end of reaction time, the heating and the agitation of the autoclave system are stopped, and the system is immediately quenched in ice.
After cooling, the autoclave system is opened and the glass volume reducer is recovered; $CaCO_3$ is then added to the obtained liquid phase, until a neutral pH is achieved. Finally, the neutralized hydrolysate is filtered in a Buchner filter: the volume of the obtained liquid phase is measured, and a fraction is further filtered with a 0.45 µL syringe filter, for HPLC analysis.
As described by Sluiter et al., a test is conducted on a sample solution, containing a known concentration of glucose and xylose, in the same reported conditions. This test allows to evaluate the degradative effect of H_2SO_4 on monosaccharides contained in the liquid fraction produced by hydrolysis of biomass substrate, and derive the corrective factors for HPLC analysis: only glucose and xylose are considered, because they are the only component of cellulose and the main component of hemicellulose, respectively.

2.3.2 Rare sugars synthesis

Catalytic tests for rare sugars synthesis have been conducted in a glass autoclave in water, heated at 110°C and stirred at 300 rpm; in these conditions, the

autogenous pressure is 1.43 bar. A scheme of the apparatus used for reactivity tests is represented in Figure 2.2.

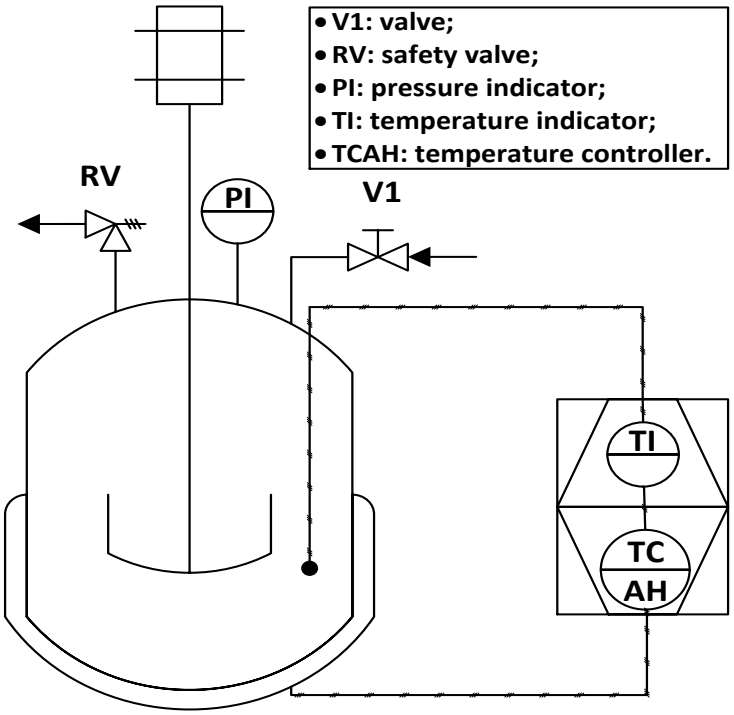

Figure 2.2 Simplified scheme of glass autoclave used for rare sugars synthesis.

In a typical test, monosaccharide (glucose, fructose or sorbose) and catalyst are loaded in a glass vessel autoclave, with a substrate/catalyst weight ratio of 2, and 40 ml of distilled water are added. The autoclave is then sealed, stirred and heated; reaction time is started when the autoclave reaches the desired temperature of 110°C. At the end of the reaction time, the heating and the agitation are stopped, and the autoclave is cooled down.

After cooling, the autoclave is opened and the reaction mixture is separated by filtration in a Buchner filter: the volume of the obtained liquid phase is measured, and a fraction is further filtered with a 0.45 µL syringe filter, for HPLC analysis.

2.3.3 HPLC analysis

Quantitative analysis of reaction products has been carried out by means of high performance liquid chromatography (HPLC); the instrument used is an *Agilent 1260 Infinity Series* HPLC system, equipped with a manual injector with a 20 µl calibrated loop.

Column and detector utilized for analysis depend on the nature of products to be identified:

- for monosaccharides an *Agilent Hi-Plex Pb* column (length = 30 cm, diameter = 7.7, particle size = 8 µm) is used, whose stationary phase is made of a divinylbenzene-styrene copolymer functionalized with Pb^{2+} ions; the column is thermostated at 80°C, and 0.6 ml/min flow of UPP water is the employed eluent. The detection of products occurs by means of a refraction index detector (RID), thermostated at 40°C;
- for degradations products of sugars, such as organic acids and furans, a *Phenomenex Rezex ROA-H* (length = 30 cm, diameter = 7.7, particle size = 8 µm) is used, whose stationary phase is made of a divinylbenzene-styrene copolymer functionalized with H^+ ions; the column is thermostated at 60°C, and 0.6 ml/min flow of 0.0025M H_2SO_4 solution is the employed eluent. The detection of products occurs by means of a UV-diode array detector (UV-DAD), recording absorbance at 253, 205, 192 nm, that at which the greater absorption for the products to be determined occurs.

2.3.4 Expression of results

Catalytic performances obtained in the hydrolysis of lignocellulose are expressed in terms of mass percentage, as reported in the following equations:

- conversion of substrate

$$X_{lignocellulose} = \frac{m_{loaded\ lignocellulose} - m_{residual\ lignocellulose}}{m_{loaded\ lignocellulose}} \cdot 100$$

- yield in monosaccharides and degradative products

$$Y_{product} = \frac{m_{product}}{m_{loaded\ lignocellulose}} \cdot 100$$

- yield in oligomers

$$Y_{cellulose\ oligomers} = \frac{m_{total\ glucose} - m_{hydrolyzate\ glucose}}{m_{loaded\ lignocellulose}} \cdot 100$$

$$Y_{hemicellulose\ oligomers} = \frac{m_{total\ xylose} - m_{hydrolyzate\ xylose}}{m_{loaded\ lignocellulose}} \cdot 100$$

As regards catalytic tests on rare sugars, performances are expressed in terms of molar percentage, normalized in function of carbon atoms number, as summarized in the following equation:

- conversion of substrate

$$X_{substrate} = \frac{(mole_{loaded\ substrate} \cdot n_{C\ atoms}) - (mole_{residual\ substrate} \cdot n_{C\ atoms})}{mole_{loaded\ substrate} \cdot n_{C\ atoms}} \cdot 100$$

- selectivity in monosaccharides and degradative products

$$S_{products} = \frac{mole_{products} \cdot n_{C\ atoms}}{(mole_{loaded\ substrate} \cdot n_{C\ atoms}) - (mole_{residual\ substrate} \cdot n_{C\ atoms})} \cdot 100$$

3. Results and Discussion

In this Chapter, the results of catalysts characterization and of reactivity experiments will be presented; in particular, relationship between results of catalytic tests and physical-chemical properties of catalysts will be searched for and discussed.

3.1 Lignocellulose hydrolysis tests

The study of lignocellulose hydrolysis with heterogeneous catalysis has been conducted focusing on a particular class of acid solid systems: transition metal phosphates.
These heterogeneous systems have been chosen because of their ability to keep strong acidic character even in polar solvents, such as water, at relatively high temperature[111, 112, 113, 114]; furthermore, as reported in literature[115, 116], these systems can be easily recovered from the reaction mixture and regenerated by thermal treatments.

The aim of this study is to investigate on the role of acid sites of different type and strength in promoting lignocellulose and cellulose hydrolysis: more specifically, the influence of Lewis and Brønsted acid features on the distribution of hydrolysis products will be examined, by comparing of conversions and yields obtained by means of tests carried out with the different metal phosphates. For this purpose, as reported in paragraph 2.1.1, both synthesized zirconium phosphate and commercial and synthesized niobium phosphate, have been tested: these two metal phosphates have been selected because of their very different performance various hydrolysis reactions, as reported in several papers[115, 116, 117, 118]. Moreover, these systems present both Lewis and Brønsted acid character: Hattori et al.[119] have attributed weak and

strong Brønsted sites in zirconium phosphate to surface P-OH groups, while, Spielbauer et al.[120], have confirmed the role of Zr^{4+} as Lewis sites. Also for niobium phosphate, Lewis acidity can be attributed to unsaturated Nb^{5+} sites, while, Brønsted sites are surface P-OH groups and, at a lesser amount, Nb-OH groups, as demonstrated by Armaroli et al[121].

Initial studies of hydrolysis were carried out on microcrystalline cellulose, that represents an easier substrate compared to lignocellulose, and which can be used to establish relationship between catalytic performance and physical-chemical properties. Both native and ball-mill pretreated cellulose were used for these catalytic tests, in order to determine the effect of pretreatment on catalytic performances. Then catalytic tests were also carried out on various lignocellulose substrates: at the beginning, we used conifer wood sawdust; then, catalytic tests were conducted on lignocellulose materials with different compositions in terms of cellulose, hemicellulose and lignin content, derived from agricultural waste, in order to estimate the influence of lignocellulose composition on catalytic performance.
Finally, in order to evaluate the actual regenerability of metal phosphates, catalysts tested for lignocellulose hydrolysis were recovered at the end of reaction, and analyzed to determine, both qualitatively and quantitatively, the nature of the insoluble substance deposited on catalyst surface.

3.1.1 Characterization of lignocellulosic substrate

Microcrystalline cellulose used for catalytic tests is a commercial Avicel PH-101, provided by Sigma-Aldrich, that presents a particle size of 50 μm.
This substrate has been employed both native and after a ball-mill pretreatment of 48 hours; *SPEX 8000M* mill, equipped with a tungsten carbide vessel, is used for the mechanical pretreatment.

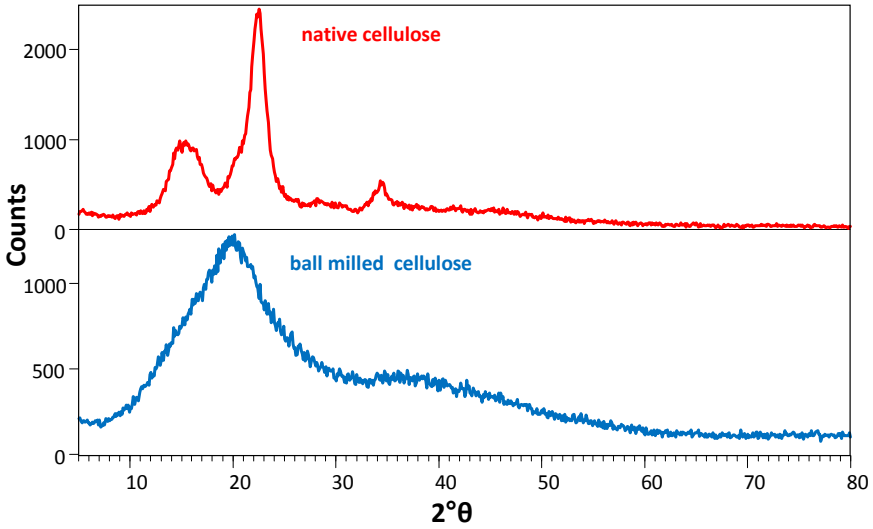

Figure 3.1 Comparison of native and ball-milled cellulose XRD patterns.

As shown in Figure 3.1, the effect of ball-mill pretreatment on commercial cellulose is that one of a drastic reduction of crystallinity, that, as described in paragraph 1.3.5, should result in an easier catalytic hydrolysis of the substrate, with consequent higher conversion and yields to hydrolysis products.

As regards lignocellulose used as substrate in catalytic tests, conifer wood sawdust, which derived from grinding and drying of forestry residues, presents a weight composition that is summarized in Figure 3.2.

Before its use in catalytic tests, conifer wood sawdust has been pretreated in ball-mill, as described for microcrystalline cellulose, for 15 minutes; this treatment is only aimed at comminuting the cellulosic material.

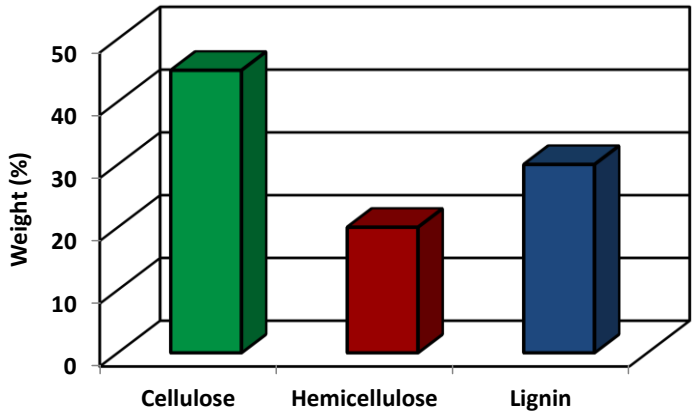

Figure 3.2 Weight percentage composition of conifer wood sawdust: ■ cellulose; ■ hemicellulose; ■ lignin**.**

Agricultural waste lignocellulose substrates, provided by Professors Monti and Zanetti of Agriculture School at Bologna University, derived from grinding and drying residues of six different crops: Jerusalem artichokes, sorghum, miscanthus, hemp, arundo and foxtail milled. The weight composition of these six substrate are shown in Figure 3.3.

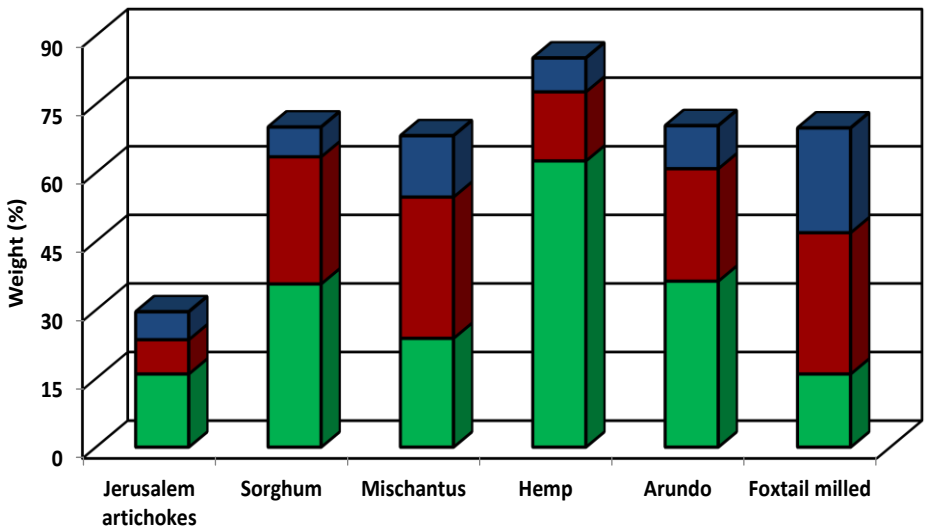

Figure 3.3 Weight percentage composition of Jerusalem artichokes, sorghum, miscanthus, hemp, arundo and foxtail milled. Legend: ■ cellulose; ■ hemicellulose; ■ lignin**.**

As reported for conifer wood sawdust, the substrates have been pretreated in ball-mill for 15 minutes before their use in catalytic tests.

3.1.2 Characterization of hydrolysis catalytic systems

The physical-chemical properties of the three metal phosphates, tested for biomass hydrolysis, i.e., synthesized zirconium phosphate (Zr/P/Osynt), commercial niobium phosphate (Nb/P/Ocomm) and synthesized niobium phosphate (Nb/P/Osynt), have been studied using different techniques: BET, XRD, ATR-IR, XRF, TPD-ammonia, FT-IR with pyridine and water-pyridine, dehydration of ethanol (model reaction).

Specific surface area (BET)

The specific surface areas of the three metal phosphates systems, calcined at 400°C, are reported in Table 3.1.

Catalytic system	BET (m^2/g)
Zr/P/Osynt	108 ± 5
Nb/P/Ocomm	133 ± 5
Nb/P/Osynt	140 ± 5

Table 3.1 Specific surface area for the three tested metal phosphates.

It is possible to observe that the surface areas of niobium phosphates, both commercial and synthesized, are slightly higher compared to that of Zr/P/Osynt; however, it is not expected that such differences will affect remarkably catalytic activity.

X-ray diffraction (XRD)

XRD allows to determine the crystalline phases present in the three catalysts; XRD patterns are shown in Figure 3.4.

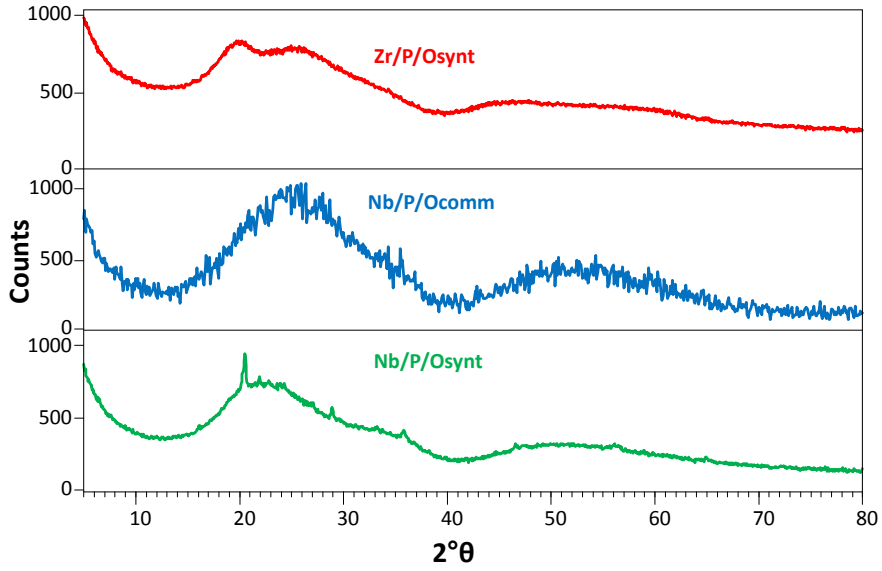

Figure 3.4 Comparison of XRD patterns of the three metal phosphates.

From the XRD patterns, is possible to note that Zr/P/Osynt and Nb/P/Ocomm, show the presence of two broad peaks in the range 10-40° and 40-70°, which are not attributable to any crystalline phase; therefore, these two materials can be considered as amorphous.

As regards Nb/P/Osynt, together with a high percentage of amorphous phase, as seen from diffuse reflections, the pattern shows the presence of weak reflections of a crystalline phase, with the main peak at 20°, which, in literature[122], is attributed to $Nb_{1.9}P_{2.8}O_{12}$.

Attenuated total reflectance IR-spectroscopy (ATR-IR)

ATR-IR spectra permit to obtain information about the molecular geometry; in Figure 3.5, are reported the ATR-IR spectra of catalysts.

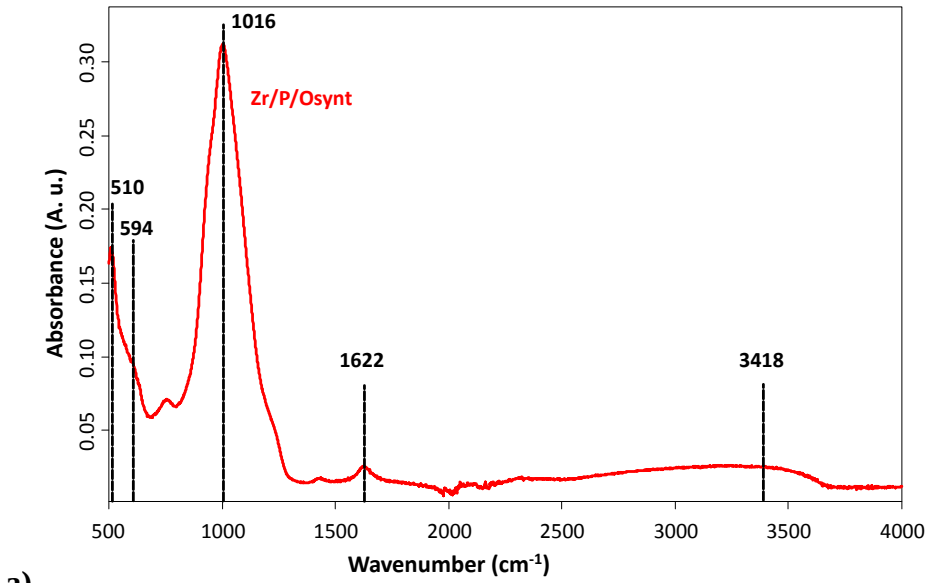

a)

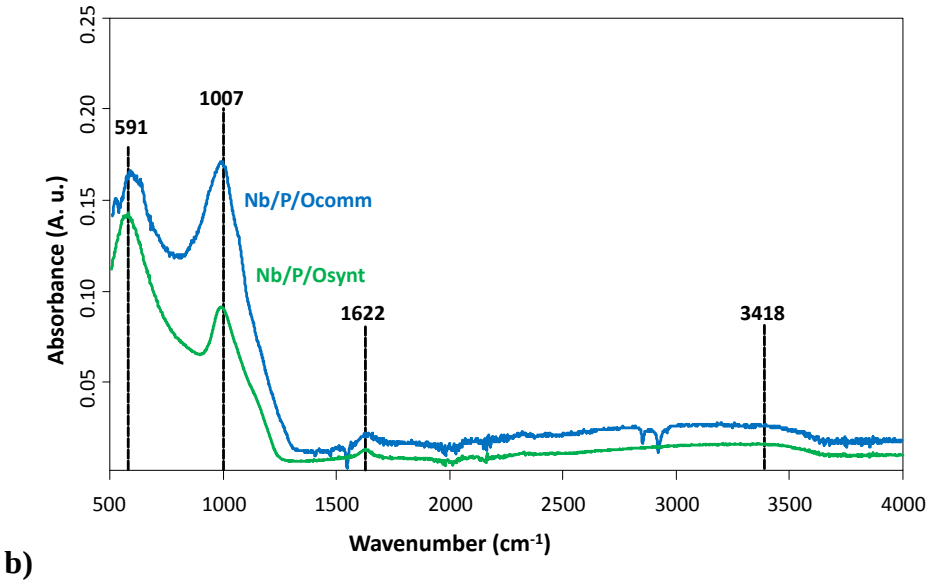

b)

Figure 3.5 ATR-IR spectra for: a) Zr/P/Osynt; b)niobium phosphates.

IR spectra of the three metal phosphates present an intense band, at 1007 cm^{-1} for niobium phosphates and 1016 cm^{-1} for Zr/P/Osynt, respectively, which is attributed to the phosphate structure: in particular it is assigned to the asymmetric stretching of phosphate O=P=O group[123]. Also bands at 1622 cm^{-1} and 3418 cm^{-1} are shown, that are attributed to adsorbed water on the catalyst surface.

Niobium phosphate spectra, both for commercial and synthesized, present another characteristic band at 591 cm^{-1}, which is assigned to the vibration of Nb-O[124]. Zr/P/Osynt spectrum shows two characteristic bands[125]: the first one at 510 cm^{-1}, that is attributed to the asymmetric stretching of Zr-O bond, and the second one at 594 cm^{-1}, due to the bending of P-OH bond.

X-ray fluorescence (XRF)

The phosphorous/metal molar ratio of the three catalysts was determined by means of XRF, and results are reported in Table 3.2.

Catalytic system	P/M (M = Zr, Nb) Molar ratio
Zr/P/Osynt	1.90 ± 0.05
Nb/P/Ocomm	0.35 ± 0.05
Nb/P/Osynt	0.65 ± 0.05

Table 3.2 Phosphorous/metal molar ratio for the three metal phosphates.

The analysis show that the P/Zr molar ratio for Zr/P/Osynt is about 2, which corresponds to the compound $Zr(HPO_4)_2$.

As regards niobium phosphates, the P/Nb ratio for Nb/P/Ocomm is comparable to that one reported by CBMM (0.29); while, for Nb/P/Osynt, the P/Nb molar ratio is closer to the ratio of $NbOPO_4$, which is suggested, in literature, to be the main phase for niobium phosphate[121].

Ammonia-temperature programmed desorption (TPD)

TPD analysis using ammonia as the probe molecule, permits to determine the total acid sites concentration, as reported in Table 3.3.

Catalytic system	Acid sites concentration (mmol/g)
Zr/P/Osynt	0.43 ± 0.05
Nb/P/Ocomm	0.10 ± 0.01
Nb/P/Osynt	0.50 ± 0.05

Table 3.3 Total acid sites concentration for the three metal phosphates.

It is shown that the three metal phosphates show different total acidity: in particular, Nb/P/Osynt, which presents the higher total number of acid sites, is five times more acid then Nb/P/Ocomm; while, Zr/P/Osynt shows a number of acid sites that is comparable to that one of Nb/P/Osynt.

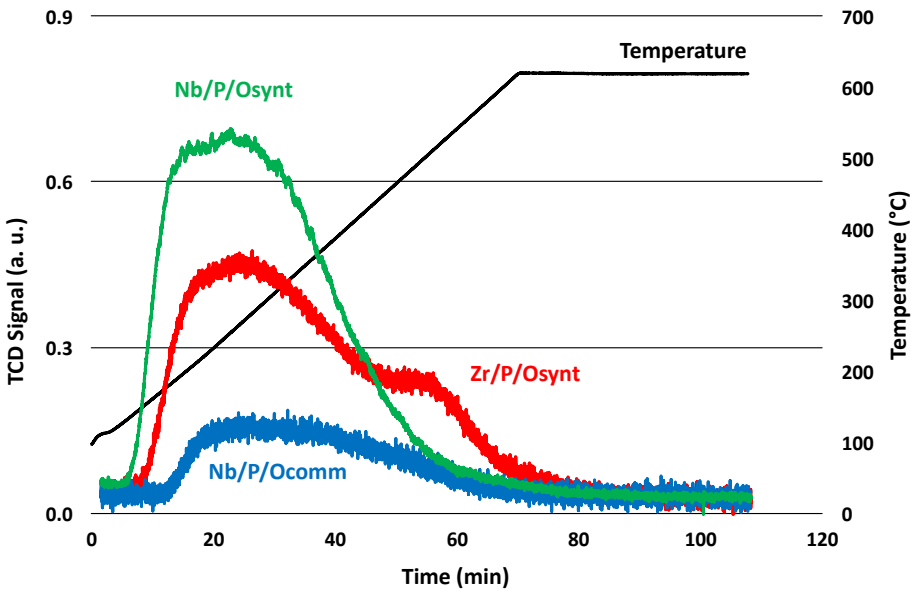

Figure 3.6 TPD-ammonia desorption analysis as function of temperature for the three metal phosphates.

From the ammonia desorption profiles, plotted in function of temperature and shown in Figure 3.6, it is possible to obtain information about the strength of acid sites. Despite the different total acid sites concentration, the desorption profiles of three metal phosphates are similar, and show that catalysts present a main fraction of low-medium acid strength sites, and a smaller fraction of stronger sites, which is more evident for Zr/P/Osynt.

Fourier transform IR-spectroscopy of adsorbed pyridine (FT-IR)

The use of pyridine as probe molecule, allows to discriminate between Lewis (L) and Brønsted (B) acid sites, thanks to the two characteristic IR absorption peaks of pyridine, respectively at 1450cm^{-1} and 1545 cm^{-1}.

Figure 3.7 shows the FT-IR spectra recorded after adsorption and desorption of pyridine, at increasing temperatures, for the three metal phosphates.

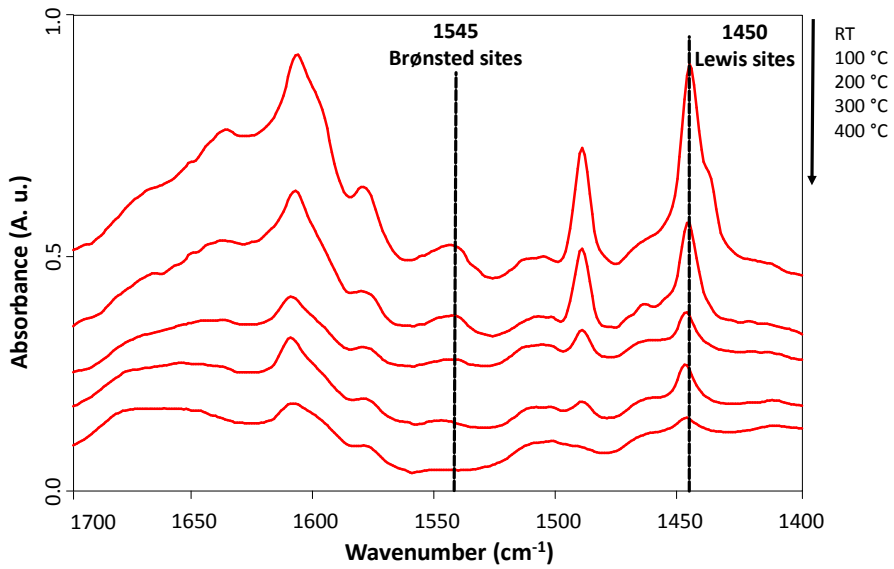

a)

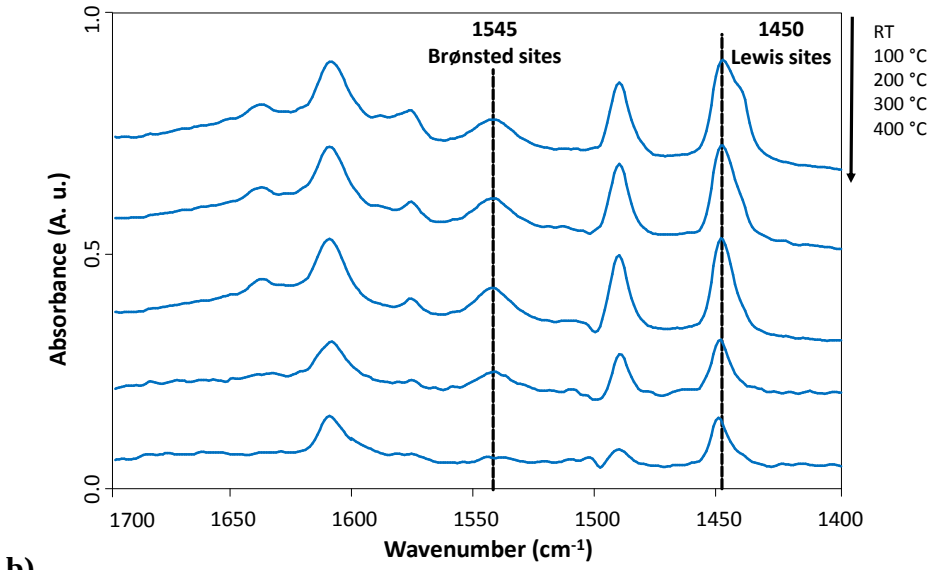

b)

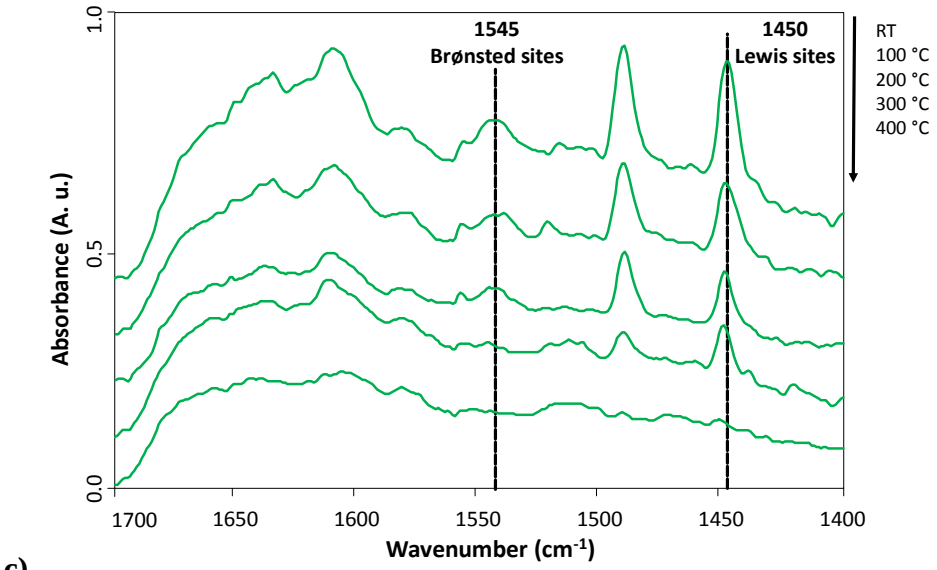

c)

Figure 3.7 FT-IR desorption spectra of pyridine, recorded at increasing temperatures, for: a) Zr/P/Osynt; b) Nb/P/Ocomm; c) Nb/P/Osynt.

It is possible to observe that, as regards B-type centers, the three catalysts show a comparable concentration and strength of acid sites: the peaks at 1545 cm^{-1} shows similar intensity and desorption trend in function of temperature.

Instead, for L centers, the situation is more complex: at room temperature, Zr/P/Osynt presents the higher concentration of L acid sites, which demonstrate a moderate strength; Nb/P/Ocomm shows somehow stronger L acidity, as it is possible to see from the still relevant concentration of adsorbed pyridine after treatment at 400°C. As regards Nb/P/Osynt, the concentration of L acid sites at room temperature is comparable to that one observed with Nb/P/Ocomm; however, the strength is more similar to that shown by Zr/P/Osynt.

In Figure 3.8 is reported the quantitative trends of Brønsted/Lewis acid sites ratio (BLR) as a function of desorption temperature, which allows to clarify the influence of the acidity type on the total strength of the three metal phosphates.

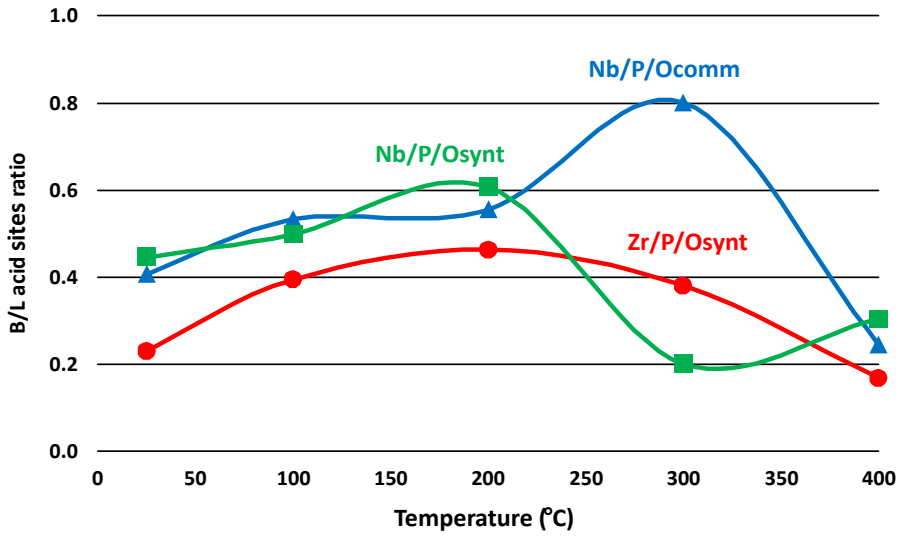

Figure 3.8 Brønsted/Lewis acid sites ratio as a function of the desorption temperature for Zr/P/Osynt, Nb/P/Ocomm, Nb/P/Osynt.

As shown in the graph, commercial and synthesized niobium phosphates present similar BLR trends until 200°C, then become very different at 300°C and finally are again similar after treatment at 400°C: therefore, also noting the desorption spectra of pyridine, it is possible to conclude that, for both niobium phosphates,

L sites show a greater strength compared to B acid sites, as demonstrated by the decrease of BLR with increasing temperature; this aspect is more relevant for Nb/P/Osynt, the BLR of which decreases at lower temperature compared to the other phosphates.

For Zr/P/Osynt, the trend highlights a different behavior: first of all, BLR is lower than values observed for niobium phosphates, that means a lower contribution of the Brønsted character; moreover, this catalyst presents L and B acid sites with a comparable strength, as shown by the lower dependence of the BLR on temperature.

The behavior of the three catalysts appears to be different when FT-IR spectra are recorded after the co-adsorption of pyridine and water, as reported in Figure 3.9 for Zr/P/Osynt and Nb/P/Ocomm.

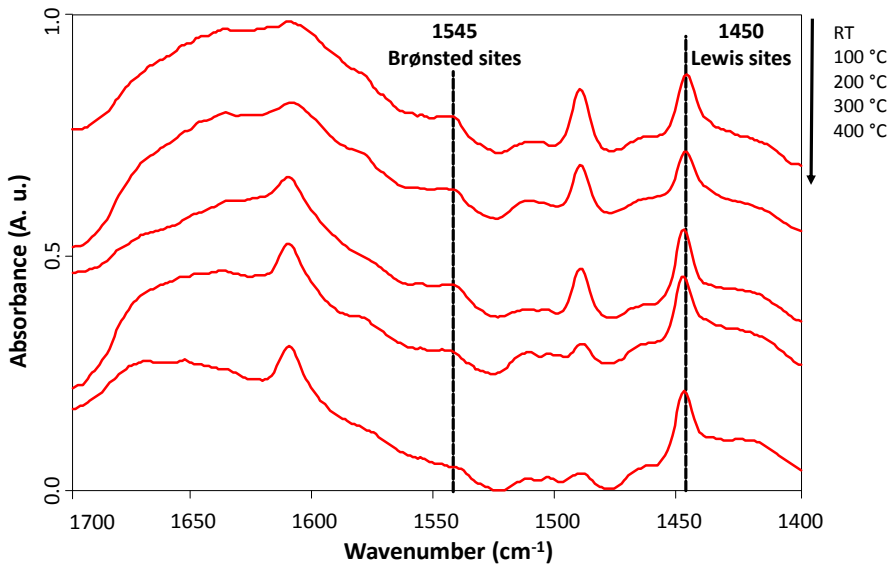

a)

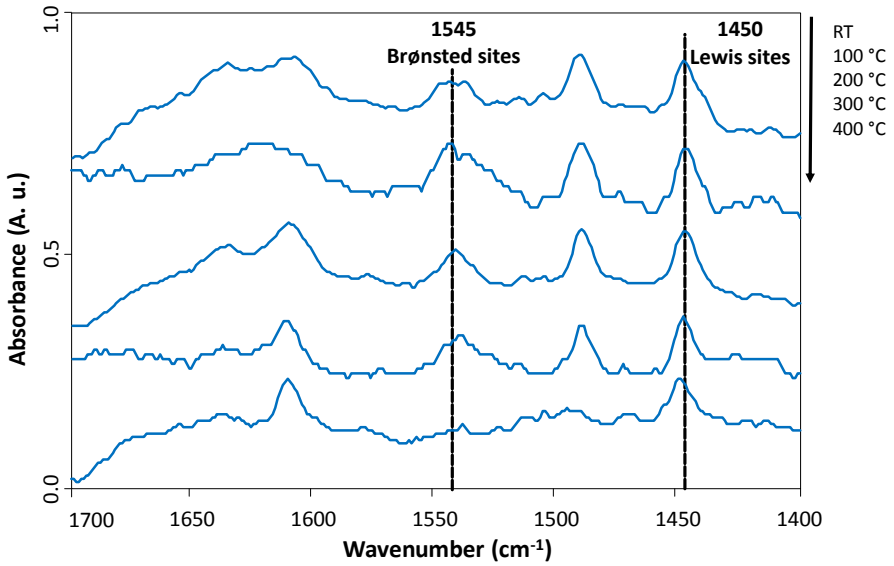

b)

Figure 3.9 FT-IR desorption spectra of co-adsorbed pyridine and water, recorded at increasing temperatures, for: a) Zr/P/Osynt; b) Nb/P/Ocomm.

A comparison of the spectra represented above with those reported in
Figure 3.7, allows to infer on the effect of water on acidity: under hydrating conditions, the metal phosphates are able to generate new strong B acid sites by transformation of a part of native L centers, with a consequent increase of B acid sites concentration and a decrease of L sites.

The relevance of this effect depends on the catalyst type, as shown by BLR trends shown in Figure 3.10.

As reported in the graph, the effect of water is very important for Nb/P/Ocomm, with a strong increase of BLR, due to the formation on new strong B centers in place of native L acid sites, that results in the predominance of Brønsted character. Conversely, for Zr/P/Osynt, the effect is milder, and, for this reason, L centers remain the prevailing ones.

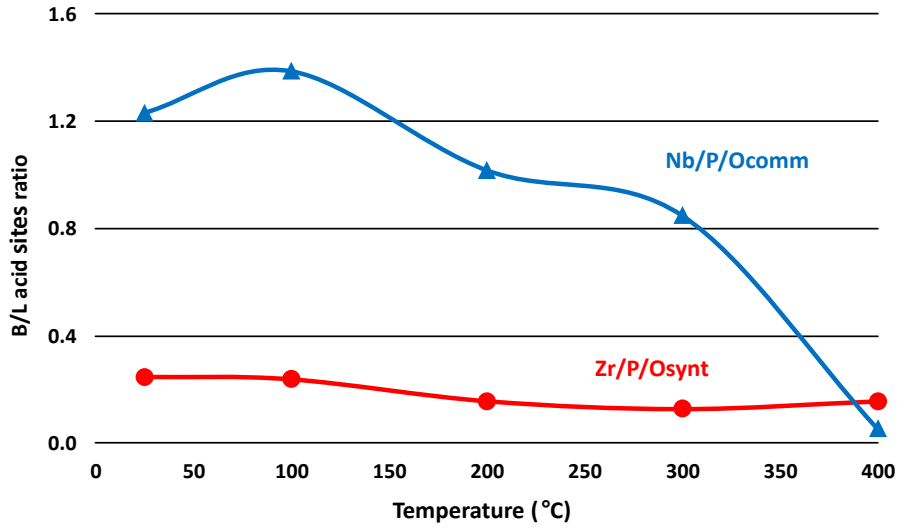

Figure 3.10 Brønsted/Lewis acid sites ratio as a function of the desorption temperature for Zr/P/Osynt, Nb/P/Ocomm after co-adsorption of pyridine and water.

Gas-phase dehydration of ethanol

The model reaction of ethanol dehydration in gas-phase provides a further proof about the type of surface acidity involved. Results are reported in Figure 3.11.

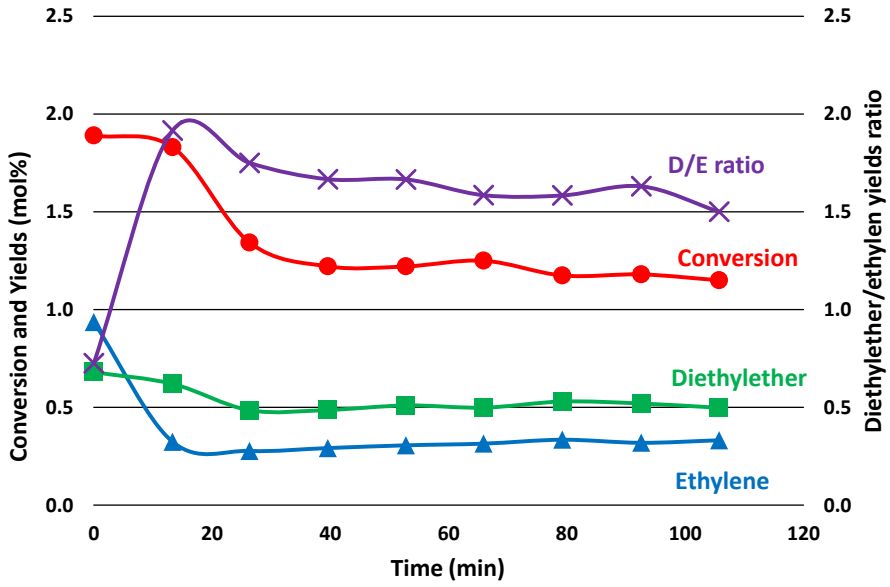

a)

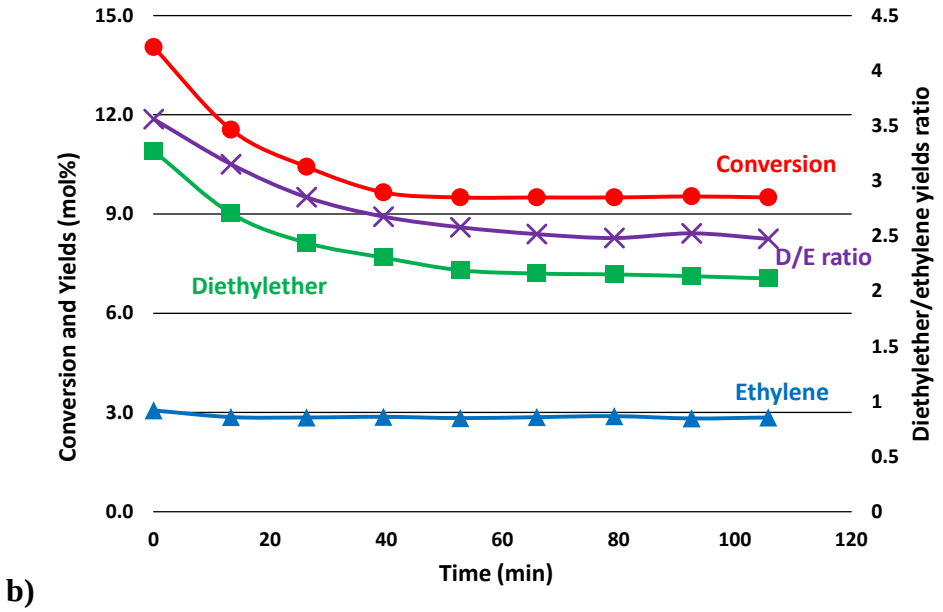

b)

Figure 3.11 Ethanol dehydration reaction in gas phase for: a) Zr/P/Osynt; b) Nb/P/Ocomm. Legend: ● ethanol conversion; ▲ Ethylene yield; ■ Diethylether yield; × Diethylether/ethylene yields ratio.

It is possible to see that Zr/P/Osynt, despite the higher total acid sites concentration, shows a lower activity in the dehydration of ethanol compared to Nb/P/Ocomm. Moreover, the two metal phosphates present a different products distribution. In fact, the diethyl ether/ethylene ratio, that are the products of ethanol dehydration, is equal to 2.0 for Zr/P/Osynt and 3.0-4.0 for Nb/P/Ocomm.

These different catalytic behaviors can be explained by taking into account the effect of water produced in-situ from ethanol dehydration: the interaction of water with catalysts L acid sites generates new strong B centers; as described in the previous paragraph, this effect is much more relevant for Nb/P/Ocomm. Therefore, the formation of new strong B acid sites in niobium phosphate explains, as reported in literature for ethanol dehydration[126], its higher activity and the higher production of diethylether compared to Zr/P/Osynt.

3.1.3 Catalytic tests of lignocellulose and cellulose hydrolysis

The catalytic behaviors of metal phosphates in acid hydrolysis of biomass are presented in this paragraph. Results will be correlated with physical-chemical properties of the three tested metal phosphate catalysts.

Microcrystalline Cellulose

Initially, the study was focused on microcrystalline cellulose, because this substrate is less complex than lignocellulose.
Hydrolysis tests were (as described in paragraph 2.3.1) were first carried out for 24 hours on native microcrystalline cellulose. Figure 3.12 compares the performance for the blank test, conducted without any catalyst, with that one of Zr/P/Osynt and Nb/P/Ocomm.

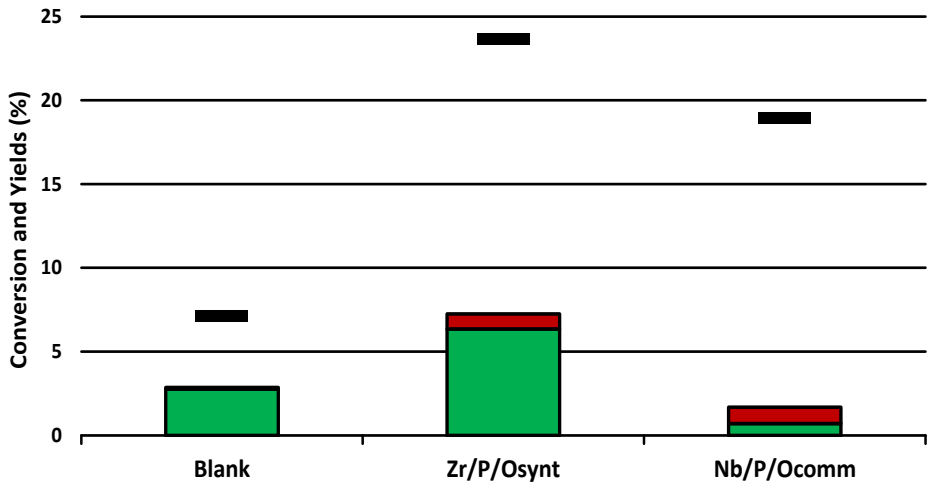

Figure 3.12 Tests for blank test, Zr/P/Osynt and Nb/P/Ocomm. Legend: – Conversion; ■ Glucose yield; ■ HMF yield.

As shown in the graph, substrate conversion achieved with metal phosphates is higher than conversion obtained without any catalyst.

Moreover, it is important to note the difference between cellulose conversion and the sum of yields to products identified; this difference, is due to the formation of products that cannot be quantified directly by means of HPLC: for example, oligomers, which are the intermediate products of cellulose hydrolysis to glucose, and humins, that, as described in paragraph 1.3.1, derive from condensation reactions involving glucose and HMF. This specification is valid for all reported hydrolysis tests, independently from substrate, catalyst or reaction conditions used. These data demonstrate that the metal phosphates are active in the hydrolysis of cellulose, but the main part of the converted reactant is transformed into either oligomers or humins. In fact, yield to glucose obtained with Zr/P/Osynt is higher than that produced by thermal hydrolysis, but in the case of Nb/P/Ocomm, the yield to glucose is very low.

We studied more in detail the kinetics of the hydrolysis for native microcrystalline cellulose: tests conducted in function of time, between 0 and 24 hours, for Zr/P/Osynt and Nb/P/Ocomm are reported in Figure 3.13.

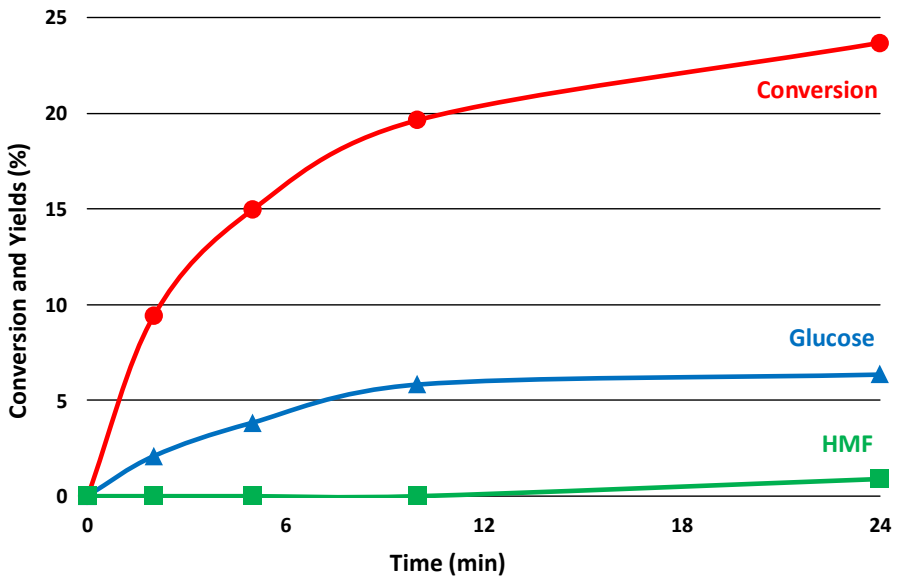

a)

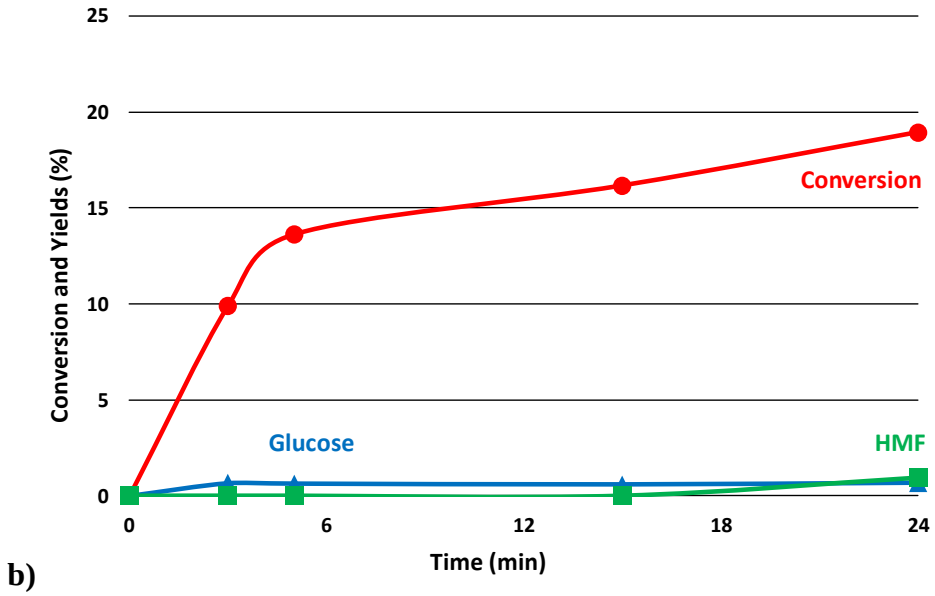

b)

Figure 3.13 Catalytic performances on native cellulose hydrolysis for: a) Zr/P/Osynt; b) Nb/P/Ocomm: Legend: ● Native cellulose conversion; ▲ Glucose yield; ■ HMF yield.

The two metal phosphates showed comparable trends for conversion and yields in function of time, but different performances in regard to both substrate conversion and products distributions:

- conversion of microcrystalline cellulose, for both catalysts, increased along with the increase of reaction time, up to 24 hours, but a different maximum value was reached, equal to 25% and 19% for Zr/P/Osynt and Nb/P/Ocomm, respectively;
- also the yield to glucose for the two systems increased along with the reaction time, but with a very different maximum value, 6% for Zr/P/Osynt and 0.7% for Nb/P/Ocomm;
- HMF, for both catalysts, formed only for prolonged reaction time, 24 hours, with a final yield of about 1%; it formed by consecutive dehydration of glucose.

From these results, it is possible to note the different catalytic behavior of the two metal phosphates: zirconium phosphate is more active in the conversion of cellulose substrate and in the production of monosaccharides, while niobium phosphate is more selective to successive degradation products. However, it should be noted that, the high resistance of native cellulose to hydrolysis caused by its crystallinity, makes any comparison between catalysts a difficult task.

For this reason, these catalytic tests were carried out even on ball-mill pretreated cellulose: as described in 3.1.1, this mechanical pretreatment drastically reduces the crystallinity of cellulose, making it a more suitable substrate for hydrolysis. The results of catalytic tests carried out as function of time, from 0 to 24 hours, on pretreated cellulose are reported in Figure 3.14.

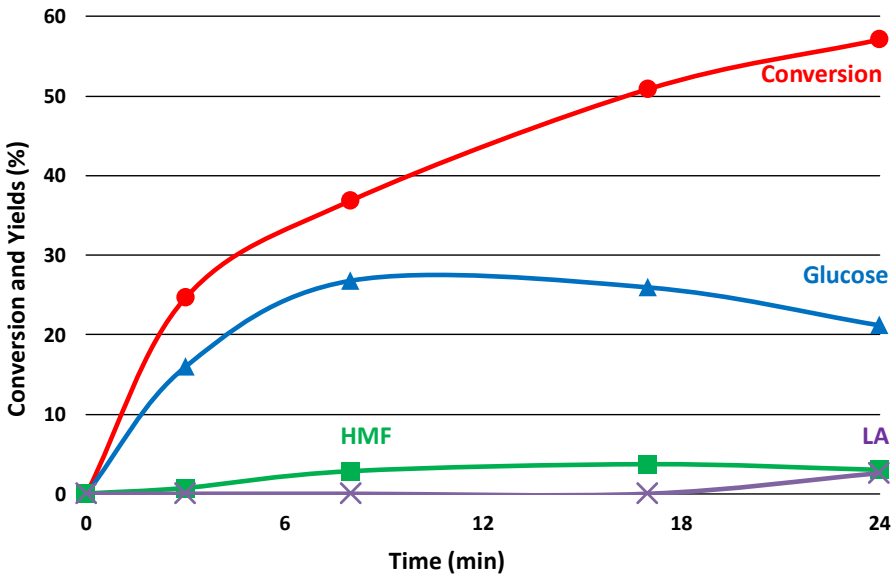

a)

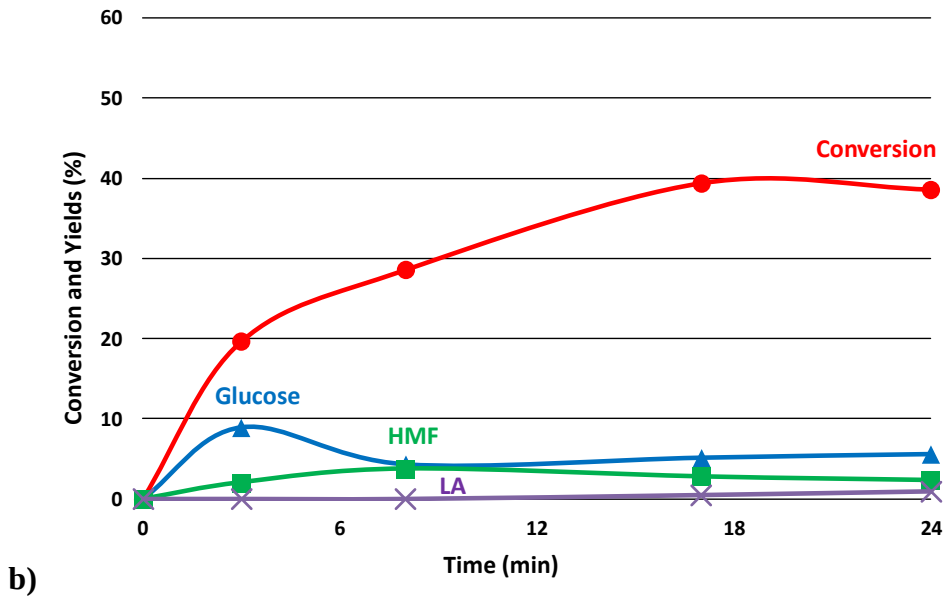

b)

Figure 3.14 Catalytic performances on ball-milled cellulose hydrolysis for: a) Zr/P/Osynt; b) Nb/P/Ocomm. Legend: ● Ball-milled cellulose conversion; ▲ Glucose yield; ■ HMF yield; × Levulinic acid yield.

It shown that the ball-mill pretreatment actually makes the hydrolysis of cellulose to occur much more easily, as shown from higher conversion and yields achieved, compared to those obtained by hydrolysis of the native cellulose.

It is also noted that the characteristic catalytic behaviors for the two metal phosphates, previously observed with microcrystalline cellulose, are confirmed by these results:

- conversion of substrate reached the maximum value, after 24 hours of reaction, of 57% for Zr/P/Osynt and 40% for Nb/P/Ocomm;
- yield to glucose initially increased with the increase of reaction time, with a maximum of 27% after 8 hours for Zr/P/Osynt and 9% at 3 hours for Nb/P/Ocomm; the subsequent reduction of glucose yield observed for a further increase of reaction time, was caused by degradative reactions;

- consequently, yield to HMF, produced by glucose dehydration, reached the maximum value at intermediate reaction times, 4% at 17 hours for Zr/P/Osynt and 40% at 8 hours for Nb/P/Ocomm, respectively; for longer reaction times, yield to HMF decreased, due to the formation of furfural (that is present in traces only, therefore it is not reported in the graphs), and levulinic acid. The latter forms by HMF hydration, and reaches its maximum value after 24 hours, equal to 2.5% for zirconium phosphate and 1% for niobium phosphate.

Therefore, these experiments demonstrate that zirconium phosphate is more active in the conversion of cellulose than niobium phosphate; moreover, Zr/P/Osynt appears to be more suitable for the production of monosaccharides, because it brings to higher glucose yield and lower formation of degradation products. Conversely, Nb/P/Ocomm is more selective in the synthesis of degradation products: in fact, the decrease of glucose yield already begins after 3 hours reaction time, whereas, for Zr/P/Osynt it starts after 8 hours.

The catalytic behaviors shown by the two metal phosphates in cellulose hydrolysis can be explained by taking into account their acid properties, as also confirmed in the literature[115, 116, 117, 118, 121]:

- for what concerns the conversion of cellulose, it is possible to say that it is closely related to the total concentration of acid sites: in fact, as emerged from ammonia-TPD analysis, reported in paragraph 2.2.3, Zr/P/Osynt presents a much greater aerial surface density of acid sites than niobium phosphate; this results in a higher activity for substrate hydrolysis and in a higher production of monosaccharides;
- instead, the products distribution is correlated to acid strength and type of acidity; Nb/P/Ocomm presents a higher amount of strong Brønsted acid sites, especially in aqueous conditions, as described in paragraph

2.2.3. Moreover, as also confirmed by results of gas-phase ethanol dehydration the Brønsted acidity is responsible for dehydration/hydration reactions. Therefore, the Nb phosphate catalyst appears to be more selective in the formation of degradation products.

This correlation between physical-chemical properties and catalytic performances is in agreement with what reported in a study, conducted in collaboration with the research group of Professor Raspolli Galletti, Pisa University[127]: this work, which is focused on the study of model dehydration reaction of fructose and inulin dehydration to HMF, carried out with the same two metal phosphates, also concluded about the importance of Brønsted acidity and strength of B acid sites, and that the Nb/P/Ocomm presents a higher activity for the formation of degradation products.

Conifer wood sawdust

After the work conducted on microcrystalline cellulose, we tested the reactivity of lignocellulose material, in particular, of conifer wood sawdust derived from the grinding and drying of forestry residue. Before catalytic tests, this substrate also underwent a mechanical pretreatment in a ball-mill for 15 minutes, in order to improve the efficiency of the hydrolysis.
The aim of this work was to determine whether the correlation found between physical-chemical properties of metal phosphates and their performances in hydrolysis of microcrystalline cellulose, was also observed for lignocellulose material, that represents a more resistant matrix, due to the presence of lignin.

Also in the case of the conifer wood sawdust, the first series of tests were conducted under the usual operative conditions. The comparison of results from the blank test, and those carried out with Zr/P//Osynt and Nb/P/Ocomm, is reported in Figure 3.15: cellulose monosaccharides represents the sum of the

yields to monosaccharides deriving from cellulose hydrolysis, i.e., glucose and fructose; monosaccharides deriving from hemicellulose hydrolysis, were xylose, arabinose, galactose and mannose.

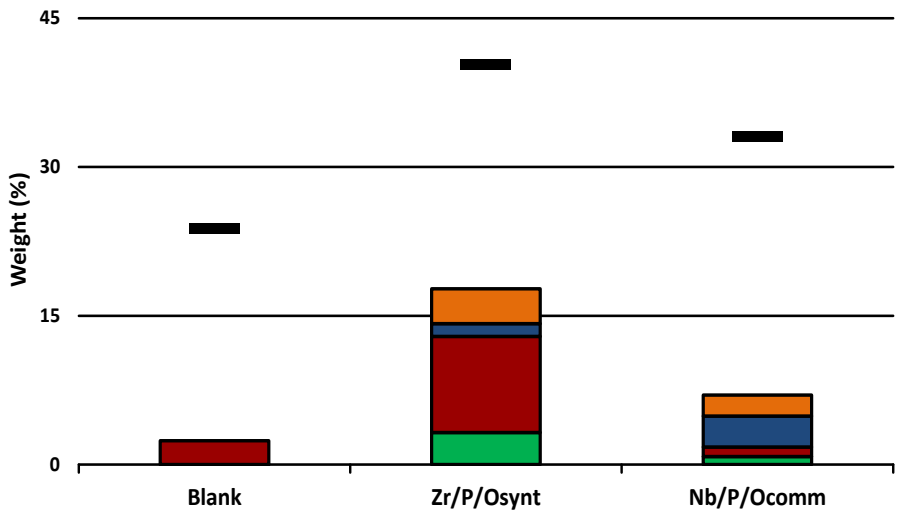

Figure 3.15 Conversion and yields for blank test, Zr/P/Osynt and Nb/P/Ocomm. Legend: – Conversion; ■ Cellulose monosaccharides yield; ■ Hemicellulose monosaccharides yield; ■ HMF yield; ■ Furfural yield.

In this case, as it was also for cellulose hydrolysis, the presence of metal phosphates improved the performance, as shown by the higher conversion and yield to products achieved.

Moreover, as already discussed for microcrystalline cellulose hydrolysis, the difference between conversion and sum of yields, was due to the presence of products that cannot be quantified by means of HPLC: oligomers and humins. As regards the humins formed, results of characterization conducted on the metal phosphates recovered at the end of the reaction (spent catalysts), are described in following paragraph.

After the comparison between blank and catalytic tests, we conducted a kinetics study of lignocellulose hydrolysis; catalytic tests were carried out in function of

time, as described in paragraph 2.3.1. Figure 3.16 shows the results obtained with Zr/P/Osynt and Nb/P/Ocomm catalysts.

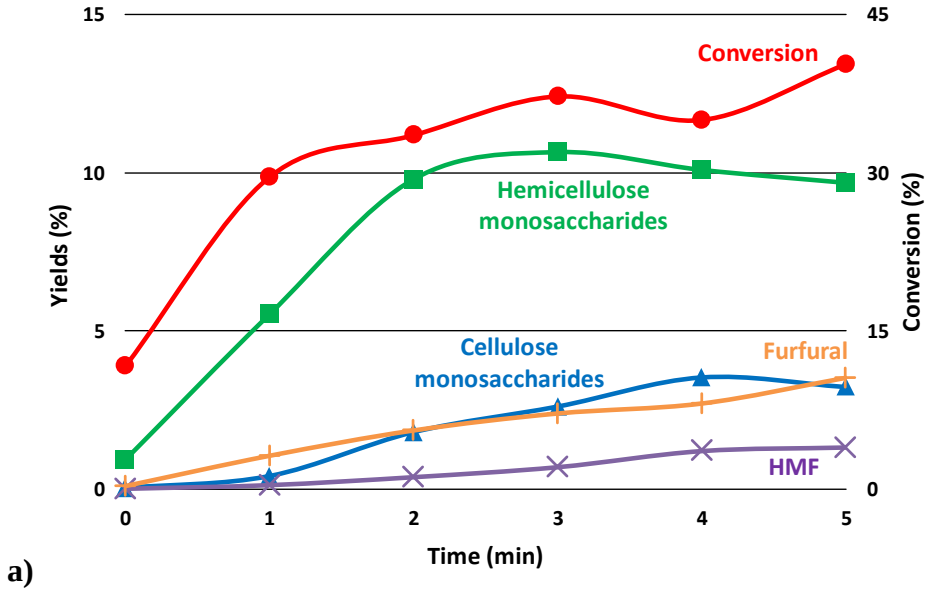

a)

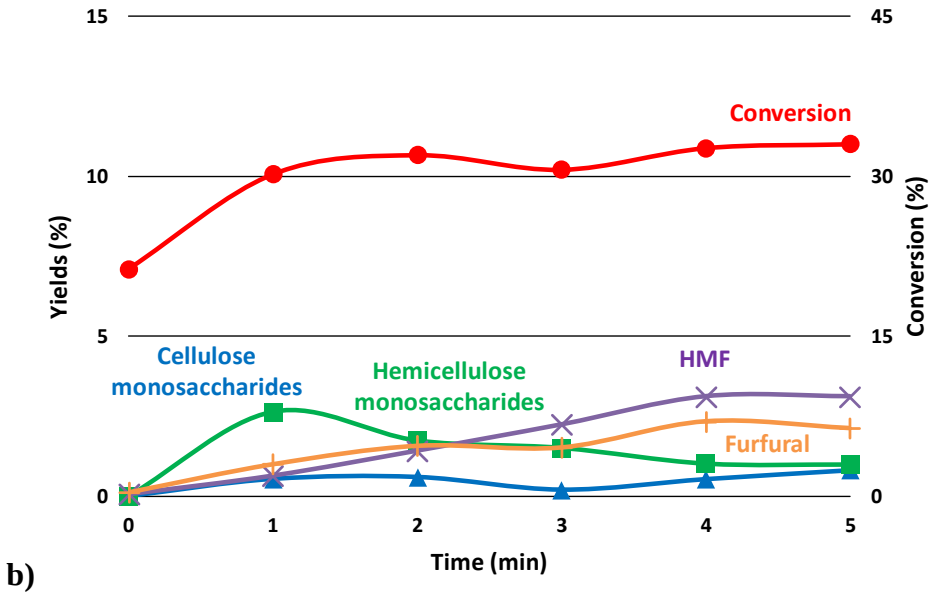

b)

Figure 3.16 Catalytic performance on conifer wood sawdust hydrolysis for: a) Zr/P/Osynt; b) Nb/P/Ocomm. Legend: ● Lignocellulose conversion; ▲ Cellulose monosaccharides yield; ■ Hemicellulose monosaccharides yield; × HMF yield; + Furfural yield.

First of all, it is important to note that, the maximum reaction time used in these experiments, that was equal to 5 hours, is lower than the 24 hours, used for experiments on microcrystalline cellulose: this is due to the easier hydrolysis of the cellulose fraction and its lower amount in lignocellulose. In fact, as shown in the figures, for both metal phosphates the conversion of lignocellulose substrate appears to be relatively high already after 5 hours of reaction, and then remained approximately constant. Moreover, it is also confirmed that the hydrolysis of hemicellulose is easier than that of cellulose: in fact, yield to monosaccharides deriving from hemicellulose was higher than yield to sugars deriving from cellulose.

In particular, from Figure 3.16, it is possible to observe the following:

- substrate conversion increased in function of reaction time up to 3 hours, then remained stable at its maximum value until 5 hours, which was equal to 40% for Zr/P/Osynt and to 33% for Nb/P/Ocomm;
- yield to cellulose monosaccharides reached a maximum of 3.5% at 4 hours for Zr/P/Osynt, then remained stable until the end of the reaction; instead, for Nb/P/Ocomm, yield to cellulose monosaccharides presented a maximum of 0.8% after 5 hours;
- yield to hemicellulose monosaccharides for both metal phosphates reached the maximum value at medium-low reaction time, respectively 10.5% at 3 hours for Zr/P/Osynt and 2.6% at 1 hour for Nb/P/Ocomm; then, in both cases yield decreased for longer times, due to the increase of decomposition products;
- yield to decomposition products, HMF and furfural, increased in correspondence of longer reaction times, and reached the highest value after 5 hours; for HMF it was equal to 1.3% for Zr/P/Osynt and 3% for Nb/P/Ocomm, while for furfural it was 3.5% for the former catalyst and 2.5% for the latter one.

These results confirm the effects already discussed for the hydrolysis of microcrystalline cellulose. Zr/P/Osynt is more active in the degradation of both cellulose and hemicellulose fractions, as shown by the higher conversion achieved with this catalyst compared to Nb/P/Ocomm. Moreover, zirconium phosphate is more suitable for the productions of sugars, because it provides higher yields to monosaccharides, both from the cellulose and hemicellulose fractions.

Conversely, Nb/P/Ocomm appears to be more selective for the formation of decomposition products. In fact, the decrease of monosaccharides yield begins after 1 hour only reaction time, especially for those deriving from the hemicellulose fraction, that is a much shorter reaction time compared to the 3 hours needed with zirconium phosphate.

Therefore, it is possible to conclude that the same relationship found between physical-chemical characteristics of metal phosphates and their performance in cellulose hydrolysis also stands in the case of the lignocellulose substrate. The higher total concentration of acid sites, shown by Zr/P/Osynt, results in a higher activity in lignocellulose conversion and consequently in a higher production of monosaccharides from both hemicellulose and cellulose hydrolysis. On the other hand, the higher amount of strong Brønsted acid sites, especially in aqueous conditions, exhibited by Nb/P/Ocomm, mainly promotes the dehydration of monosaccharides, those deriving from both cellulose and hemicellulose, to the successive degradation products, i.e., HMF and furfural.

Various agricultural lignocellulose substrates

Having been established that the catalytic behavior of metal phosphates in hydrolysis reaction is closely related to the catalyst acid properties also in the case of the lignocellulose substrate, the relationship between catalytic performances and lignocellulose composition has been investigated. For this

reason, catalytic tests with two metal phosphates were carried out on various lignocellulose substrates, that differ for their composition and amount of the three main components (cellulose, hemicellulose and lignin), as reported in paragraph 3.1.1.

In Figure 3.17, are represented the results of catalytic tests conducted at 150°C for 1 hour with Zr/P/Osynt and Nb/P/Ocomm with the six different agricultural lignocellulosic residues; also these substrates, before catalytic tests, were mechanically pretreated in ball-mill for 15 minutes, in order to break the material into smaller and more homogeneous pieces and finally favor the hydrolysis. Moreover, in these tests also oligomers, indicates as total oligomers, deriving from the hydrolysis of both cellulose and hemicellulose, were quantified, using the method reported in paragraph 2.3.1; therefore, the difference between conversion and the sum of the reported yields is only due to the formation of humins. In these graphs, total monosaccharides includes all the six more common sugars, deriving from both cellulose and hemicellulose, i.e., glucose, fructose, xylose, galactose, arabinose and mannose. Total successive products indicates the sum of yields to HMF, furfural, levulinic acid, formic acid, oxalic acid, acetic acid and tartaric acid.

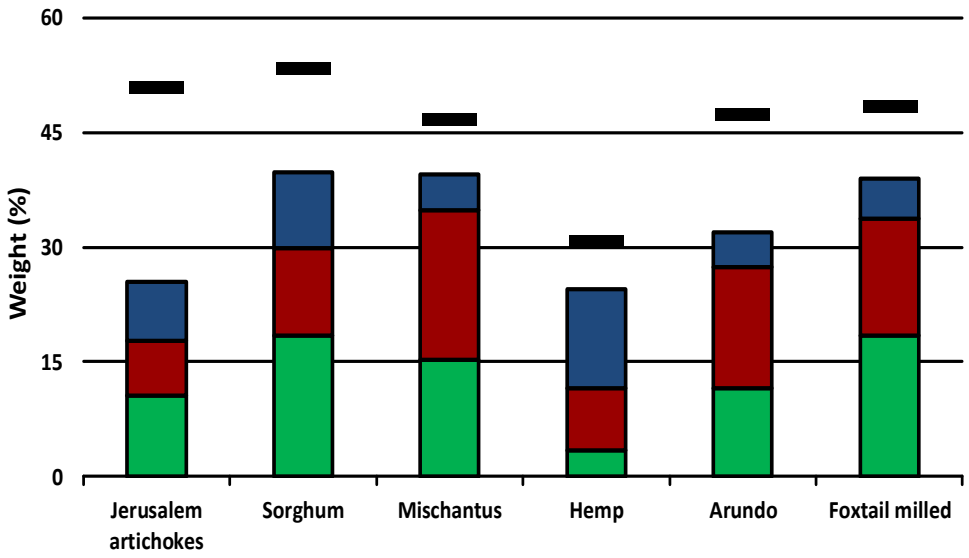

a)

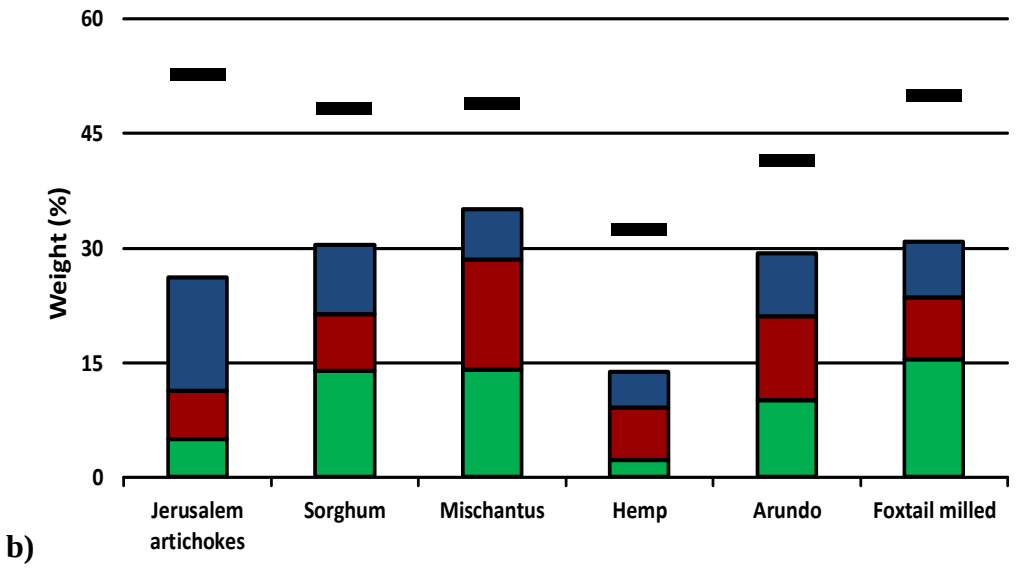

Figure 3.17 Catalytic performances in lignocellulose substrates hydrolysis for: a) Zr/P/Osynt; b) Nb/P/Ocomm. Legend: ‒ Conversion; ■ Total monosaccharides yield; ■ Total oligomers yield; ■ Total successive products yield**.**

From the comparison of the results reported, it is possible to observe that catalytic performances are affected by the composition of substrates:

- the amount of cellulose, which is harder to hydrolyze compared to hemicellulose, affects the degree of conversion achieved: hemp, which contains 63% cellulose, shows the lower conversion with both metal phosphates, 30.5% with Zr/P/Osynt and 32.5% with Nb/P/O; whereas Jerusalem artichoke shows the highest conversion, 51% with Zr/P/Osynt and 52% with Nb/P/Ocomm, thanks to the lower cellulose content, equal to 16% only;
- on the other hand, the hemicellulose content affected the distribution of products: in particular, due to its easier hydrolysis, it is readily converted into oligomers and monosaccharides, reducing the amount of successive products. In fact, miscanthus shows the higher yield to total monosaccharides and oligomers, respectively 15% and 20% with Zr/P/Osynt and 14% and 14.5% with Nb/P/Ocomm, while the amount of

successive products is the lower, respectively 4.5% with Zr/P/Osynt and 6.5% with Nb/P/Ocomm, because of its relatively high hemicellulose content, equal to 31%;

- the lignin fraction, that is not converted, does not show a significant influence on catalytic performance.

The correlation of catalytic behavior with acid properties previously described for conifer wood sawdust, is confirmed also for the six agricultural lignocellulose substrates. The average of conversion values turns out to be the higher with Zr/P/Osynt, thanks to its greater total concentration of acid sites, and consequently, also average yields for total monosaccharides and oligomers results to be higher. Conversely, Nb/P/Ocomm presents higher average yield values for decomposition products, due to the greater amount of strong Brønsted acid sites in aqueous medium.

The study of the hydrolysis of the six lignocellulose substrates was then carried out with a different type of niobium phosphate: Nb/P/Osynt, prepared according to the method reported by Mal and Fujiwara, described in paragraph 2.1.1. This niobium phosphate shows completely different acid properties compared to those observed for the other metal phosphates prepared and tested, as summarized in paragraph 3.1.2; therefore, it is interesting to investigate on the relationship between acid properties and catalytic performances for this new catalyst. Figure 3.18 reports the results of catalytic tests conducted at 150°C for 1 hour with Nb/P/Osynt, on the six different lignocellulosic residues.

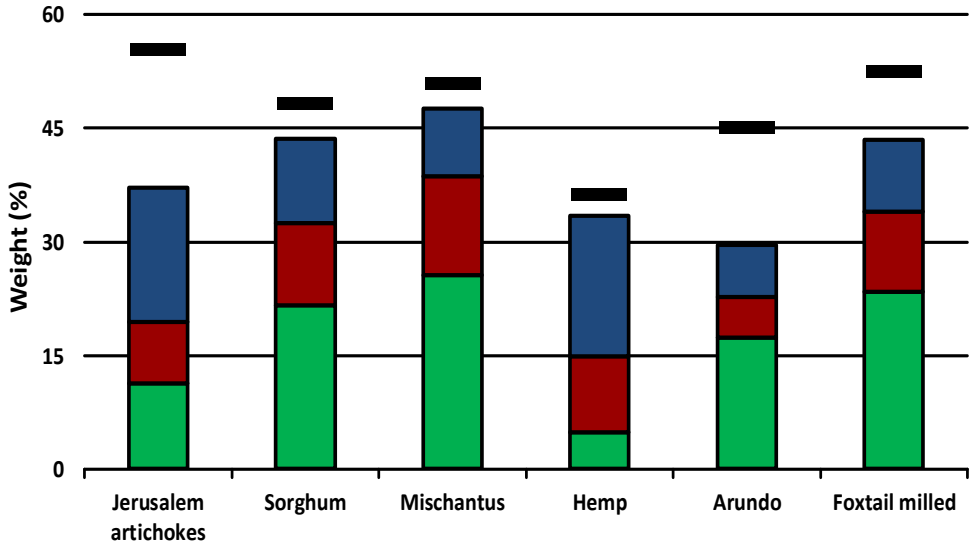

Figure 3.18 Catalytic performances on lignocellulose substrates hydrolysis for Nb/P/Osynt.

Legend: - Conversion; ■ Total monosaccharides yield; ■ Total oligomers yield; ■ Total successive products yield**.**

Once again the same relationship previously discussed between catalytic performances and substrate composition, is confirmed with this catalyst type: the substrate with the higher cellulose fraction (i.e., hemp) is the harder to be hydrolyzed, as demonstrated by the lower conversion achieved, 36%; while miscanthus, that presents the higher hemicellulose fraction, shows the greater yield to total monosaccharides and oligomers, 26% and 13% respectively, and the lower yield to successive products, 9%.

Furthermore, by comparing these results with those obtained from catalytic tests carried out with Zr/P/Osynt and Nb/P/Ocomm, reported in Figure 3.17, it is possible to confirm also for Nb/P/Osynt the correlation between catalytic behavior and physical-chemical properties.

As reported in the paragraph dealing with acid characterization of catalysts (paragraph 3.1.2), the synthesized niobium phosphate presents the highest total acid sites concentration amongst the metal phosphates here studied, which allows this system to be the most active in the conversion of lignocellulose

substrates, as evident from the high conversion values achieved; consequently, also the formation of monosaccharides and oligomers turns out to be the highest with this system. As regards the type acidity, Nb/P/Osynt shows a significant presence of strong Brønsted acid sites, which is comparable to that observed in Nb/P/Ocomm; for this reason, also the yield of successive products is highly favored with this catalyst.

3.1.4 Characterization of spent catalytic systems

The metal phosphates recovered at the end of a reaction, independently from the substrate tested and operative conditions used, showed the presence of black and sticky substances deposited on their surface. These insoluble products, as described in paragraph 1.3.1, are made of humins, which derived from condensation reactions, involving glucose and HMF, promoted by acid conditions. The composition and the amount of humins depends on several factors, such as the substrate and catalytic system employed and reaction conditions.

The easiest way to analyze, both qualitatively and quantitatively, these undesired products, is to study the properties of catalytic systems recovered after reaction, the so-called spent catalysts. Therefore, Zr/P/Osynt and Nb/P/Ocomm recovered after conifer wood sawdust hydrolysis for 1 hour at 150°C, were analyzed by means of thermogravimetry and ATR-IR analysis; before these tests, catalytic systems were washed with distilled water and dried overnight at 80°C in oven.

Thermogravimetry analysis (TGA)

The amount of humins deposited on the two metal phosphates have been determined by thermogravimetry analysis, conducted in air flow: in this way, as

represented in Figure 3.19, carbonaceous compounds are combusted to CO_2, and this conversion is detected as weight change: the two spent catalysts showed different weight loss, equal to 17% for Zr/P/Osynt and 11% for Nb/P/Ocomm.

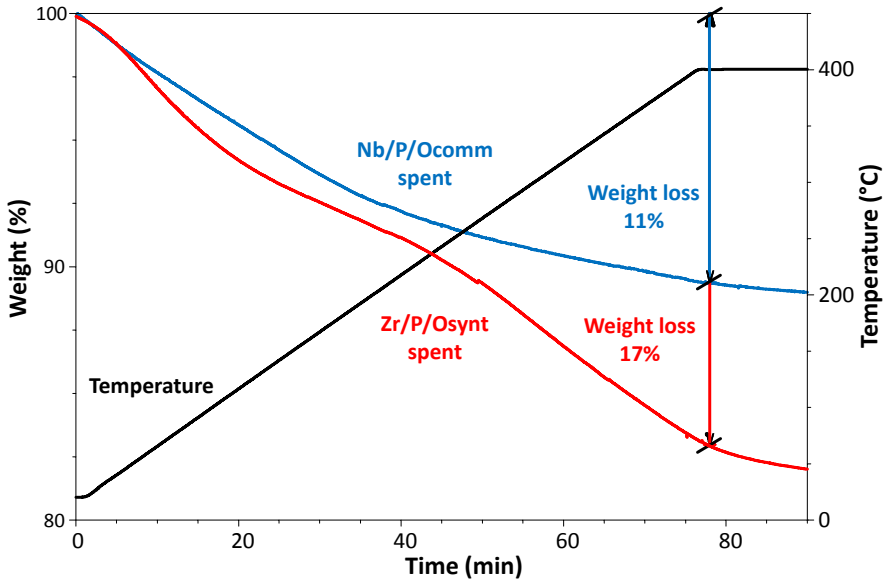

Figure 3.19 TGA analysis in air flow of spent metal phosphates.

From these graphs, it is also possible to observe that the combustion of humins is complete at 400°C, that is the calcination temperature of the metal phosphates. This means that carbonaceous residues can be totally removed by oxidative treatment under relatively mild conditions; moreover, metal phosphates appears to be stable systems and suitable catalysts to be reused several times.

Attenuated total reflectance IR-spectroscopy (ATR-IR)

ATR-IR spectroscopy allows to gain information on the chemical composition of humins and, by comparison of spectra of the fresh catalyst with the used one, the effect that these products have on acid sites.

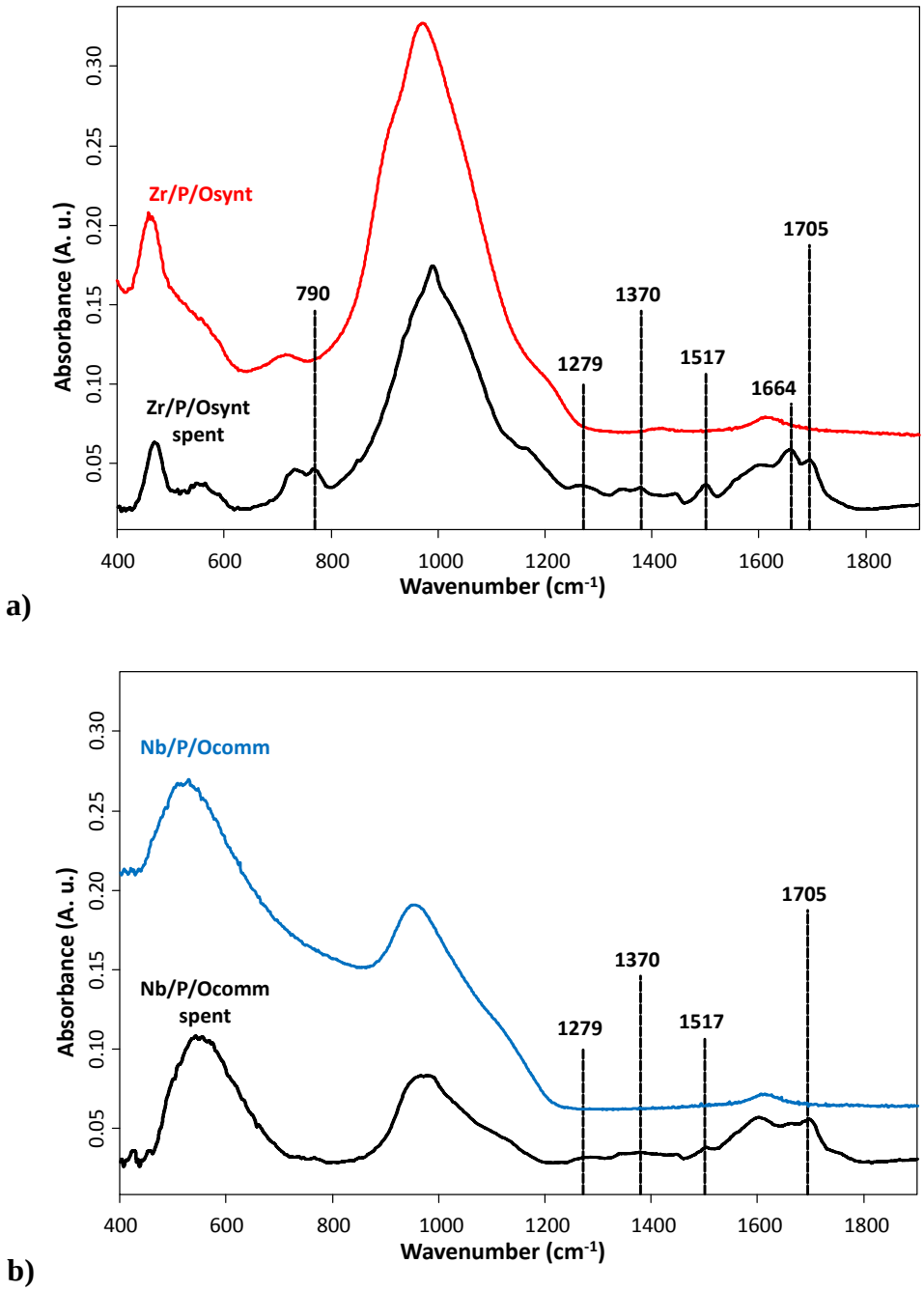

Figure 3.20 Comparison of fresh and spent ATR-IR spectra for: a) Zr/P/Osynt, b) Nb/P/Ocomm.

In Figure 3.20, the comparison between fresh and spent catalysts for Zr/P/Osynt and Nb/P/Ocomm is reported. First of all, it is possible to note that characteristic bands of fresh metal phosphates appear to be less intense for the spent systems;

this is due to the presence of organic residues deposited on the catalyst surface, which involves a weaker interaction of the metal phosphates with IR radiation, and probably also reduces the catalytic activity of these systems.

Moreover, the ATR-IR spectra of spent catalysts show the presence of new bands, which are not seen in fresh spectra, that are attributable to deposited compounds, confirming the carbonaceous nature of humins[128, 129, 130]: both metal phosphates exhibit bands at 1279 cm^{-1}, 1370 cm^{-1}, 1517 cm^{-1} and 1705 cm^{-1} that can be assigned to the stretching of ether C-O bonds, stretching of furan ring C-O-C bonds, stretching of C=C bond in furan and aromatic compounds and stretching of carbonyl C=O bonds, respectively. Moreover, the spectrum of used Zr/P/Osynt, shows two bands at 790 cm^{-1} and 1664 cm^{-1} attributed to the bending of =C-H bond in furan and aromatic compounds.

3.2 Rare sugars synthesis

The study on the synthesis of rare sugars from glucose was focused on the use of titanium-based heterogeneous catalysts; in particular, as described in paragraph 1.4.4, the choice of this element is related to its well-known Lewis acid property, which is fundamental in order to promote this class of reactions[78, 81, 91, 97]. More in detail, the aim of this work is to determine the role that the various species of titanium play in promoting the different reactions of glucose rearrangement.

For this purpose, two types of heterogeneous catalysts containing titanium have been studied: titanium oxide grafted on silica and titanium silicalite.

At first, these catalysts were characterized, in order to define both the amount and type of the different titanium species. Then, results were correlated with performances achieved in catalytic tests of glucose rearrangement, in order to establish relationships between titanium specie and type of sugar formed.

Finally, a hypothesis on the reaction network for glucose structural rearrangement in acid conditions has been proposed.

3.2.1 Characterization of titanium oxide grafted on silica catalysts

The physical-chemical properties of five synthesized grafted systems (TOS), that differ for the amount of titanium oxide loaded, were determined using different techniques: XRF, ATR-IR and DR-UV spectroscopy.

X-ray fluorescence (XRF)

The amount of titanium oxide, expressed as weight percentage of Ti, for the five grafted systems synthesized was determined by means of XRF analysis; the analytical and the nominal values (amount of titanium loaded during the synthesis step) are reported in Table 3.4.

Catalytic system	Nominal Ti (%w)	Measured Ti (%w)
TOS-A	0.50	0.50 ± 0.05
TOS-B	1.00	1.00 ± 0.05
TOS-C	2.00	1.60 ± 0.05
TOS-D	4.00	2.10 ± 0.05
TOS-E	8.00	2.30 ± 0.05

Table 3.4 Titanium weight percentage for the five synthesized grafted systems.

As shown in the table, the difference in terms of titanium amount between nominal and measured value appears to be more relevant at increasing Ti content: in particular, for systems with the higher titanium amount (TOS-D and

TOS-E) the difference is very significant. This is due to the maximum amount of metal that is possible to load on silica support, which, as reported in the synthesis method described by Hamilton et al.[109], is about 2-3 w%.

Attenuated total reflectance IR-spectroscopy (ATR-IR)

ATR-IR analysis allows to evaluate the effect of titanium grafting on the structure of silica support and on the nature of Ti sites; Figure 3.21 reports the comparison of spectra for pure SiO_2 and grafted systems.

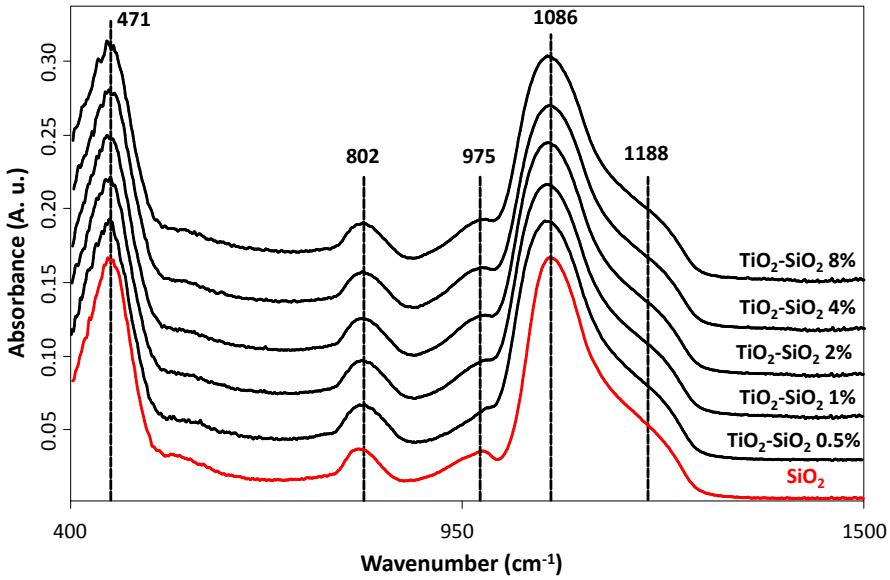

Figure 3.21 Comparison of silica (red) and titanium grafted systems (black) ATR-IR spectra.

It is possible to observe that all spectra show the characteristic bands of silica with comparable intensity of bands: 471 cm^{-1} which corresponds to the bending of Si-O-Si group; 802 cm^{-1} and 1086 cm^{-1} that are assigned to Si-O-Si symmetric stretching; 975 cm^{-1} attributed to of Si-OH bond vibration; and 1188 cm^{-1} attributed to the asymmetric stretching of Si-O-Si group.

Therefore, these analysis confirm that the grafting procedure used does not modify the structure of the support. A band at ca 970-980 cm^{-1} attributed to the Si-O-Ti bond was also expected, but it was overlapped by the silica band falling in the same spectral region.

Diffusive reflectance UV-spectroscopy(DR-UV)

The coordination of Ti grafted onto the silica support can be determined by means of DR-UV spectroscopy, spectra are reported in Figure 3.22.

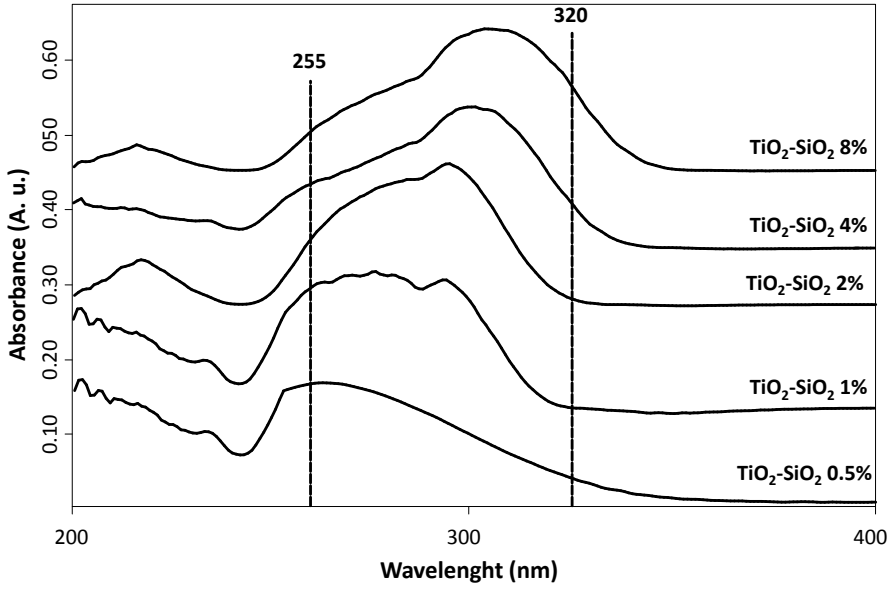

Figure 3.22 DR-UV spectra for the five synthesized grafted systems.

The band at 255 nm can be attributed to isolated Ti(IV) species in octahedral coordination; this band is the only one observed for the sample containing the lowest Ti amount (TOS-A). On increasing the Ti content, a shift of the band is observed at progressively increasing wavelength. Upon changing the degree of Ti condensation, from isolated species until oligomeric/polymeric and bulk titanium dioxide, the characteristic charge-transfer band is shifted towards

higher wavelength numbers. In fact, as reported in literature[131], DR-UV spectrum of anatase shows a band at ca 320 nm; while the other crystalline form of titanium oxide, rutile, exhibits an absorption band at 340 cm^{-1}.

Therefore, differences of spectra can be attributed to the different condensation level of Ti specie, as also described in literature for grafted systems[109, 131, 132], at low concentration of titanium, TiO_2 is distributed as monomeric species, highly dispersed on silica surface; while, on increasing the amount of Ti loaded more aggregated species, which can be identified as oligomeric species, are formed.

3.2.2 Characterization of titanium-silicalites

As described in 2.1.2, the three titanium-silicalites studied for rare sugars synthesis, were provided by an external company. We characterized the physical-chemical properties of TS-1 systems in depth, using different techniques: BET, XRD, ATR-IR, XRF DR-UV, TPD and FT-IR.

Specific surface area (BET)

The specific surface areas of the three titanium-silicalites are reported in Table 3.5.

Catalytic system	BET (m^2/g)
TS-1A	470 ± 5
TS-1B	450 ± 5
TS-1C	465 ± 5

Table 3.5 Specific surface area for the three TS-1 catalysts.

The three catalysts showed similar values of surface area.

X-ray diffraction (XRD)

XRD allows to determine the crystalline structure of the three catalysts; the comparison of the XRD patterns is represented in Figure 3.23.

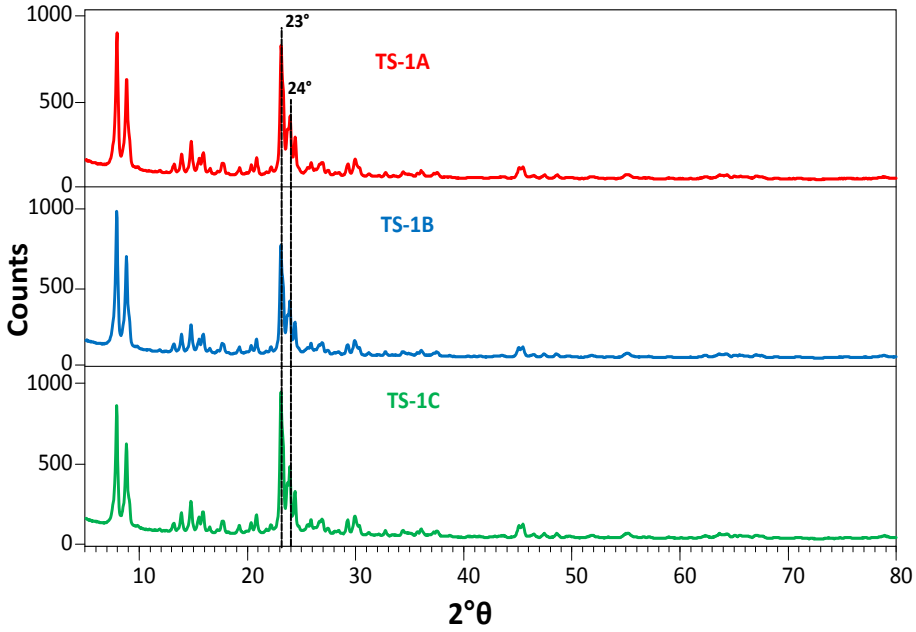

Figure 3.23 Comparison of XRD patterns of the three titanium-silicalite catalysts.

The XRD patterns were the same for the three samples, with two strong reflections at 23° and 24°; the pattern corresponds to the orthorhombic structure, which is characteristic for TS-1: in fact, these patterns are similar to those of titanium-silicalite reported in literature[104].

Attenuated total reflectance IR-spectroscopy (ATR-IR)

ATR-IR spectra permits to obtain information about molecular geometry of the three titanium-silicalites; Figure 3.24 shows the comparison of ATR-IR spectra.

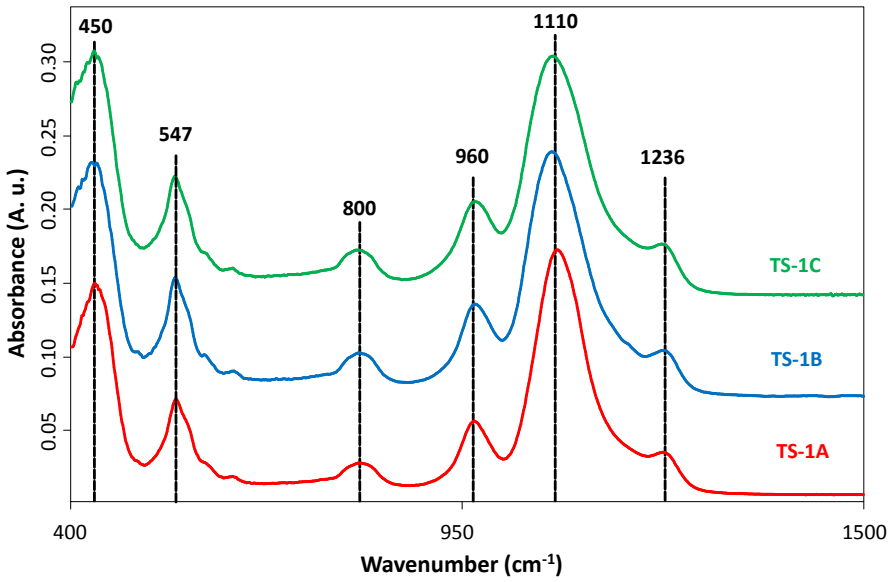

Figure 3.24 Comparison of ATR-IR spectra for the three TS-1 catalysts.

The ATR-IR spectra of the three TS-1 catalysts show the same characteristic bands: those at 450 cm^{-1}, 800 cm^{-1} and 1100 cm^{-1} are attributed to vibrations of tetrahedral -[SiO4]- structure; bands at 547 cm^{-1} and 1230 cm^{-1} are assigned to vibrations of the crystalline structure of titanium-silicalite; finally, the band at 960 cm^{-1} is attributed to the symmetric stretching of Si-O-Ti bond.

X-ray fluorescence (XRF)

The amount of titanium, expressed as weight percentage, present in the three TS-1 catalysts was determined by means of XRF, and results are reported in Figure 3.25.

Catalytic system	Measured Ti (%w)
TS-1A	2.20 ± 0.05
TS-1B	2.40 ± 0.05
TS-1C	2.40 ± 0.05

Figure 3.25 Titanium weight percentage for the three tested TS-1 systems.

The analysis show that catalysts present a comparable content of Ti, slightly higher for TS-1B and TS-1C: this suggests that these two catalysts may present species of titanium other than framework Ti.

Diffusive reflectance UV-spectroscopy (DR-UV)

DR-UV spectroscopy allowed us to determine the Ti species present in the three titanium-silicalites; spectra are reported in Figure 3.26.

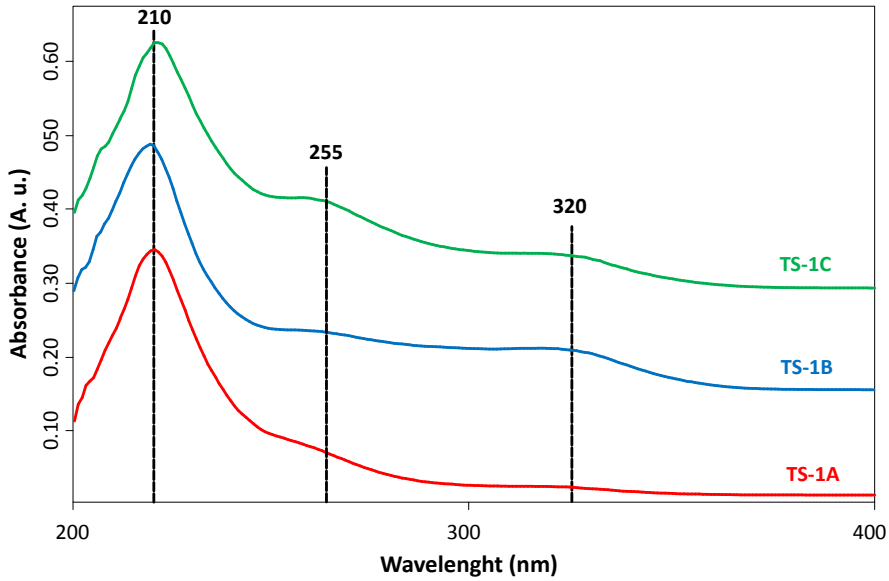

Figure 3.26 Comparison of DR-UV spectra for the three tested TS-1.

It is shown that the three TS-1 show different absorption bands, which correspond to the three characteristic species of Ti(IV) that can be present in titanium-silicalite, as described in paragraph 1.4.4:

- the band at 210 nm is attributed to framework Ti, that is a tetrahedral titanium species which replaces a Si atom in the silicalite structure;

- the band at 255 nm is assigned to amorphous Ti, which is situated in octahedral sites, but whose chemical nature has not yet been definitely ascertained in the literature;
- the band between 290 nm and 320 nm is attributed to bulk Ti, that is titanium oxide (TiO_2) in the anatase form; this band is similar to that one observed in DR-UV spectra of titanium oxide grafted on silica.

However, the DR-UV spectra differ for the relative amount of the three different Ti species; by means of spectra deconvolution, it was possible to observe that TS-1A hold mainly framework Ti with traces of amorphous Ti, but it does not present bulk Ti oxide; besides framework Ti, TS-1B and TS-1C also exhibit bulk Ti and an amount of amorphous Ti that is higher for TS-1C (about twice as much that of TS-1B).

Ammonia temperature programmed desorption (TPD)

TPD with ammonia as probe molecule permits to determine the total acid sites concentration, as reported in Table 3.6.

Catalytic system	Acid sites concentration (mmol/g)
TS-1A	0.068 ± 0.005
TS-1B	0.033 ± 0.005
TS-1C	0.066 ± 0.005

Table 3.6 Total acid sites concentration for the three tested TS-1 systems.

From these analysis it is possible to conclude that TS-1A and TS-1C show a comparable total concentration of acid sites, that is twice as much that one held

by TS-1B; however, the acid sites concentration shown by all TS-1 catalysts was very low.

Moreover, the ammonia desorption profiles plotted in Figure 3.27, show that the three TS-1 systems catalyst hold a similar low strength of acid sites: in fact, the maximum of the desorption profile is in all cases at ca 200°C.

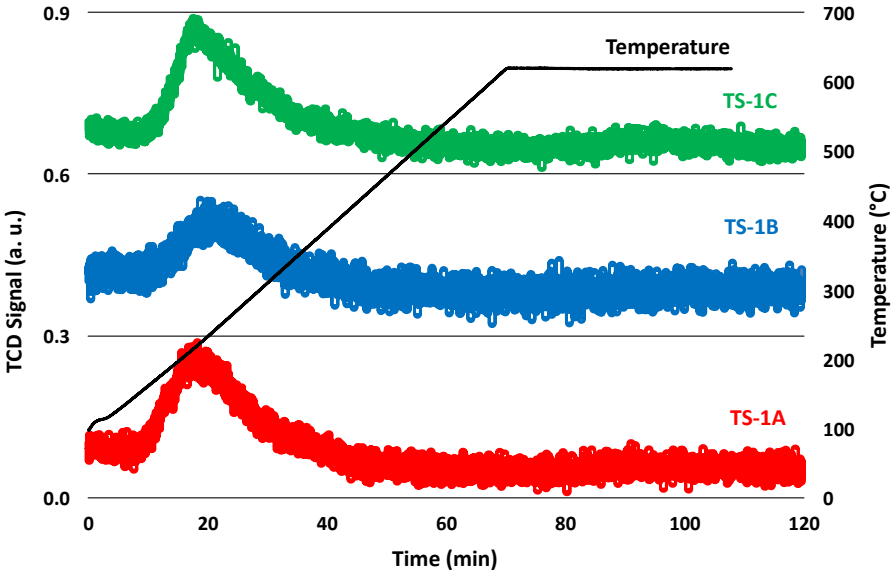

Figure 3.27 TPD-ammonia desorption profiles for the three TS-1 catalysts.

Fourier transform IR-spectroscopy of adsorbed pyridine (FT-IR)

Using pyridine as a probe molecule, and recording the FT-IR spectra at increasing desorption temperatures, allows to discriminate between Lewis (L) and Brønsted (B) acid sites, and their relative strength as well, thanks to the two characteristic vibration bands of adsorbed pyridine over different acid sites: at 1450cm^{-1} and 1545 cm^{-1} for L and B sites, respectively. The FT-IR desorption spectra of pyridine, recorded at increasing temperatures, for the three titanium-silicalite samples are shown in Figure 3.28.

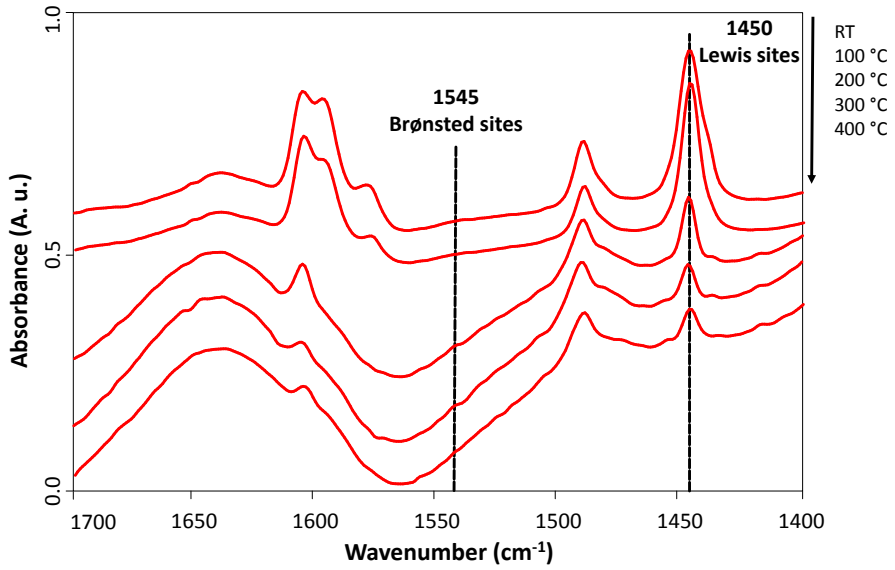
1.0
0.5
0.0
Absorbance (A. u.)
1700
1650
1600
1550
1500
1450
1400
Wavenumber (cm-1)
1450
Lewis sites
1545
Brønsted sites
RT
100 °C
200 °C
300 °C
400 °C

a)

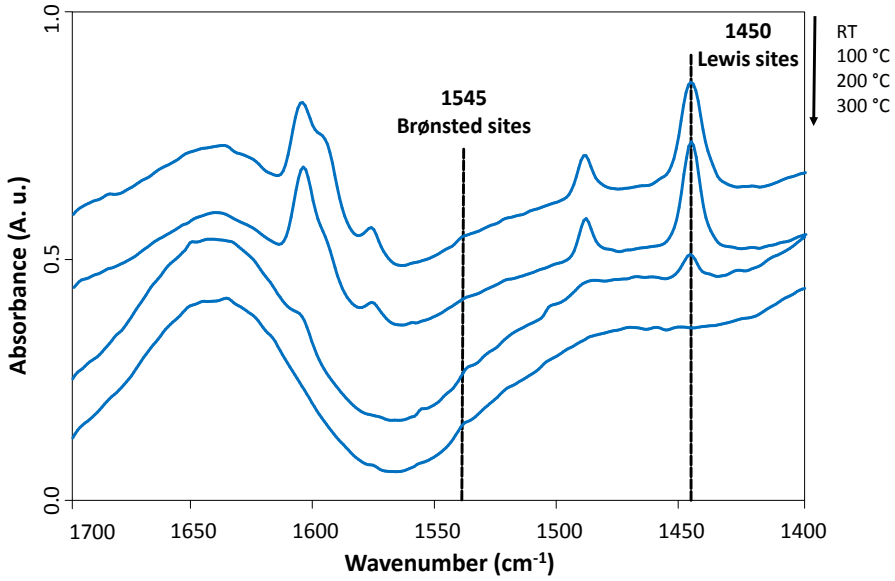
1.0
0.5
0.0
Absorbance (A. u.)
1700
1650
1600
1550
1500
1450
1400
Wavenumber (cm-1)
1450
Lewis sites
1545
Brønsted sites
RT
100 °C
200 °C
300 °C

b)

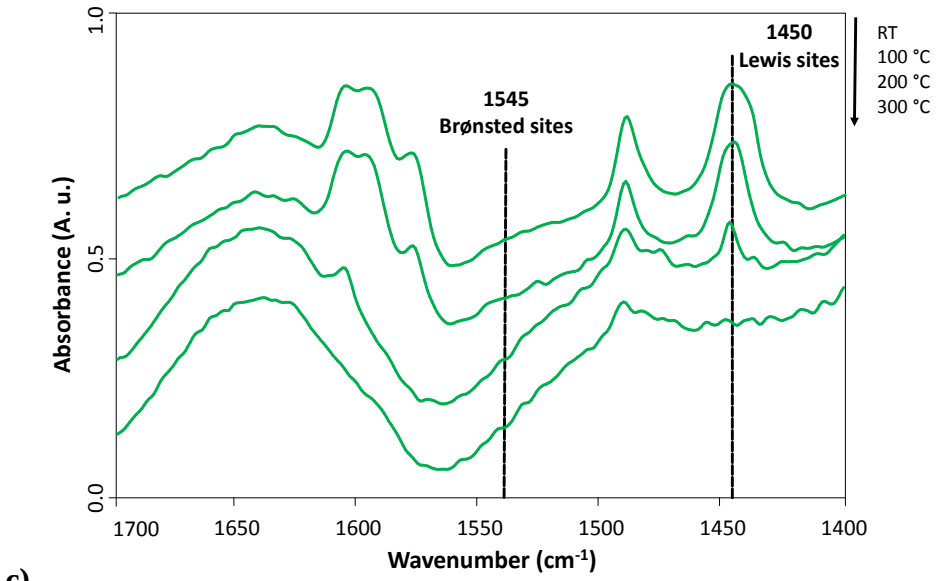

c)

Figure 3.28 FT-IR desorption spectra of pyridine, recorded at increasing temperatures, for: a) TS-1A; b) TS-1B; c) TS-1C.

These analysis confirm that titanium-silicalite present only Lewis acid character, associated to Ti atoms: in fact, spectra did not show the peak at 1545 cm^{-1}. Moreover, it is possible to observe that samples are weakly acid: especially for TS-1B and TS-1C the desorption of pyridine is complete already at 300°C. In the case of TS-1A, instead, after treatment at 300°C still some residual adsorbed pyridine is shown. This suggests that the structural tetrahedral Ti is the site holding the stronger Lewis-type acid feature.

3.2.3 Catalytic tests for the synthesis of rare sugars

The catalytic performances of titanium based heterogeneous catalysts in the synthesis of rare sugars starting from glucose, are presented in this paragraph: results will be correlated to the different species of titanium.

Titanium oxide grafted on silica (TOS)

In order to establish the effect of the different species of titanium on glucose rearrangement, catalytic tests were initially conducted with Ti grafted catalysts.

First of all, we investigated the thermal effect on glucose rearrangement: for this purpose, a blank tests (without any catalyst) was carried out at 110°C for 5 hours, using the same operative conditions (described in paragraph 2.3.2) also used in catalytic tests. The blank test showed that no rearrangement occurs in the absence of catalyst: in fact, the conversion of glucose was almost zero, and only traces of HMF and furfural were detected.

After that, the influence of silica, used as the support for grafting titanium oxide, was analyzed; a kinetic study was carried out as function of time, from 0 to 5 hours, using only pure silica (Grace DAVICAT SI-1301) as catalyst: Figure 3.29 displays results obtained.

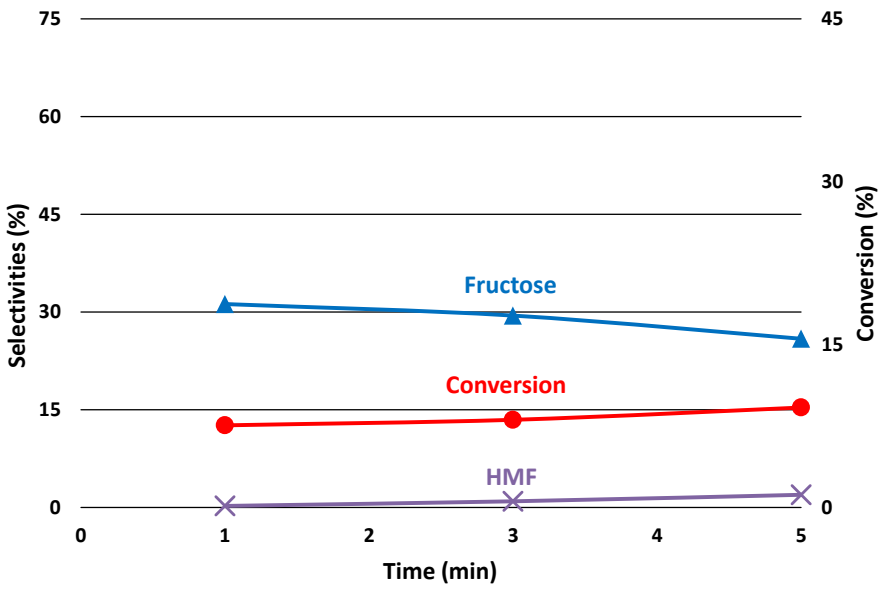

Figure 3.29 Catalytic performances of rare sugars synthesis starting from glucose for silica. Legend: ● Glucose conversion; ▲ Fructose selectivity; × HMF selectivity.

It is shown that silica alone is active in glucose conversion, with fructose as the only product formed.

Therefore, it is possible to conclude that silica holds an acidity which is enough to promote isomerization of glucose to fructose, but is not suitable for the synthesis of mannose and sorbose.

Moreover, the trends for conversion and product selectivities suggest that:

- glucose conversion shows a minimal growth along with the increase of reaction time, with a maximum of 9% after 5 hours;
- selectivity to fructose is 31% after 1 hour, then decreases for longer reaction times, due to degradation reactions;
- consequently, selectivity to HMF, produced by fructose dehydration, increases with reaction times, with a maximum of 3% at 5 hours.

It is also important to note that the sum of selectivities is very low, less than 40%, due to the formation of products that cannot be quantified by means of HPLC: they are mainly made of humins, that, as described in paragraph 1.3.1, derive from condensations involving glucose and HMF. Moreover, other products, which were detected by means of HPLC but were not identified also formed: these products are probably due to degradative reactions that involves monosaccharides.

Synthetized silica-grafted titanium oxide catalysts were tested in glucose rearrangement; Figure 3.30 shows the results of catalytic performances for the five grafted systems, that differ for the weight content of Ti and degree of Ti agglomeration. The kinetic studies were carried out at 110°C, in function of reaction time between 0 and 5 hours.

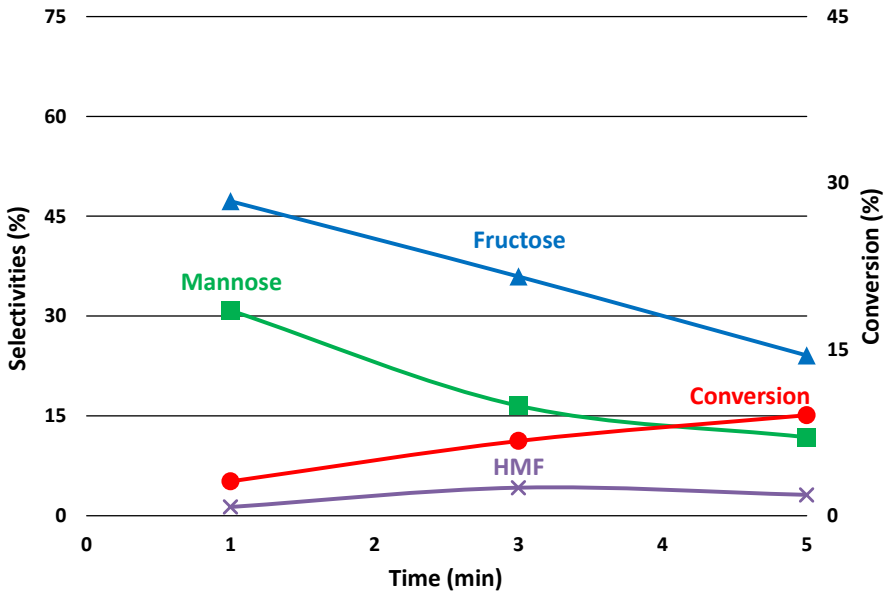
75
60
45
30
15
0
45
30
15
0
Selectivities (%)
Conversion (%)
Fructose
Mannose
Conversion
HMF
0
1
2
3
4
5
Time (min)

a)

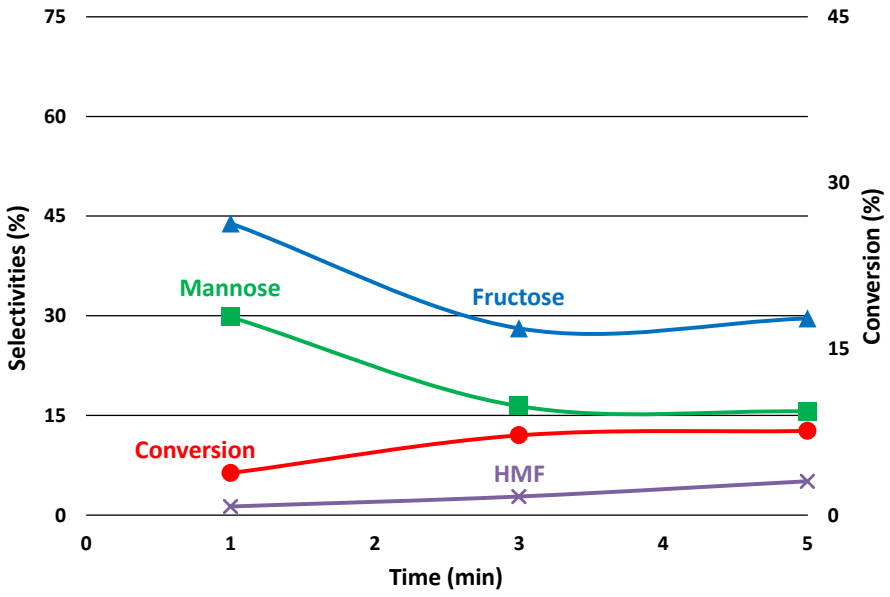
75
60
45
30
15
0
45
30
15
0
Selectivities (%)
Conversion (%)
Mannose
Fructose
Conversion
HMF
0
1
2
3
4
5
Time (min)

b)

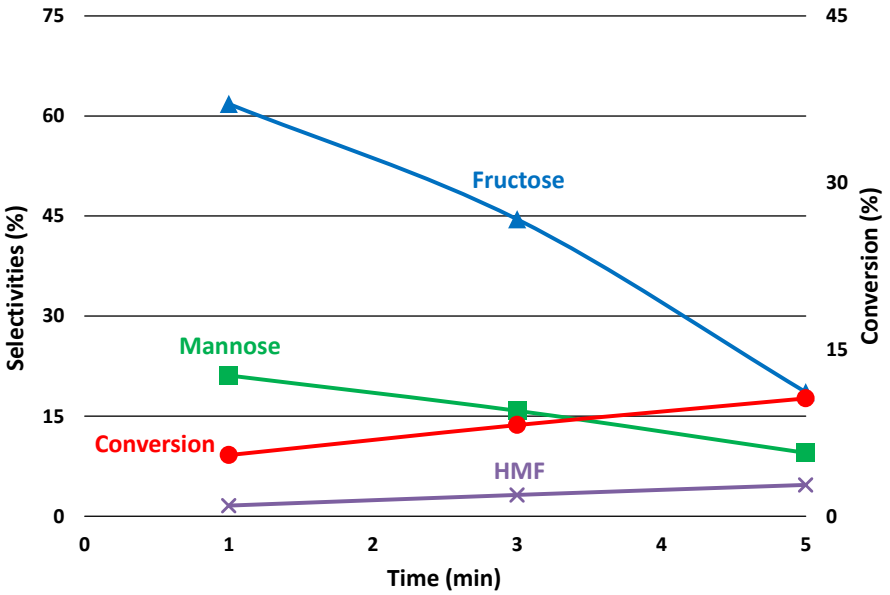
75
60
45
30
15
0
45
30
15
0
Selectivities (%)
Conversion (%)
Fructose
Mannose
Conversion
HMF
0
1
2
3
4
5
Time (min)

c)

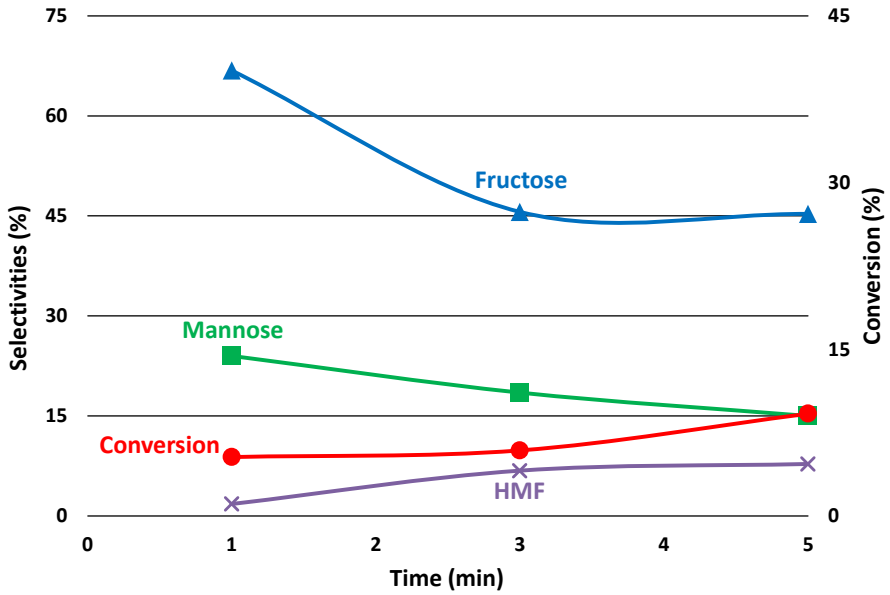
75
60
45
30
15
0
45
30
15
0
Selectivities (%)
Conversion (%)
Fructose
Mannose
Conversion
HMF
0
1
2
3
4
5
Time (min)

d)

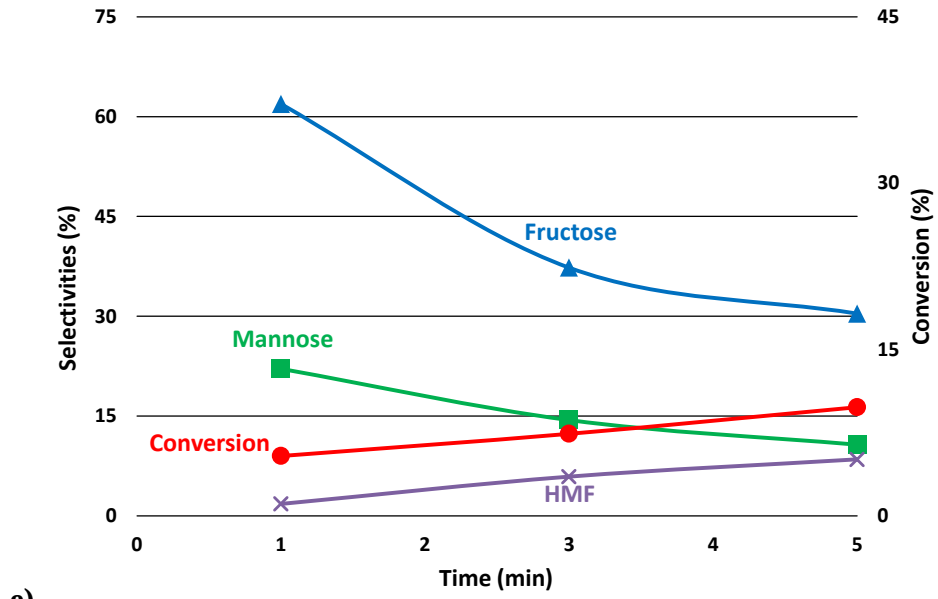

e)

Figure 3.30 Catalytic performances of rare sugars synthesis starting from glucose for: a) TOS-A; b) TOS-B; c) TOS-C; d) TOS-D; e) TOS-E. Legend: ● Glucose conversion; ▲ Fructose selectivity; ■ Mannose selectivity; × HMF selectivity.

At first, is possible to note that the presence of octahedral Ti promotes both isomerization and epimerization: in fact, compared to experiments conducted with pure silica, Ti grafted catalysts are able to form not only fructose with higher selectivity compared to silica support, but also mannose, in significant quantities; the other product of isomerization, sorbose, was not observed with these catalytic systems.

As regards glucose conversion, all catalysts show comparable trends: in fact, conversion grew along with the increase of reaction time, with a maximum of about 10% after 5 hours; therefore, conversion of glucose was not affected by the amount of Ti loaded in grafted systems. It should also be noted that similar values of glucose conversion were achieved with silica alone, and that this value was much lower compared to the equilibrium value reported in literature for glucose rearrangement reactions[94, 133]. Overall, it seems that silica catalyzes glucose isomerization to fructose, whereas octahedral Ti catalyzes epimerization

to mannose. On the other hand, it is shown that on increasing the Ti loading on silica, that is, by developing more agglomerated Ti species (until the formation of bulk anatase), the mannose-to-fructose selectivity ratio decrease. This suggests that the formation of bulkier Ti oxide species are inductive to the formation of fructose.

In regard to the selectivity to each product, the following noticed:

- selectivity to fructose and mannose is higher at 1 hour, then decreases for longer reaction times, due to degradation reactions; however, on increasing the Ti content, catalysts become more selective to fructose, and less to mannose;
- consequently, selectivity to HMF (also furfural formed in traces amount, but is not reported in the figures), produced by degradation of monosaccharides, increases along with reaction time, with a maximum value of 8.5% for TOS-E after 5 hours;
- the sum of selectivities at low reaction time is high, about 80-90%, then decreases for longer times, due to the formation of humins and unknown degradative products.

As reported above, the Ti content in grafted catalysts influenced the distribution of monosaccharides. From the comparison of mannose/fructose selectivity ratio (MFSR) at the beginning of reaction (i.e. after 1 hour) for the different catalysts, it is shown that MSFR decreases with the increase of Ti content: in fact, this ratio changes from 0.67 for catalysts with low Ti amount (TOS-A and TOS-B), to 0.33 for TOS-C; then, the ratio remains stable for catalysts having the greater amount of Ti (TOS-D and TOS-E), because, as reported in paragraph 3.2.1, the real amount of titanium is similar for catalysts with a nominal content of Ti higher than 2%.

The effect of titanium content on products distribution can be correlated to the aggregation degree of Ti species, as shown by the DR-UV spectroscopy study reported in paragraph 3.2.1: at low amount, titanium is present as isolated species dispersed on silica support surface (monomeric species), that, as observed from catalytic experiments, show a higher specificity in mannose synthesis. On increasing the content, titanium becomes more aggregated and forms oligomeric/bulk species, that lead to the preferred formation of fructose at the detriment of mannose.

This aspect was also confirmed by kinetic study carried out with commercial TiO_2 in the form of anatase (CristalACTi G5); results of this test, conducted at 110°C, are shown in Figure 3.31.

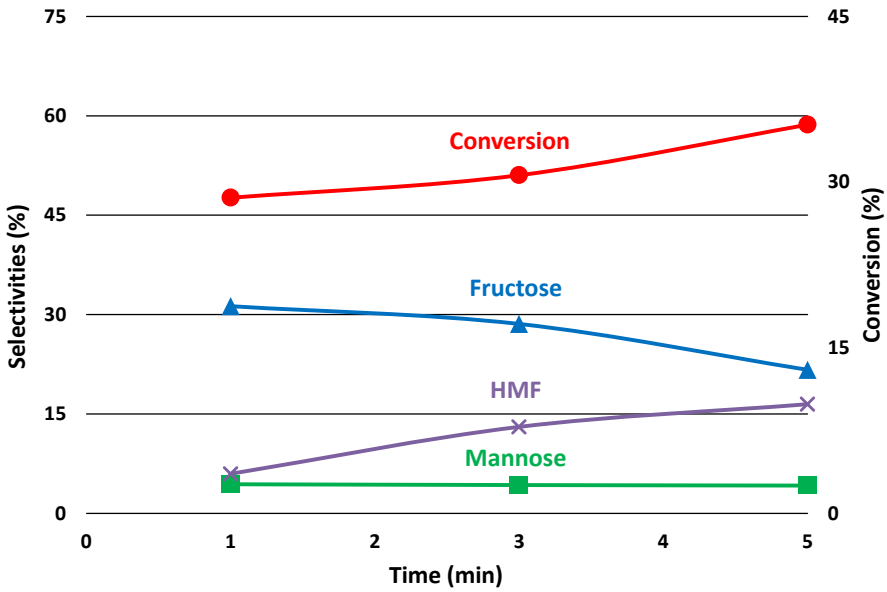

Figure 3.31 Catalytic performances on rare sugars synthesis starting from for anatase. Legend: ● Glucose conversion; ▲ Fructose selectivity; ■ Mannose selectivity; × HMF selectivity.

This graph shows that with titanium oxide in the form of bulk anatase, the MFSR at the beginning of the reaction (i.e., after 1 hour) drops down to 0.15:

this confirms that more condensed species of Ti and bulk titanium oxide promote the preferential formation of fructose.

Titanium silicalite (TS-1)

The role of titanium in glucose rearrangement was then studied by carrying out reactivity experiments with titanium-silicalites; as described in paragraph 3.2.2, the three TS-1 catalysts differed in the amount and type of Ti: in particular, they showed the presence of three Ti species, characterized by different coordination and aggregation degree.

Figure 3.32 reports the performances obtained in catalytic tests conducted at 110°C in function of time, with the three TS-1 catalysts.

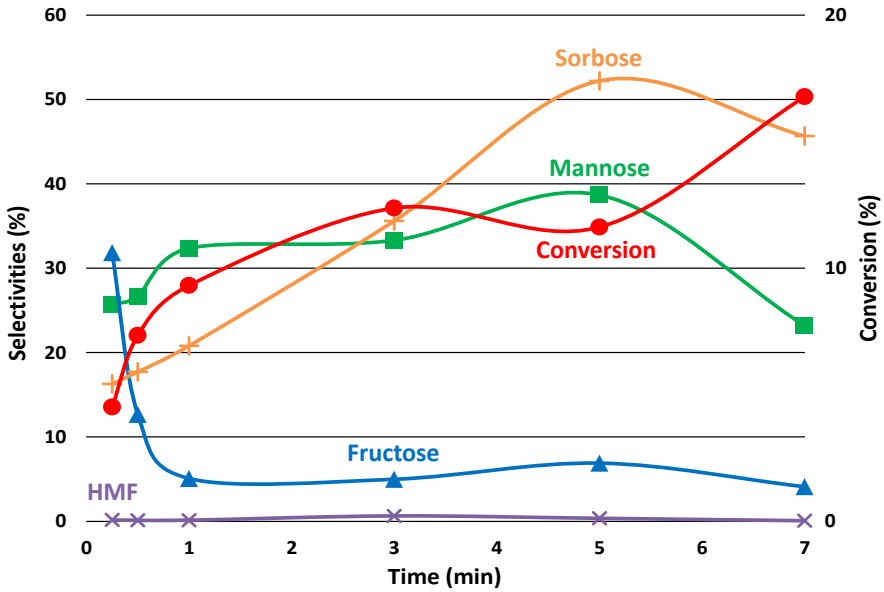

a)

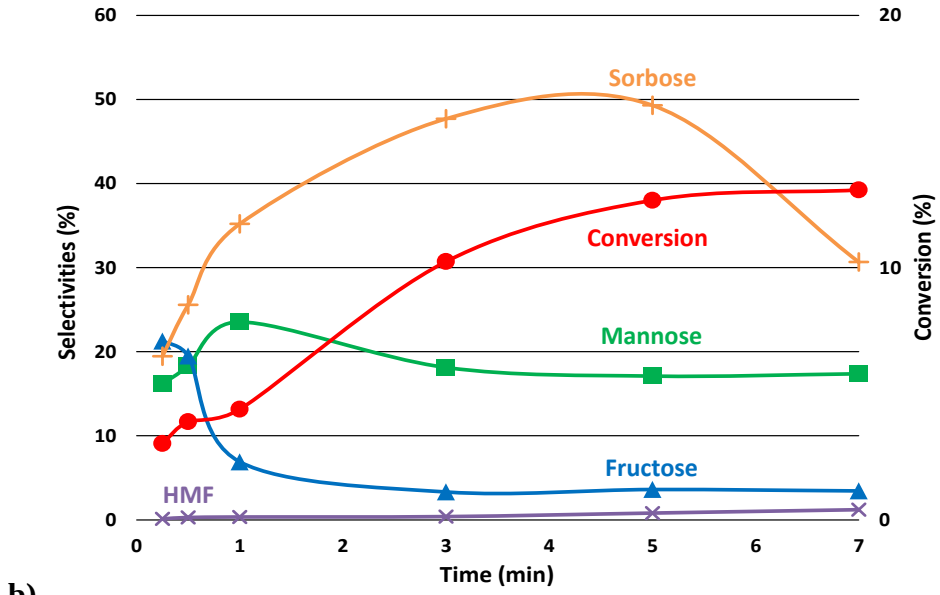

b)

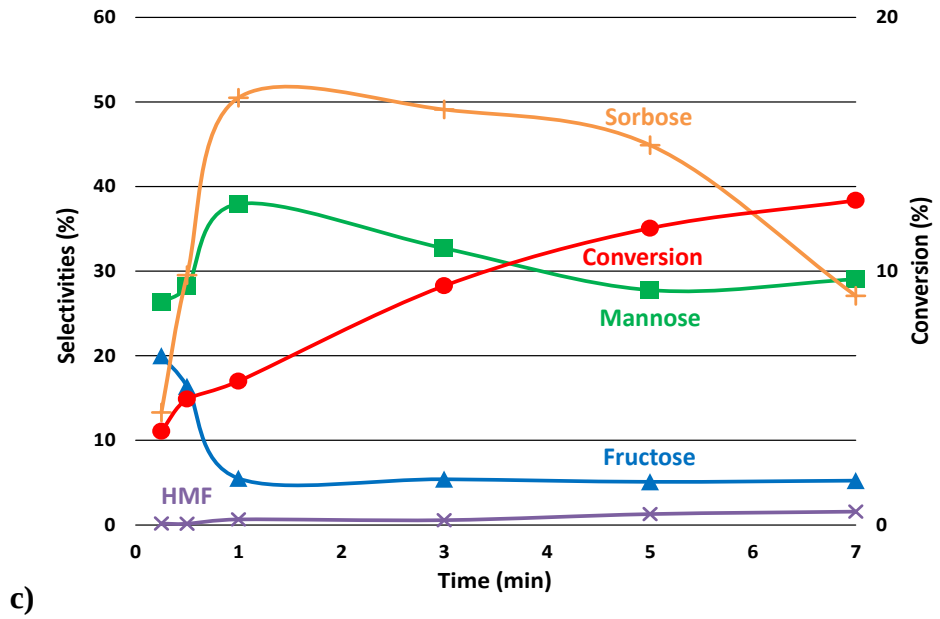

c)

Figure 3.32 Catalytic performances on rare sugars synthesis starting from glucose for: a) TS-1A; b) TS-1B; c) TS-1C. Legend: ● Glucose conversion; ▲ Fructose selectivity; ■ Mannose selectivity; + Sorbose selectivity; × HMF selectivity.

The catalysts showed similar trends for conversion and products selectivities, but different performance:

- conversion of glucose grows along with reaction time, with the maximum value at 7 hours; TS-1A exhibits the higher conversion value of 17%;
- selectivity to fructose is higher at the beginning of the reaction (the greater value is 32%, shown by TS-1A); then it decreases very quickly and, after 1 hour, remains stable at about 5%;
- selectivity to mannose initially grows along with the increase of reaction time, with a maximum value shown after 1 hour (TS-1C exhibits the higher selectivity, 38%), then gradually decreases for longer reaction times, due to the increased contribution of degradation reactions;
- also selectivity to sorbose initially increases with reaction time, but with a very different rates for the three systems: TS-1C shows both the higher maximum value and rate, with a selectivity of 51% after 1 hour. Then, for longer reaction times selectivity decreases due to degradation reaction;
- consequently, selectivity to HMF, produced by dehydration of monosaccharides, increases along with reaction time, and TS-1C exhibits the highest value of 1.5% after 7 hours;
- at low reaction times, the sum of selectivities is high, about 90-95%, but then decreases for longer times, due to formation of humins and unknown products of monosaccharides degradation (especially for sorbose).

As regards conversion, it is possible to note that TS-1 exhibits a slightly higher conversion compared to those achieved with TiO_2-SiO_2 catalysts; however, also for titanium-silicalites, conversions obtained are lower than equilibrium value for glucose rearrangement.

Moreover, is possible to say that the activity of TS-1 in glucose conversion is a function of acidity: in fact, as described in paragraph 3.2.2, TS-1A shows the higher total concentration and strength of acid sites, that results in a higher conversion of glucose; on the other hand, TS-1B, the catalyst with the lower acidity, is the least active in glucose conversion.

For what concerns selectivity, it is important to note that the nature of Ti species has an important influence on products distribution. First, compared to the grafted systems, titanium-silicalites promote both epimerization to mannose, and isomerization to fructose and sorbose.

At the beginning of reaction, the isomerization to fructose results to be the kinetically favored reaction, and therefore fructose is the predominant product. However, the products distribution completely changes when the reaction time is increased: isomerization to sorbose and, at a lesser extent, epimerization to mannose (its reaction rate is also high at the beginning of the reaction) gradually increase their contribution, at the detriment of isomerization to fructose. Therefore, sorbose becomes the main product.

The remarkable change of products distribution during reaction, led us to the formulate two different hypotheses:

- the trends of selectivities experimentally observed seems to suggest the presence of consecutive reactions, that convert fructose into sorbose and/or mannose; however, the hypothesis of the role of fructose as an intermediate compound is in disagreement with the mechanism reported in literature for these reactions[91, 133];
- according to the hypothesized mechanism, it is possible to propose the shift of the equilibrium for glucose isomerization (which can be summarized as fructose ↔ glucose ↔ sorbose) towards the formation of sorbose, at the detriment of fructose.

Therefore, in order to distinguish between these assumptions, a catalytic test was carried out using fructose as the substrate, at 110°C, in function of time; the catalyst employed was TS-1C, because it showed to be the most active one in sorbose synthesis. Results are reported in Figure 3.33.

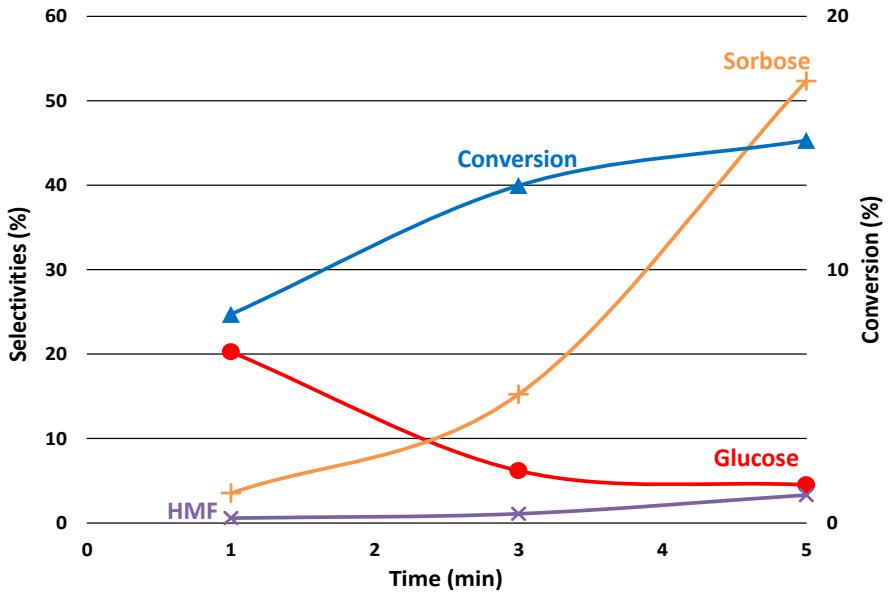

Figure 3.33 Catalytic performances on rare sugars synthesis starting from fructose for TS-1C. Legend: ▲ Fructose conversion; ● Glucose selectivity; + Sorbose selectivity; × HMF selectivity.

Results lead to the following conclusions:

- conversion of fructose proportionally grows along with the increase of reaction time, with a maximum value of 15% at 5 hours;
- selectivity to glucose is the higher (20%) at the beginning of the reaction (1 hour), then decreases for long reaction times;
- on the other hand, selectivity to sorbose increases along with the increase of reaction time, with a maximum value of 52% at 5 hours;
- mannose is not detected in this experiment.

These results suggest that initially, glucose is the only product obtained by fructose isomerization. Thereafter, with the increase of reaction time, glucose is transformed into sorbose via isomerization; consequently, fructose is continuously converted. Overall, the hypothesis of an equilibrium shift for isomerization turns out to be the most likely hypothesis to explain results observed during glucose rearrangement catalyzed by TS-1.

Moreover, this assumption is also supported by arguments based on reactants and products diffusivity. At the beginning of the reaction, glucose molecules interact first with the surface of TS-1, where nano-domains of bulk Ti are present; as demonstrated in catalytic tests conducted with titanium grafted systems, this Ti species promotes mainly isomerization to fructose and, at a lesser amount, epimerization to mannose. As the reaction time increases, glucose molecules can also diffuse inside the channels of the silicalite, and interact with the framework and amorphous Ti species; in this way, isomerization to sorbose is promoted, to the detriment of fructose synthesis. In particular, the isomerization to sorbose appears to be closely related to the Ti amorphous species: in fact, the rate for this reaction increases from TS-1A to TS-1C, in agreement with the increase of the concentration of amorphous Ti.

4. Conclusions

The work carried out during my PhD, and presented in this thesis, has been focused on the study and development of new heterogeneous catalytic systems for the transformation of renewable raw materials into valuable chemicals, in order to contribute to the development of a modern, environmentally and economically sustainable model of production, able to replace the conventional industry, based on fossil resources.
In particular, the conversion of lignocellulosic biomasses, the most abundant renewable source presents on Earth, has been studied by using the acid-catalyzed hydrolysis. The sugars obtained from this transformation represent important intermediates: in fact, these can be functionalized to obtain bio-building blocks, which show several industrial applications; otherwise, sugars from lignocellulose hydrolysis are used to synthesize other relevant industrial monosaccharides, called rare sugars, that cannot be obtained in appreciable amount from natural resources.

In the first part of my work, the use of heterogeneous metal phosphate catalysts for the acid hydrolysis of biomass has been described: the physical-chemical features and reactivity of synthetized zirconium phosphate and commercial niobium phosphate were compared. Both systems showed interesting performance, in terms of conversion and yields, for the hydrolysis of both cellulose and lignocellulose, comparable to the performance obtained with best commercial catalysts (i.e. acid functionalized resins), reported in literature. In particular, this study has demonstrated the decisive influence of acid properties on catalytic behavior of metal phosphates: the total concentration of acid sites plays a fundamental role in determining catalyst activity in lignocellulose conversion. Conversely, the distribution of products is mainly conditioned by the type of acidity, in particular by the ratio between Brønsted and Lewis acid

sites. For these reasons, synthetized zirconium phosphate showed higher conversion and consequently a higher production of monosaccharides, thanks to its greater acidity. On the other hand, the stronger Brønsted character exhibited by commercial niobium phosphate, especially in aqueous conditions, promoted mainly the formation of successive decomposition products by sugars dehydration.

The further catalytic hydrolysis tests carried out on lignocellulose substrates derived from agricultural waste (which also allowed us demonstrate the role of biomass composition on hydrolysis performance), with synthesized niobium phosphate catalyst, confirmed the close relationship between acid characteristics and catalytic performances: in fact, thanks to its higher acidity and greater amount of strong Brønsted acid sites, the synthetized niobium catalyst showed the highest activity and the greatest production of monosaccharides, but also the formation of successive products turned out to be promoted. Therefore, metal phosphates appear to be flexible catalysts for the hydrolysis of lignocellulose: in particular, it is possible to model their composition, and consequently their acid properties, in order to modulate the performance in biomass hydrolysis.

Finally, characterization study conducted on spent catalysts, has shown that metal phosphate catalysts can be recovered in mild conditions, thus suggesting the ease reuse for these systems for several hydrolysis reactions.

In the second part, the effectiveness of heterogeneous catalysts containing titanium for glucose rearrangement and the influence of the different species of Ti on products distribution, have been investigated.

Titanium species in the form of oligomeric and bulk (like in anatase) octahedral Ti, both in grafted systems and TS-1 catalysts, promoted the isomerization to fructose and epimerization to mannose, with a selectivity ratio influenced by the aggregation degree of Ti species; in fact, the increase of titanium content, that results in the formation of more condensed species, mainly favored the formation of fructose.

Amorphous Ti specie and characteristic framework Ti in TS-1, catalyzed the formation of sorbose by isomerization. In particular, the presence of a non-well characterized amorphous specie, was closely related to sorbose formation: in fact, TS-1C, thanks to its greater concentration of amorphous Ti species, showed both the higher rate of sorbose formation and selectivity to this compound.

Moreover, by combining the role played by the various Ti species in promoting different glucose rearrangement reactions, with diffusional effects of reactants inside TS-1 porosity, it was possible to explain the experimental data by invoking a shift of equilibrium predominance for glucose isomerization from the formation of fructose to that one of sorbose.

5. References

[1] http://unfccc.int/meetings/paris_nov_2015/items/9445.php

[2] P. Fornasiero, M. Graziani, Renewable Resources and Renewable Energy, CRC press, 2012.

[3] F. Cavani, S. Albonetti, F. Basile, A. Gandini, Chemicals and Fuels From Bio-based Building Blocks, Wiley-VCH, 2016.

[4] B. Kamm, P. R. Gruber, M. Kamm, Biorefineries-Industrial Processes and Products: Status Quo and Future Directions, Wiley-VCH, 2010.

[5] R. Luque, Curr. Green Chem., 2015, **2**, 90-95.

[6] S. Rama Mohan, Biores. Technol., 2016, **215**, 76-83.

[7] J. C. Serrano-Ruiz, R. Luque, Chem. Soc. Rev., 2011, **40**, 5266–5281.

[8] S. G. Wettstein, D. M. Alonso, E. I. Gürbüz, J. A. Dumesic, Curr. Opt. Chem. Eng., 2012, **1**, 218-224.

[9] K. Shimizu, A. Satsuma, Ener. Environ. Sci., 2011, **4**, 3140-3153.

[10] H. Chen, Lignocellulose Biorefinery Engineering, Woodhead Publishing, 2015.

[11] P. L. Dhephe, A. Fukuoka, Chem. Sus. Chem., 2008, **1**, 969-975.

[12] R. Rinaldi, F. Schüth, Ener. Environ. Sci., 2009, **2**, 610-626.

[13] S. Van de Vyver, J. Geboers, P. A. Jacobs, B. F. Sels, Chem. Cat. Chem., 2011, **3**, 82-94.

[14] P. Kumar, D. M. Barret, M. J. Delwiche, P. Stroeve, Ind. Eng. Chem. Res., 2009, **48**, 3713-3729.

[15] P. Gallezot, Chem. Soc. Rev., 2012, **41**, 1538-1558.

[16] B. Kamm, M. Kamm, Appl. Microbiol. Biotechnol., 2004, **64**, 137-145.

[17] C. Xu, R. A. D. Arancon, J. Labidi, R. Luque, Chem. Soc. Rev., 2014, **43**, 7485-7500.

[18] S. Laurichesse, L. Averous, Pro. Polym. Sci., 2014, **39**, 1266-1290.

[19] E. Windeisen, G. Wegener, Polymer Science: A Comprehensive Reference, Elsevier, 2012.

[20] P. Calvini, Cellulose, 2005,**12**, 445-447.

[21] J. T. Edward, Chem. Ind., 1955, **3**, 1102-1104.

[22] T. P. Nevell, W. R. Upton, Carbohyd. Res., 1976, **49**, 163-174.

[23] B. Philipp, V. Jacopian, F. Loth, W. Hirte, G. Schultz, Adv. Chem. Ser., 1979, **181**, 127-143.

[24] X. Qian, M. R. Nimlos, D. K. Johnson, M. E. Himmel, Appl. Biochem. Biotechnol., 2005, **124**, 989-997.

[25] E. Palmqvist, B. Hahn-Hagerdal, Biores. Technol., 2000, **74**, 25-33.

[26] K. Freudenberg, G. Blomqvist, Ber. Dtsch. Chem. Ges., 1935, **68**,2070-2082.

[27] H. G. Higgins, A. W. McKenzie, J. Polym. Sci., 1958, **32**, 247-252.

[28] H. Krassig, J. Schurz, R. G. Steadman, K. Schliefer, W. Albrecht, M. Mohring, H. Schlosser, Ullmann's Encyclopedia of Industrial Chemistry, Wiley-VCH, 2004.

[29] H. A. Krassig, Cellulose: Structure Accessibility and Reactivity Polymer Monographs, Gordon and Breach Science Publishers, 1992.

[30] B. G. Ranby, R. H. Marchessault, J. Polym. Sci., 1959, **36**, 561-564.

[31] J. Horvat, B. Klaic, B. Metelko, V. Sunjic, Tetra. Lett., 1985, **26**, 2111–2114.

[32] D. W. Rackemann, W. O. S. Doherty, Biofuels Bioprod. Bioref., 2011, **5**, 198-214.

[33] R. S. Assary, P. C. Redfern, J. R. Hammond, J. Greeley, L. A. Curtiss, J. Phys. Chem. B, 2011, **114**, 9002–9009.

[34] B. Girisuta, B. Danon, R. Manurung, L. P. B. M. Janssen, H. J. Heeres, Biores. Technol., 2008, **99**, 8367–8375.

[35] J. M. Lee, Y. C. Kim, I. T. Hwang, N. J. Park, Y. K. Hwang, J. S. Chang, J. S. Hwang, Biofuels, Bioproducts and Biorefineries, Wiley-VCH, 2008.

[36] S. McKibbins, J. F. Harris, J. F. Saeman, W. K. Neill, Forest Prod. J., 1962, **12**, 17-23.

[37] I. Van Zandvoort, Y. Wang, B. C. Rasrendra, E. R. H. Van Eck, P. C. A. Bruijnincx, H. J. Heeres, B. M. Weckhuysen, Chem. Sus. Chem., 2013, **6**, 1745-1758.

[38] S. K. R. Patil, C. R. F. Lund, Ener. & Fuels, 2011, **25**, 4745-4755.

[39] S. P. Teong, G. Yi, Y. Zhang, Green Chem., 2014, **16**, 2015-2026.

[40] R. J. Van Putten, J. C. Van der Waal, E. De Jong, C. B. Rasrendra, H. J. Heeres, J. G. de Vries, Chem. Rev., 2013, **113**, 1499-1597.

[41] A. Mukherjee, M. Dumont, V. Raghavan, Biomass Bioenerg., 2015, **72**, 143-183.

[42] I. Agirrezabal-Telleria, I. Gandarias, P. L. Arias, Catal. Today, 2014, **234**, 42-58.

[43] T. Werpy, G. Petersen, National Renewable Energy Laboratory (NREL) Report, 2004.

[44] T. Wang, M. W. Nolte, B. H. Shanks, Green Chem., 2014, **16**, 548-572.

[45] P. J. Deuss, K. Barta, J. G. De Vries, Catal. Sci. Technol., 2014, **5**, 1174-1196.

[46] W. L. Faith, Ind. Eng. Chem., 1945, **37**, 9-11.

[47] E. E. Harris, E. Beglinger, US Department of Agriculture, 1946.

[48] F. Bergius, Ind. Eng. Chem., 1937, **29**, 247-253.

[49] P. L. Ragg, P. R. Fields, P. B. Tinker, Philos. Trans R. Soc. London, 1987, **321**, 537-547.

[50] R. A. Antonopolis, H. W. Blanch, R. P. Freitas, A. F. Sciamanna, C. R. Wilke, Biotechnol. Bioeng., 1983, **25**, 2757-2773.

[51] D. R. Thompson, H. E. Grethlein, Ind. Eng. Chem. Prod. Res. Dev., 1979, **18**, 166-169.

[52] J. F. Harris, A. J. Baker, A. H. Conner, T. W. Jeffries, J. L. Minor, R. C. Petersen, E. L. Springer, R. W. Scott, T. H. Wegner, J. I. Zerbe, US Department of Agriculture, 1985.

[53] V. M. Ghorpade, M. A. Hanna, Patent US 5859263, 1999.

[54] S. W. Fitzpatrick, Patent US 5608105, 1997.

[55] T. Marzialetti, M. B. Valenzuela Olarte, C. Sievers, T. J. C. Hoskins, P. K. Agrawal, C. W. Jones, Ind. Eng. Chem. Res., 2008, **47**, 7131-7140.

[56] D. Bianchi, A. M. Romano, G. Franzosi, A. Bosetti, Patent WO 069516A2, 2010.

[57] G. Ertl, H. Knozinger, F. Schuth, J. Weitkamp, Handbook of Heterogeneous Catalysis, Wiley-VCH, 2008.

[58] D. M. Lai, L. Deng, J. Li, B. Liao, Q. X. Guo, Y. Fu, Chem. Sus. Chem., 2011, **4**, 55-58.

[59] R. L. De Souza, H. Yu, F. Rataboul, N. Essayem, Challenges, 2012, **3**, 212-232.

[60] S. Van de Vyver, J. A. Geboers, P. A. Jacobs, B. F. Sels, Chem. Cat. Chem., 2011, **3**, 82-94.

[61] A. Onda, T. Ochi, K. Yanagisawa, Green Chem., 2008, **10**, 1033-1037.

[62] A. Takagaki, C. Tagausagawa, A. Iguchi, K. Takanabe, J. N. Kondo, K. Ebitani, T. Tatsumi, K. Domen, Angew. Chem. Int. Ed., 2010, **49**, 1128-1132.

[63] S. De, S. Dutta, B. Saha, Catal. Sci. Techol., 2016, **6**, 7364-7385.

[64] R. Rinaldi, F. Schuth, R. Palkovits, Angew. Chem. Int. Ed., 2008, **47**, 8047-8050.

[65] J. Hegner, B. De Boef, C. Pereira, B. L. Lucht, Tetra. Lett., 2010, **51**, 2356-2358.

[66] M. Todal, A. Takagaki, M. Okamura, J. N. Kondo, S. Hayashi, K. Domen, M. Hara, Nature, 2005, **438**, 178.

[67] L. Bhatia, S. Johri, R. Ahmad, AMB Express, 2012, **2**, 1-19.

[68] P. Kumar, D. M. Barrett, M. J. Delwiche, P. Stroeve, Ind. Eng. Chem. Res., 2009, **48**, 3713-3729.

[69] D. J. Hayes, J. Ross, M. H. B. Hayes, S. Fitzpatrick, Biorefineries: Industrial Processes and Products**,** Wiley-VCH, 2006.

[70] R. N. Maeda, V. I. Serpa, V. Alves Lima Rocha, R. Aparecida Alves Mesquita, L. M. Melo Santa Anna, A. Machado de Castro, C. E. Driemeier, C. E. Nei Pereira Jr., I. Polikarpov, Process Biochem., 2011, **46**, 1196-1201.

[71] B. Yang, Z. Dai, S. Y. Ding, C. E. Wyman, Biofuels, 2011, **2**, 421-450.

[72] Y. H. P. Zhang, L. R. Lynd, Biotechnol. Bioeng., 2004, **88**, 797-824.

[73] H. Kobayashi, Y. Ito, T. Komanoya, Y. Hosaka, P. L. Dhepe, K. Kasai, K. Hara, A. Fukuoka, Chem. Sus. Chem., 2010, **3**, 440-443.

[74] C. H. Zhou, X. Xia, C. X. Lin, D. S. Tong, J. Beltramini, Chem. Soc. Rev., 2011, **40**, 5588-5617.

[75] X. Tan, W. Deng, M. Liu, Q. Zhang, Y. Wang, Chem. Commun., 2009, **46**, 7179-7181.

[76] T. K. Lindhorst, Essential of Carbohydrate Chemistry and Biochemistry, Wiley-VCH, 2003.

[77] P. Y. Bruice, Organic Chemistry, Pearson Higher Education, 2013.

[78] I. Delidovich, R. Palkovits, Chem. Sus. Chem., 2016, **9**, 547-561.

[79] K. K. Makinen, Int. J. Dent., 2010, **1**, 1-23.

[80] B. Hahn-Hägerdal, M. Galbe, M. F. Gorwa-Grauslund, G. Lidén, G. Zacchi, Trends Biotechnol., 2006, **24**, 549-556.

[81] S. J. Angyal, Glycoscience: Epimerisation, Isomerisation and Rearrangement reactions of carbohydrates, Springer-Verlag, 2001.

[82] J. W. Pelley, Integrated Biochemistry, Elsevier, 2008.

[83] J. A. Muntz, R. E. Carroll, J. Biol. Chem., 1959, **235**, 1258-1260.

[84] M. Hara, K. Nakajima, K. Kamata, Sci. Technol. Adv. Mater., 2015, **16**, 1-22.

[85] R. Gounder, M. E. Davis, J. Catal., 2012, **308**, 176-188.

[86] T. J. Harrison, G. R. Drake, J. Org. Chem., 2005, **70**, 10872-10874.

[87] J. M. Carraher, C. N. Fleitman, J. P. Tessonier, ACS Catal. 2015, **5**, 3162-3173.

[88] A. Corna, M. Renz, Chem. Commun., 2004, **5**, 550-551.

[89] W. R. Gunther, Y. Wang, Y. Ji, V. K. Michaelis, S. T. Hunt, R. G. Griffin, Y. Román-Leshkov, Nature Commun., 2012, **3**, 1109-1117.

[90] M. Moliner, Y. Román-Leshkov, M. E. Davis, Proc. Natl. Acad. Sci., 2010, **107**, 6164-6168.

[91] R. Bermejo-Deval, R. Gounder, M. E. Davis, ACS Catal., 2012, **2**, 2705-2713.

[92] Y. Takasaki, T. Ohya, Patent US 5240717A, 1993.

[93] T. Zhang, Z. Pan, C. Qian, X. Chen, Carbohyd. Res., 2009, **344**, 1687-1689.

[94] V. Bilik, Chem. Zvesti, 1972, **86**, 183-186.

[95] A. Kusin, Ber. Dtsch. Chem. Ges., 1936, **69**, 1041–1049.

[96] S. Yoshikawa, Inorg. Chem., 1988, **27**, 4085-4094.

[97] M. E. Davis, R. Gounder, Patent US 9255120 B2, 2016.

[98] M. Taramasso, G. Perego, B. Notari, Patent US 4410501, 1983.

[99] R. Millini, E. Previde Massara, G. Perego, G. Bellussi, J. Catal., 1992, **137**, 497-503.

[100] G. Perego, Stud. Surf. Catal., 1986, **28**,129.

[101] R. Catlow, Modeling of Structure and Reactivity in Zeolites, Academic Press, 1992.

[102] J. Čejka, H. Van Bekkum, Zeolites and Ordered Mesoporous Materials: Progress and Prospects, Elsevier, 2005.

[103] J. Su, G. Xiong, J. Zhou, W. Liu, D. Zhou, G. Wang, X. Wang, H. Guo, J. Catal., 2012, **288**, 1-7.

[104] A. Vasile, A. M. Tomoiaga, Mater. Res. B., 2012, **47**, 35-41.

[105] M. G. Clerici, G. Bellussi, Patent EU 315247, 1992.

[106] T. Tatsumi, N. Nakamura, S. Negishi, H. Tominaga, Chem. Commun., 1990, 476-477.

[107] Y. Kamiya, S. Sakata, Y. Yoshinaga, R. Ohnishi, T. Okuhara, Catal. Lett., 2004, **94**, 45-47.

[108] N. K. Mal, M. Fujiwara, Chem. Commun., 2002, **22**, 2702–2703.

[109] N. Hamilton, T. Wolfram, G. T. Muller, M. Havecker, J. Krohmert, C. Carrero, R. Schomacker, A. Trunschke, R. Schlogl, Catal. Sci. Technol., 2012, **2**, 1346-1359.

[110] A. Sluiter, B. Hames, R. Ruiz, C. Scarlata, J. Sluiter, D. Templeton, National Renewable Energy Laboratory (NREL) Technical Report, 2008.

[111] Y. Zhang, J. Wang, J. Ren, X. Liu, X. Li, Y. Xia, G. Lu, Y. Wang, Catal. Sci. Technol., 2012, **2**, 2485–2491.

[112] P. Carniti, A. Gervasini, S. Biella, A. Auroux, Catal. Today, 2006, **118**, 373–378.

[113] I. Jiménez-Morales, A. Teckchandani-Ortiz, J. Santamaría-González, P. Maireles-Torres, A. Jiménez-López, Appl. Catal. B: Environ., 2016, **144**, 22–28.

[114] P. Khemthong, P. Daorattanachai, N. Laosiripojana, K. Faungnawakij, Catal. Commun., 2012, **29**, 96–100.

[115] I. Nowak, M. Ziolek, Chem. Rev., 1999, **99**, 3603–3624.

[116] A. Jain, A. M. Shore, S. C. Jonnalagadda, K. V. Ramanujachary, A. Mugweru, Appl. Catal. A: Gen., 2015, **489**, 72–76.

[117] G. Gliozzi, A. Innorta, A. Mancini, R. Bortolo, C. Perego, M. Ricci, F. Cavani, Appl. Catal. B: Environ., 2014, **145**, 24-33.

[118] P. Carniti, A. Gervasini, F. Bossola, V. Dal Santo, Appl. Catal. B: Environ., 2016, **193**, 93–102.

[119] T. Hattori, A. Ishiguro, Y. Murakami, J. Inorg. Nucl. Chem., 1978, **40**, 1107–1111.

[120] D. Spielbauer, G. A. H. Mekhemer, T. Riemer, M. I. Zaki, H. Knözinger, J. Phys. Chem. B, 1997, **101**, 4681–4688.

[121] T. Armaroli, G. Busca, C. Carlini, M. Giuttari, A. M. Raspolli Galletti, G. Sbrana, J. Molec. Catal. A: Chem., 2000, **151**, 233-243.

[122] J. J. Zah-Letho, A. Verbaere, A. Jouanneaux, F. Taulelle, Y. Piffard, M. Tournoux, J. Sol. Sta. Chem., 1995, **116**, 335-342.

[123] V. V. Ordomsky, V. L. Sushkevich, J. C. Schouten, J. Van der Schaaf, T. A. Nijhuis, J. Catal., 2013, **300**, 37–46.

[124] A. S. Rocha, A. M. S. Forrester, M. H. C. De la Cruz, C. T. Da Silva, E. R. Lachter, Catal. Commun., 2008, **9**, 1959–1965

[125] M. Helen, B. Viswanathan, S. S. Murthy, J. Membr. Sci., 2007, **292**, 98–105.

[126] W. Alharbi, E. Brown, E. F. Kozhevnikova, I. V. Kozhevnikov, J. Catal., 2014, **319**, 174–181.

[127] C. Antonetti, M. Melloni, D. Licursi, S. Fulignati, E. Ribecchini, S. Rivas, J. C. Parajo, F. Cavani, A. M. Raspolli Galletti, App. Catal B: Environ., 2017, **206**, 364-377.

[128] C. S. Rasrendra, M. Windt, Y. Wang, S. Adisasmito, I. G. B. N. Makertihartha, E. R. H. Van Eck, D. Meier, H. J. Heeres, J. Anal. Appl. Pyrol., 2013, **104**, 299–307.

[129] A. Chuntanapum, Y. Matsumura, Ind. Eng. Chem. Res., 2009, **48**, 9837–9846.

[130] M. Tatzber, M. Stemmer, H. Spiegel, C. Katzlberger, G. Haberhauer, A. Mentler, M. H. Gerzabek, J. Plant Nutr. Soil Sci., 2007, **170**, 522–529.

[131] Q. Yuan, A. Hagen, F. Roessner, App. Catal. A: Gen., 2006, **303**, 81-87.

[132] M. Cozzolino, M. Di Serio, R. Tesser, E. Santacesaria, App. Catal. A: Gen., 2007, **325**, 256-262.

[133] H. Nguyen, V. Nikolakis, D. G. Vlachos, ACS Catal., 2013, **6**, 1497-1504.